Université Mohamed Khider – Biskra
Faculté des Sciences et de la technologie
Département : Génie Civil et Hydraulique
Ref : …………………………………

جامعة محمد خيضر بـسكرة
كـلية العلــوم والتكــنولوجيـــا
قسم : الهندسة المدنية و الري
المـرجع : ....

Thèse présentée en vue de l'obtention

Du diplôme de

Doctorat LMD en Voies et ouvrages d'art

Option : Modélisation numérique en Travaux publics

Analyse numérique du comportement mécanique des colonnes ballastées renforcées de géosynthétiques dans des sols mous

---

Soutenue publiquement le : **29/06 /2025**

Devant le jury composé de :

Mr. BELOUNAR Lamine	**Professeur**	**Président**	**Université de Biskra**
Mr. HOUHOU Mohamed Nabil	**Professeur**	**Rapporteur**	**Université de Biskra**
Mr. BENMEBAREK Sadok	**Professeur**	**Examinateur**	**Université de Biskra**
Mr. BENMOUSSA Samir	**Maitre de conférences A**	**Examinateur**	**Université de Batna**
Mr. REMADNA Mohamed Saddek	**Professeur**	**Invité**	**Université de Biskra**

Thesis presented with a view to obtaining

LMD Doctorate in Roads and Engineering Structures

Option: Numerical modeling in Public Works

Numerical analysis of the mechanical behavior of geosynthetic reinforced stone columns in soft soils

Presented by:

BAHI Selma

Publicly supported on: **29/06/2025**

Before the jury composed of:

Mr. BELOUNAR Lamine	Professeur	President	University of Biskra
Mr. HOUHOU Mohamed Nabil	Professeur	Rapporteur	University of Biskra
Mr. BENMEBAREK Sadok	Professeur	Examiner	University of Biskra
Mr. BENMOUSSA Samir	Maitre de conférences A	Examiner	University of Biskra
Mr. REMADNA Mohamed Saddek	Professeur	Invited	University of Biskra

DEDICATION

To my dear parents, *BAHI Lkhdar & DERBAL Mlika,*

For their endless love, sacrifices, and unwavering belief in me.

Your strength and encouragement have been my greatest source of motivation.

To my sister and brothers, *Souhir, Saif Eddine, and Mohamed,*

For their constant support and for standing by my side through every challenge.

And to all those who believed in me,

This work is dedicated to you with heartfelt gratitude.

Bahi Selma

ACKNOWLEDGEMENTS

ABSTRACT

Soft soils, characterized by high compressibility and low shear strength, present significant challenges for infrastructure construction, necessitating innovative soil improvement techniques. Among these, geosynthetic-encased stone columns (GESC) have emerged as a highly effective solution. This thesis explores the mechanical behavior of GESC in soft soils through advanced three-dimensional numerical analyses using Plaxis 3D, aiming to enhance our understanding and optimize design methods for infrastructure projects.

The first part of the study focuses on optimizing ground improvement with encased stone columns through a detailed 3D numerical analysis in very soft clay. Different types of columns were studied, including short and floating columns, ordinary stone columns, and geosynthetic-encased stone columns within a unit cell model. The investigation demonstrates the superior performance of geosynthetic encasement in reducing bulging and settlement compared to ordinary stone columns. The results emphasize the importance of considering realistic installation effects, highlighting how geosynthetic encasement significantly improves performance by preventing lateral expansion and maintaining structural integrity.

The second part of the study delves into the advanced 3D modeling of a group of geosynthetic-encased stone columns in soft clay beneath embankments. Using Plaxis 3D software, this analysis evaluates the installation effects using a realistic lateral expansion method alongside the effects of geosynthetic reinforcement. The simulations reveal that geosynthetic encasement, combined with realistic installation methods, substantially enhances the load-bearing capacity and stability of stone columns. The findings validate the effectiveness of the lateral expansion method for simulating installation effects, showing that geosynthetic encasement greatly improves the performance of stone columns under various loading conditions.

This thesis significantly advances the understanding of GESC behavior in soft soils, offering practical guidelines for designing more resilient and efficient infrastructure. The findings emphasize the necessity of incorporating realistic installation effects and a comprehensive range of parameters in design practices to achieve optimal performance.

Keywords: stone column, Embankment, Numerical modeling, Geosynthetic, Bearing capacity, soft soil, Settlement

RESUME

Les sols mous, caractérisés par une compressibilité élevée et une faible résistance au cisaillement, présentent des défis importants pour la construction d'infrastructures, nécessitant des techniques innovantes d'amélioration des sols. Parmi celles-ci, les colonnes ballastées enveloppées de géosynthétiques (GESC) se sont révélées être une solution très efficace. Cette thèse explore le comportement mécanique des GESC dans les sols mous à travers des analyses numériques tridimensionnelles avancées utilisant Plaxis 3D, visant à améliorer notre compréhension et à optimiser les méthodes de conception pour les projets d'infrastructure.

La première partie de l'étude se concentre sur l'optimisation de l'amélioration des sols avec des colonnes ballastées enveloppées à travers une analyse numérique 3D détaillée dans de l'argile très molle. Différents types de colonnes ont été étudiés, y compris les colonnes courtes et flottantes, les colonnes ordinaires et les colonnes ballastées enveloppées de géosynthétiques dans un modèle de cellule unitaire. L'investigation démontre la performance supérieure de l'enveloppement géosynthétique dans la réduction du renflement et de l'affaissement par rapport aux colonnes ordinaires. Les résultats soulignent l'importance de considérer les effets réalistes de l'installation, mettant en évidence comment l'enveloppement géosynthétique améliore significativement la performance en empêchant l'expansion latérale et en maintenant l'intégrité structurelle.

La deuxième partie de l'étude s'intéresse à la modélisation 3D avancée d'un groupe de colonnes ballastées enveloppées de géosynthétiques dans de l'argile molle sous les remblais. En utilisant le logiciel Plaxis 3D, cette analyse évalue les effets de l'installation en utilisant une méthode réaliste d'expansion latérale ainsi que les effets du renforcement géosynthétique. Les simulations révèlent que l'enveloppement géosynthétique, combiné à des méthodes d'installation réalistes, améliore considérablement la capacité portante et la stabilité des colonnes ballastées. Les résultats valident l'efficacité de la méthode d'expansion latérale pour simuler les effets de l'installation, montrant que l'enveloppement géosynthétique améliore grandement la performance des colonnes ballastées sous diverses conditions de charge.

Cette thèse fait progresser de manière significative la compréhension du comportement des GESC dans les sols mous, offrant des lignes directrices pratiques pour la conception d'infrastructures plus résilientes et efficaces. Les résultats mettent en évidence la nécessité d'incorporer des effets réalistes d'installation et une gamme complète de paramètres dans les pratiques de conception pour atteindre une performance optimale.

Mots clé : Colonne ballastée, remblai, modélisation numérique, géosynthétique, capacité portante, sol mou, tassement.

الملخص

تُعتبر التربة اللينة، التي تتميز بارتفاع قابلية الانضغاط وانخفاض قوة القص، من التحديات الكبيرة في بناء البنية التحتية، مما يتطلب تقنيات مبتكرة لتحسين التربة. من بين هذه التقنيات، أصبحت الأعمدة الحجرية المحاطة بالجيوسينتيك (GESC) حلًا فعّالًا للغاية. تستعرض هذه الأطروحة السلوك الميكانيكي لـ GESC في التربة اللينة من خلال تحليلات عددية ثلاثية الأبعاد متقدمة باستخدام برنامج Plaxis 3D ، بهدف تحسين فهمنا وتحسين طرق التصميم لمشاريع البنية التحتية. تتمحور الجزء الأول من الدراسة حول تحسين التربة باستخدام الأعمدة المحاطة بالجيوسينتيك من خلال تحليل رقمي ثلاثي الأبعاد مفصل في الطين اللين جداً. تم دراسة أنواع مختلفة من الأعمدة، بما في ذلك الأعمدة القصيرة والعائمة، والأعمدة الحجرية العادية، والأعمدة الحجرية المحاطة بالجيوسينتيك ضمن نموذج وحدة الخلية. تُظهر التحقيقات الأداء المتفوق للتغليف الجيوسينيتيكي في تقليل الانتفاخ والهبوط مقارنة بالأعمدة العادية. تؤكد النتائج على أهمية أخذ تأثيرات التثبيت الواقعية في الاعتبار، مع تسليط الضوء على كيفية تحسين الأداء بشكل كبير بواسطة التغليف الجيوسنيتيكي من خلال منع التوسع الجانبي والحفاظ على السلامة الهيكلية. يتناول الجزء الثاني من الدراسة النمذجة ثلاثية الأبعاد المتقدمة لمجموعة من الأعمدة الحجرية المحاطة بالجيوسينتيك في الطين اللين تحت الردم، باستخدام برنامج 3D Plaxis ، تقيم هذه التحليلات تأثيرات التثبيت باستخدام طريقة واقعية للتوسع الجانبي بجانب تأثيرات التعزيز الجيوسنيتيكي. تكشف المحاكاة أن التغليف الجيوسنيتيكي، جنبًا إلى جنب مع الطرق الواقعية للتثبيت، يعزز بشكل كبير القدرة التحملية واستقرار الأعمدة الحجرية. تؤكد النتائج فعالية طريقة التوسع الجانبي في محاكاة تأثيرات التثبيت، موضحة أن التغليف الجيوسنيتيكي يحسن بشكل كبير أداء الأعمدة الحجرية تحت ظروف تحميل متنوعة. تسهم هذه الأطروحة بشكل كبير في تعزيز فهم سلوك GESC في التربة اللينة، مقدمةً إرشادات عملية لتصميم بنية تحتية أكثر مرونة وكفاءة. تبرز النتائج الحاجة إلى دمج تأثيرات التثبيت الواقعية ونطاق واسع من المعلمات في ممارسات التصميم لتحقيق الأداء الأمثل.

الكلمات المفتاحية: عمود الحجري،ردم، النمذجة الرقمية، الجيوسينتيك، القدرة التحميلية، التربة الرخوة، الهبوط.

LIST OF ABBREVIATIONS

$K_{a,c}$: Active earth pressure exerted by the column material.

C_u: Undrained shear strength.

$E_{oed,ref}$: Reference constrained modulus of the soil, indicating its stiffness under confined conditions.

$E_{oed,s}$: constrained modulus of soft soil.

F_0 : Tensile resistance in quick wide strip test.

h_0 : Initial length of the column.

$K_{0,s}$: At-rest earth pressure coefficient for the soil.

$K_{a,c}$: Active earth pressure of column material.

K_a: The active earth pressure

K_c : Permeability coefficient of column material.

K_p: The passive coefficient earth pressure

K_s : Permeability coefficient of soil in the smeared zone.

n_s : Stress concentration factor, representing the ratio between the vertical stress on top of the column and the vertical stress on top of the surrounding soil at the end of primary consolidation.

P^* : Effective vertical stress in middle of soft soil layer

P_{ref}: Reference effective vertical stress

r_0 : Initial radius of the column.

r_{geo} : Original radius of the geosynthetic encasement.

S_c : Settlement of the column.

S_{mr} : d_s/d_c =Ratio between the smeared zone diameter ($_s$) and the column's diameter ($_c$).

S_s: Settlement of the surrounding soil.

v_s : Poisson's ratio of soft soil.

Δr_c : Change in the radius of the column.

$\Delta \sigma_{h,c}$: Horizontal stress acting on the column.

$\Delta \sigma_{h,diff}$: Net horizontal stress difference.

$\Delta \sigma_{h,geo}$: Horizontal stress developed on the geosynthetic encasement.

$\Delta \sigma_{h,s}$: Horizontal stress acting on the surrounding soil.

$\Delta \sigma_{v,c}$: Vertical stress on top of the column.

$\Delta \sigma_{v,s}$: Vertical stress on top of the surrounding soil.

$_,$: Constrained modulus of the soft soil.

F'_M: Consolidation function.

: Soil horizontal (or radial) permeability.

: Modified time factor.

: Area replacement ratio, which is the ratio of the area occupied by columns to the total area.

c' : The effective cohesion of the soil

: Coefficient of horizontal consolidation, considering radial flow.

: Diameter of the unit cell.

, : Volumetric compressibility coefficient of the column.

, : Volumetric compressibility coefficient of the surrounding soil.

: Specific unit weight of water.

Δr_{geo} : Variation in the geosynthetic encasement radius.

ARR: Area replacement ratio.

C_c: Indicators of Compressibility.

C_g: Constant coefficient related to columns arrangement.

C_s: Indicator of settlement.

CSE: Columns supported embankments.

C_u: undrained shear strength.

d_e: Diameter of the unit cell.

ESC: encased stone column. F:

The hoop ("ring") force. FEM:

Finite element methods. FOS:

factor of safety.

GC: Geocomposite.

GEC: Geosynthetic encased column.

Geofoam: GFM.

Geopipe: GPP.

GESC: geosynthetic encased stone column.

GGR: Geogrid.

GMB: Geomembrane.

GNT: Geonet.

GRSC: geosynthetic reinforced stone column.

GTX: Geotextile.

HRSC: horizontal layers horizontally reinforced stone column.

J: the tensile stiffness modulus.

m: exponent coefficient.

OCR: Over consolidation ratios.

OSC: Ordinary stone columns.

PE: polyethylene.

PM: Polyamides.

PP: polypropylene.

PS: Polyesters.

PVC: Polyvinyl chloride.

q_s: Average vertical stress acting on the soft soil.

RF_{amb} : Reduction factor for chemical and environmental damages.

RF_{dm} : Reduction factor for mechanical damage.

RF_f : Reduction factor for creep.

RF_{joint} : Reduction factor for joints/seams, if exists.

S: geogrid spacing.

SC: Stone column.

U (t) = U: Degree of consolidation due to radial water flow at a given time.

VESC: Vertical encasement stone column.

$\Delta\sigma_0$: Total Vertical Stress from Embankment.

 : Dry density of soil.

LIST OF FIGURES

CHAPTER I

OVERVIEW OF SOIL IMPROVEMENT TECHNIQUES USING GEOSYNTHETIC-REINFORCED STONE COLUMNS

Chapter II

Calculation Approaches for Encased Stone Column Ground Improvement

Chapter III

Review of Published Studies on the Effects of Various Parameters on the Performance of

Geosynthetic-Encased Stone Columns in Soft and Very Soft Soils

Chapter IV

3D Numerical Modeling of Encased Stone Columns for Soft Clay Stabilization

Chapter V

Advanced 3D Modeling of Geosynthetic-Encased Stone Column Group Installation and Performance in Soft Clay Beneath Embankment

LIST OF TABLES

Chapter I

Overview of Soil Improvement Techniques Using Geosynthetic-Reinforced Stone Columns

Chapter 2

Calculation Approaches for Encased Stone Column Ground Improvement

Chapter 3: Review of Published Studies on the Effects of Various Parameters on the Performance of

Geosynthetic-Encased Stone Columns in Soft and Very Soft Soils

Chapter 4

3D Numerical Modeling of Encased Stone Columns for Soft Clay Stabilization

Chapter 5

Advanced 3D Modeling of Geosynthetic-Encased Stone Column Group Installation and Performance

in Soft Clay Beneath Embankment

General introduction

General introduction

Soft soils present considerable challenges due to their high compressibility and low shear strength, complicating the construction of structures like road embankments, dams, bridges, and storage reservoirs. Geotechnical engineers often face difficulties when working with such soils. To address these issues, various soil improvement techniques are employed, among which stone columns stand out as a highly effective and economical solution. This approach involves substituting a portion of the soft soil with vertical columns made of compacted aggregates, resulting in a composite material that offers greater shear strength, improved permeability, and decreased compressibility. The primary objectives of this method are to enhance bearing capacity, minimize settlement, expedite consolidation, and reduce the risk of liquefaction.

In extremely soft soils such as peat or marine clays, traditional granular columns may fail to perform effectively due to the lack of adequate confinement from the surrounding soil. To enhance lateral confinement and improve the bearing capacity of stone columns in these very soft soils, the columns can be encased in a highly rigid, creep-resistant polymer material called geosynthetic. The geosynthetic encasement offers radial support, preventing the column from expanding and the aggregates from spreading laterally. This results in minimal aggregate loss and allows for faster installation of the columns.

Geosynthetic-encased stone columns are an innovative method that has been effectively utilized in numerous embankment projects on soft soils. To optimize this technique, it is crucial to gain a deeper understanding of the factors that influence the performance of stone columns, necessitating further research. Several analytical methods have been developed for designing this soil improvement technique, mainly relying on the unit cell concept and assuming that the granular column and the surrounding soil settle uniformly. These methods do not factor in the enhancement from installation effects and are designed to predict unit cell behavior under long-term drained conditions using elasticity theory. They also consider the surrounding soil as homogeneous, which limits their ability to address nonlinear issues and complex multilayered soil conditions.

Recently, numerous in-situ and laboratory studies have been carried out to assess the effectiveness of geosynthetic-encased stone columns. These investigations have explored different designs, including partial and full encasement, as well as both conventional and floating columns. While these tests provide insights into the fundamental aspects of the technique, they are often conducted under 1g conditions, which do not accurately replicate the stress levels and scaling found in real-world environments. Additionally, using experimental methods for initial design can be both time-intensive and expensive.

In recent years, many researchers have employed finite element numerical methods to study the behavior of geosynthetic-encased stone columns, often using axisymmetric analyses and the unit cell concept. However, experimental studies have pointed out the limitations of this approach, revealing that the underlying assumptions in these formulations can be restrictive and confirming that the issue is fundamentally three-dimensional in nature.

As a result, conducting three-dimensional numerical analysis for foundation systems (whether circular or rectangular) or embankments on very soft soils reinforced with geosynthetic-encased stone columns has become essential. This approach allows for a better understanding of the complex interactions that occur due to group effects, the installation of columns, and loading asymmetry. According to previous research findings, complex interactions between the soil, geosynthetic material, and aggregate control how well stone columns covered with geosynthetic material function when subjected to loads from embankments or shallow foundations. Consequently, numerical models of these structures, when compared to data from instrumented sites or laboratory experiments, often show variations, largely because of the challenges in replicating real-world construction conditions and accurately estimating lateral stress changes near the columns. To enhance the understanding of these interactions and improve design practices, further advanced numerical and experimental studies are necessary. In this context, the current research is dedicated to the numerical investigation of the mechanical behavior of geosynthetic-reinforced stone columns subjected to axial loading in very soft soils.

The installation of stone columns is a commonly employed ground improvement method in geotechnical engineering, known for its ability to significantly enhance the characteristics of soft and unstable soils. Compressed stone or aggregate is used to make these columns, which are designed to improve load-bearing capacity, minimise settlement, increase shear strength, accelerate consolidation, provide lateral support, improve stiffness, improve drainage, and minimise ground vibrations in a range of soil conditions (Grizi et al., 2022; Kelesoglu and Durmus, 2022). These benefits are essential for stabilising and strengthening soils, particularly in building projects on challenging or soft terrain.

Grasping the influence of stone column installation on the surrounding soil is essential for precise design and performance forecasting. The literature identifies three main methods for simulating these effects, each with a distinct approach to modeling soil-column interactions and mechanical behavior (Al Ammari and Clarke, 2018; Kelesoglu and Durmus, 2022).

In the first simulation method, the initial ground pressure coefficient (K_0) is intentionally raised to represent the increased stiffness that stone columns give. This method adjusts the mechanical properties of the soil matrix in numerical simulations, enabling engineers to consider the structural reinforcement introduced by the columns (Al Ammari and Clarke, 2016; Benmebarek *et al*., 2018; Elshazly *et al.,* 2008). Although this approach is simple and computationally efficient, it presumes a uniform stiffness distribution around the stone columns. This assumption may not accurately represent the variability in soil behavior, particularly in cases where the soil is heterogeneous or anisotropic, potentially leading to inaccuracies in predicting the soil's response to loading.

The second method simulates the preloading of stone columns, assuming that they behave elastically with a higher modulus compared to the surrounding soil. This approach takes into account soil stiffening and column-soil interaction, providing a practical solution for many engineering applications (Ellouze *et al.*, 2017; Guetif *et al.,* 2007; Remadna *et al.,* 2020). While this method effectively models the initial stages of soil improvement, it does not always reflect the true nonlinear behavior of stone columns, especially under high loads or in long-term scenarios. Stone columns often exhibit complex mechanical behavior that cannot be fully captured by assuming linear elasticity, necessitating more sophisticated modeling approaches to improve accuracy.

The third approach for simulating stone columns involves applying radial displacement, typically defined as a percentage of the column diameter, to model the radial expansion of the columns. This method is particularly effective in analyzing columns in soft soils, where lateral expansion significantly influences performance (Nguyen et al., 2007). By incorporating lateral expansion, this technique offers a more accurate depiction of column behavior, capturing the interactions between the columns and the surrounding soil matrix. Experimental and numerical studies have supported the validity of this method, showing its effectiveness in representing the deformation characteristics of stone columns (Elshazly et al., 2008). However, determining accurate radial displacement values is complex and requires careful consideration of soil properties and column design parameters.

The present research is focused on two main aspects of numerical modeling to examine the behavior and performance of stone columns. A variety of stone column types are covered in the first chapter, including ordinary and geosynthetic-encased stone columns (OSC and GESC), as well as short and floating columns. In particular, the study evaluates how installing geosynthetic encasement and using the lateral expansion approach affect column performance. An extensive numerical study in three dimensions (3D) is carried out with the explicit finite element code PLAXIS 3D. This analysis examines the influence of installation techniques on settlement reduction ($ß$), lateral displacement (U_x), and vertical displacement (U_z) across different values of lateral expansion, ranging from 0% to 15%. By simulating these parameters, the research aims to understand how variations in lateral expansion affect the mechanical behavior and stability of the stone columns.

The findings from the numerical analysis highlight the superior performance of geosynthetic-encased stone columns (GESC). Among the types of columns analyzed, short columns are found to outperform floating ones, demonstrating a more effective load-bearing capacity and settlement reduction. This improved performance is due to the combined impacts of geosynthetic encasement and higher lateral expansion, which significantly reduce lateral displacement ( ) at the column's edge and vertical displacement ($_z$) beneath the rigid footing. These results underscore the importance of using geosynthetic encasement and optimizing lateral expansion to improve the efficiency and effectiveness of stone columns in geotechnical applications.

The second chapter comprehensively analyzes geosynthetic-encased stone columns (GESC) in soft clay soils beneath embankments using advanced 3D modeling with Plaxis 3D software, validated against field data from

the Penchala Toll Plaza project. The research highlights the significant benefits of incorporating both installation effects and geosynthetic reinforcement in embankment design, emphasizing realistic installation techniques. The lateral expansion method for stone column installation, varying from 0% to 10%, shows a noticeable reduction in settlement, with geosynthetic wrapping further enhancing performance. A detailed parametric study provides insights into optimal geosynthetic properties, installation methods, and column arrangements. Findings reveal that increased geosynthetic stiffness enhances load-bearing capacity and stability, with combined horizontal and vertical reinforcement (VESC + HRSC) being most effective in minimizing vertical displacement. Higher friction angles of stone column materials and triangular arrangements of GESC significantly reduce settlement, highlighting the importance of material selection and column configuration. This research uniquely investigates the radial expansion method for stone column installation and explores various factors affecting settlement mitigation. Overall, the study advances the understanding and application of GESC in geotechnical engineering, offering crucial insights for designing resilient infrastructure in challenging geotechnical environments.

The thesis is divided into two main parts: bibliographic research and numerical analysis .

The bibliographic research part contains three chapters:

Chapter 01: Overview of Soil Improvement Techniques Using Geosynthetic-Reinforced Stone Columns: This chapter provides a general overview of various soil improvement techniques, emphasizing the advantages of using geosynthetic-reinforced stone columns.

Chapter 02: Bibliographic Review on Bearing Capacity Improvement and Settlement Reduction of Shallow Foundations and Embankments Reinforced by Encased Granular Columns: This chapter reviews existing literature on how encased granular columns improve bearing capacity and reduce settlement in shallow foundations and embankments.

Chapter 03: Review of Published Studies on the Effects of Various Parameters on the Performance of Geosynthetic-Encased Stone Columns in Soft and Very Soft Soils: This chapter analyzes studies on the impact of different parameters on the effectiveness of geosynthetic-encased stone columns in very soft soils.

The numerical analysis part contains two chapters:

Chapter 04: 3D Numerical Modeling of Encased Stone Columns for Soft Clay Stabilization: This chapter explores the behavior of various stone column types, such as short and floating columns, along with ordinary and geosynthetic-encased stone columns, through a 3D unit cell numerical analysis.

Chapter 05: Advanced 3D Modeling of Geosynthetic-Encased Stone Column Group Installation and Performance in Soft Clay Beneath Embankment: This chapter analyzes geosynthetic-encased stone columns in soft clay soils beneath embankments using advanced 3D modeling with Plaxis 3D software, validated.

FIRST PART: BIBLIOGRAPHIC STUDY

Chapter 1

Chapter 1

Overview of Soil Improvement Techniques Using Geosynthetic-Reinforced Stone Columns

1. Introduction

Constructing earthen structures such as dams, dikes, and road or rail embankments on soft soil presents significant challenges due to the soil's high compressibility and low shear strength, which contribute to instability. Research into the behavior of soft soils has advanced within the field of ground improvement and can be explored through experimental methods (Rashid *et al.*, 2018), numerical analysis (Ye *et al.*, 2017), and fieldwork (Sadaoui and Bahar, 2019).

Researchers proposed four major ways to improve the performance of classical stone columns in excessively soft soils:

1- **Incorporating Stabilizing Agents:** Adding materials like cement or lime to the cohesion less material of stone columns transforms them into rigid inclusions, significantly increasing their strength (Dobson & Slocombe, 1982).

2- **Internal Reinforcement with Horizontal Elements:** Various methods have been explored to reinforce stone columns internally. AlObaidy (2000) added isolated concrete discs along the column's length. Ayadat et al. (2008) conducted experiments by embedding horizontal wire meshes inside granular columns, while Sharma et al. (2004) developed a laboratory model using geogrid rings placed at specific intervals. These wire meshes were made from different materials, including plastic, steel, and aluminum. More recently, Prasad and Satyanarayana (2016) introduced circular geogrid discs to enhance stone column performance.

3- **Reinforcement with Vertical Nails:** Shivashankar et al. (2010) suggested reinforcing stone columns by driving small-diameter steel bars along the column's circumference, improving stability and load-bearing capacity.

4- **Encasement with Geosynthetics:** Using geotextiles, geogrids, or polymer sleeves to encase stone columns is another effective method. Encasement not only enhances the stiffness and strength of the columns but also prevents lateral spreading of fill materials during installation, particularly in extremely soft soils (Gniel & Bouazza, 2009). Ayadat (1990) recommended this approach for dealing with collapsible soils. The current study focuses on improving ordinary stone columns through encasement, highlighting its effectiveness in challenging soil conditions.

Geosynthetics are used to reinforce stone columns. Numerous investigations have been conducted on test specimens of geosynthetic-reinforced ballasts of varying densities and configurations. The absence of reinforcement results in a large amount of lateral distortion in the column's head, as well as an excessive amount of settlement, which leads to failure due to expansion. The implementation of the backfill on compressible soil treated by stone columns results in horizontal displacements at the slope's foot, which decreases the confinement force of the columns. As a result, the continuing growth of compressible soil treatment necessitates reinforcement, either by horizontal layers or by confinement of the columns by geosynthetics.

2. Performance of the technic

2.1. Material properties selection

2.1.1. Compressible soil

All types of soils exhibit compressibility, meaning they experience settlement when subjected to vertical loads. The degree and rate of this settlement can vary significantly based on the soil type. Generally, soils that have formed recently are less suitable for supporting structures like buildings but can be used for embankments if managed properly.

Recent soils, often a few thousand years old, frequently contain varying amounts of organic matter and are categorized into three main types: silts and soft clays, peat, and sebkha soils. The Unconfined Compression Test is employed to evaluate the compressive strength of these soils by applying a force until the soil breaks apart. This test also assesses the soil's strain under pressure (Lambe and Whitman, 1969). Table I.1 provides a classification of soils based on results from the unconfined compression test.

Table. I. 1 Classification of Soil According to the Unconfined Compression Test.

Soil Properties	Unconfined Compression Strength (kg/cm^2)
Very soft	< 0.25
Soft	$0.25 - 0.50$
Firm	$0.5 - 1$
Stiff	$1 - 2$
Very stiff	$2 - 4$
Hard	> 4

The effectiveness of stone columns is greatly affected by the surrounding soil's properties, such as its undrained shear strength, in situ lateral stress, and radial pressure deformation characteristics (Hughes *et al.,*

1975). For example, in very soft soils, granular columns might have limited load-bearing capacity due to inadequate lateral confinement. The undrained shear strength of the surrounding soil is crucial for evaluating the suitability of ground improvement methods.

In a laboratory investigation, Ayadat (1990) tackled the problem of reduced lateral support in collapsible soils by encasing stone columns with geotextile. This approach aimed to improve the performance of standard stone columns in such soils. However, its effectiveness with finer soil types remains uncertain.

2.1.2. Granular column material

To evaluate the geotechnical characteristics of granular column fill materials, laboratory tests such as direct shear and triaxial tests are routinely used. These assessments are essential for determining parameters needed for numerical and analytical evaluations. While these tests are standard in the industry, their outcomes are critical. For geosynthetic-encased columns (GEC), the fill material should ideally be clean, crushed stone, and free from any organic or harmful substances. The material should show less than 45% degradation in the Los Angeles abrasion test and have a particle size between 12 and 75 mm (Castro, 2017). Table I.2 summarizes parameters for effective Vibro-replacement techniques, based on over five decades of experience with conventional stone column methods (Greenwood, 1970; FHWA, 1983).

Table. I. 2 General recommendations for material and geometry of granular columns (FHWA, 1983).

Conditioning Factors	Recommendations
% Of soft clay going	15% to 30%
% Of soft clay going through the 200 sieves	Between 15 kPa up to 50 kPa (*)
Diameter of columns	0.6 m to 1.0 m
Spacing between columns	1.5 m to 3.0 m
Length of columns	Between 3 m up to 15 m
Grain diameter of the column material	20 mm to 75 mm
Friction angle of the granular soil	36° to 45°
Stone column Young's modulus	60 − 100 MPa (lower range for design)

(*) FHWA (1983) reports cases with S_u values as low as 7.5 kPa and column lengths up to 20 m.

2.1.3. Geosynthetic encasement

Since the 1990s, foundation systems with geotextile-encased columns have been used for soil improvement and, in particular, road embankment foundations in Germany, Sweden, and the Netherlands (Raithel et al., 2004; Raithel et al., 2005).

a. Definitions and Types of Geosynthetics

The term 'Geosynthetics' is made up of two parts: the prefix 'geo,' which refers to an end-use associated with improving the performance of civil engineering works involving earth/ground/soil, and the suffix 'synthetics,' which refers to the fact that the materials are almost entirely man-made. The materials used in the production of geosynthetics are primarily synthetic polymers derived from crude petroleum oils; however, rubber, fiberglass, and other materials are also occasionally used in the production of geosynthetics. Geosynthetics is a generic term for a wide range of polymeric-based planer products, the most common of which are geotextiles, geogrids, geonets, geomembranes, and Geocomposite the Figs.I.4-8 illustrate the different types of geosynthetics, which are used in contact with soil, rock, and/or any other civil engineering-related material as an integral part of a man-made project, structure, or system (Shukla, S. K., and Yin, J. H., 2006).

- **Geotextiles:** are permeable materials made from woven, non-woven, or knitted polymers used in geotechnical and civil engineering applications. They serve various functions in soil management, including separation, filtration, and reinforcement. Geotextiles are essential components in many engineered projects, structures, or systems.

- **Geogrids:** are a type of geosynthetic material designed to enhance soil stability. They consist of a flat polymer structure with an open, regular network of elements that resist traction. Geogrids are produced through extrusion, bonding, or interlacing processes, and feature openings large enough to accommodate and interlock with soil particles, thereby providing soil reinforcement.

- **Geocomposites:** are created by combining two or more geosynthetic materials during manufacturing. These combinations can include geotextiles with geonets, geotextiles with geogrids, geotextiles with geomembranes, geomembranes with geonets, and geotextiles with polymer nuclei or three-dimensional cell-like structures. The range of possible and useful geocomposites is extensive, allowing for various applications in geotechnical engineering, such as separation, reinforcement, and wear courses, particularly for repair purposes. Geosynthetics are predominantly made from synthetic fibers due to their cost-effectiveness and durability against soil's chemical and biological effects.
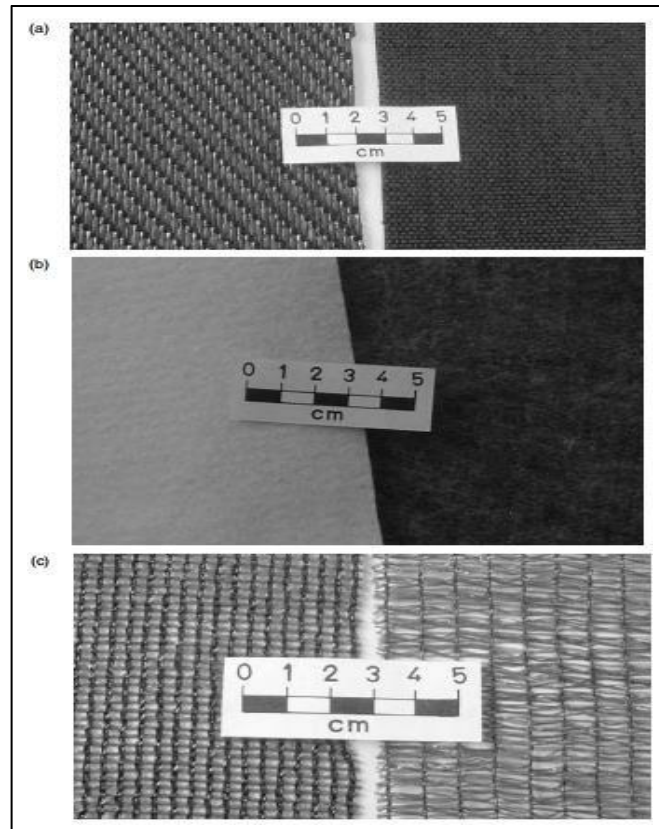
Fig.I.1 Typical geotextiles: (a) woven; (b) nonwoven; (c) knitted (S.K. and Yin, J.-H, 2006).
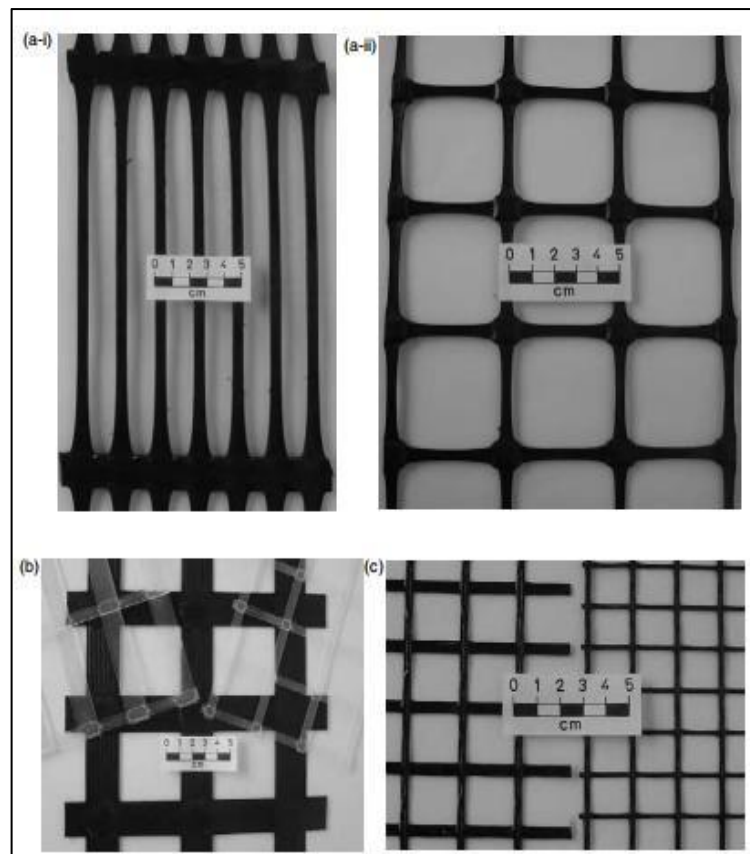
Fig. I. 2 Typical geogrids: (a) extruded- (i) uniaxial; (ii) biaxial; (b) bonded. (c) woven (S.K. and Yin, J.-H., 2006).
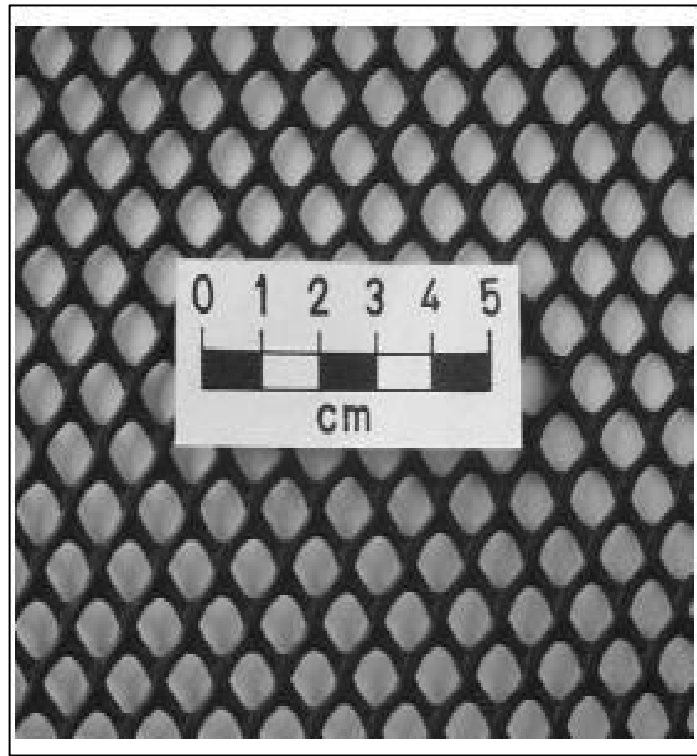
Fig. I. 3 Typical geonet (S.K. and Yin, J.-H., 2006).
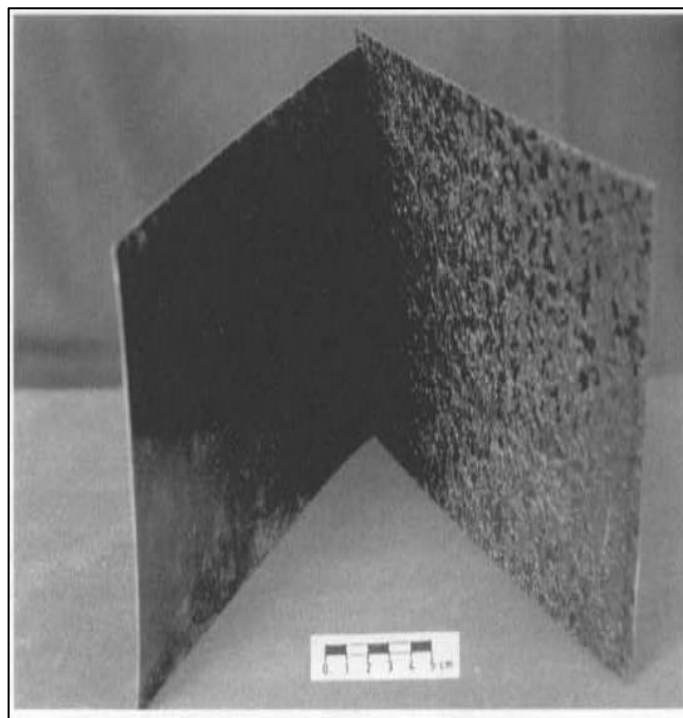
Fig. I. 4 Typical geomembranes (S.K. and Yin, J.-H., 2006).
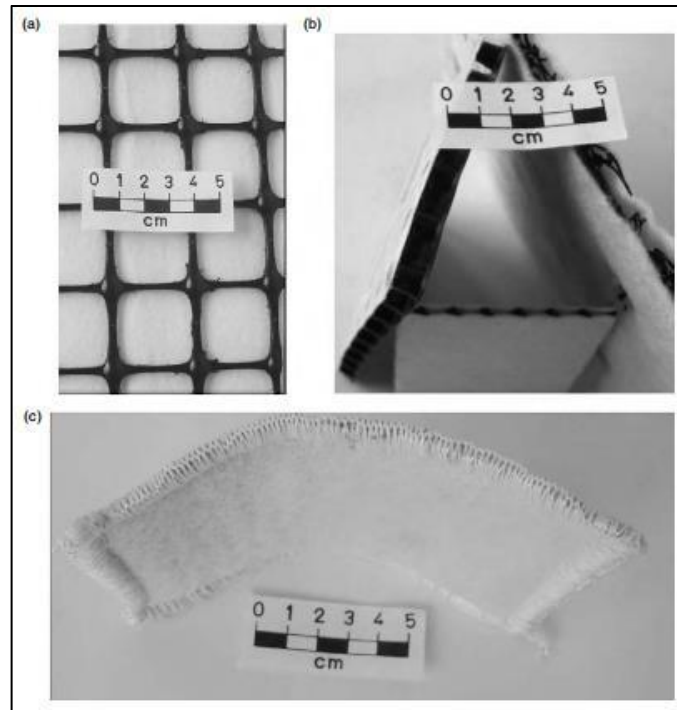
Fig.I.5 Typical Geocomposites: (a) reinforced drainage separator; (b) drainage composites; (c) geosynthetic clay line (S.K. and Yin, J.-H., 2006).

b. Functions of Geosynthetics

Geosynthetics are versatile tools in civil engineering with a broad range of uses. Initially, their primary application was in road construction, where they proved to be highly effective. In this context, geotextiles serve multiple purposes, including acting as separators, reinforcements, filters, and drainage solutions, as well as combating slope erosion. These materials typically fulfill one or more of the following key roles: Reinforcement, Separation, Filtration, Drainage, Fluid Barrier, and Protection. Table I.3 outlines the selection criteria for geosynthetics according to their specific functions.

The main role of geosynthetics is well-established, but they also often serve additional secondary functions depending on the application. It is crucial to consider both these primary and secondary functions when performing calculations and designing features. Geotextiles, for example, vary widely in tensile strength and stiffness, making them suitable for various reinforcement tasks, including soil stabilization in structures like retaining walls and encased stone columns (ESC).

Table. I. 3 Selection of geosynthetics based on their functions

Functions to be performed by the geosynthetics		Geosynthetics that can be used
Separation	Primary	GTX, GCP, GFM
	Secondary	GTX, GGR, GNT, GMB, GCP, GFM
Reinforcement	Primary	GTX, GGR, GCP
	Secondary	GTX, GCP
Filtration	Primary	GTX, GCP
	Secondary	GTX, GCP
Drainage	Primary	GTX, GNT, GCP, GPP
	Secondary	GTX, GCP, GFM
Fluid barrier	Primary	GMB, GCP
	Secondary	GCP
Protection	Primary	GTX, GCP
	Secondary	GTX, GCP

Notes:

GTX: Geotextile, GGR: Geogrid, GNT: Geonet, GMB: Geomembrane, Geofoam: GFM, Geopipe: GPP, GC: Geocomposite.

2.2. Methods of constructions

The construction of geosynthetic-encased columns (GEC_s) involves three main techniques, which differ in whether they displace the surrounding soft soil or not. Each technique offers specific advantages that cater to various site conditions, ensuring optimal performance and stability of the encased columns.

2.2.1. Replacement method

The replacement method, which involves removing soft soil within a pipe, is the first technique used for constructing encased stone columns. As illustrated in Fig.I.6, this method entails driving an open steel casing down to the bearing layer and using an auger to excavate the soil within the casing. This technique is particularly suited for soils with relatively high penetration resistance or in situations where minimizing the vibration impact on nearby structures and roads is crucial. The replacement method offers precision in installation and is ideal for urban environments where disturbances must be minimized.

| Casing pushed into the soft soil resting on rigid layer. | Helical auger is used to remove the soft clay inside the casing. | Geogrid sleeve is then placed inside the empty casing. | Geogrid sleeve is filled with stone aggregate using funnel. | Casing is raised around the encased granular column. | Geogrid encased granular column is completed. |
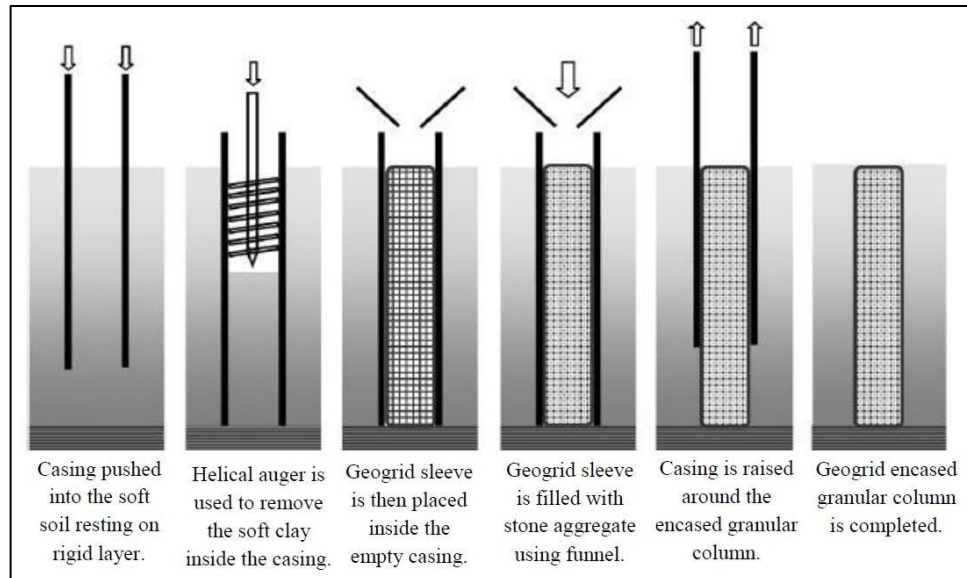
Fig.I.6 Phases of the Replacement Technique for Encased Column Installation (Gniel and Bouazza, 2010).

2.2.2. Displacement method

The process involves inserting a steel pipe with a sealed end into soft soil, followed by the installation of a circular geotextile within the pipe. This geotextile is then filled with sand or crushed stone aggregate. A visual representation of this technique for installing encased stone columns can be seen in Fig. I.7. Columns created using this method generally have a diameter of about 0.80 meters, with the geotextile's diameter ideally matching the inner diameter of the pipe to ensure proper fit and support (Alexiew *et al*., 2005). These columns are spaced between 1.5 and 2.5 meters apart, facilitating effective load distribution and soil stabilization. The geotextile employed in this approach has a tensile stiffness modulus (J) ranging from 1500 kN/m to 4000 kN/m, which contributes to its strength and durability (Kempfert *et al*., 2002). This technique is highly effective for improving the mechanical properties of soft soils, making it suitable for projects requiring strong foundation support.
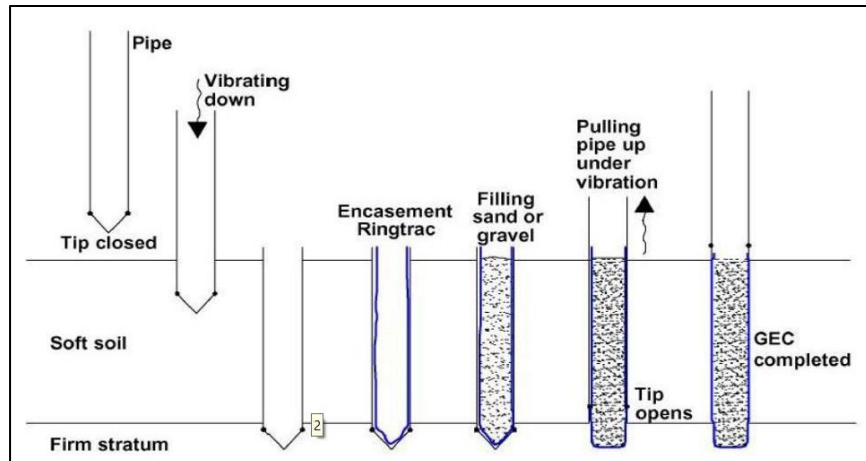
Fig.I.7 Displacement Technique for Geosynthetic-Encased Column Installation (Alexiew et al. 2005).

2.2.3.   Partially encased stone columns

Lee *et al.* (2008) developed a novel method for constructing partially encased stone columns that enhances their performance. This technique involves using a polyester geogrid tailored to the column's diameter (0.8 m) and extending 2 to 3 times the diameter in length. The construction process, illustrated in Fig. I.8, begins with drilling using an auger, followed by casing installation and soil removal. Stones, each 25 mm in diameter, are layered and compacted within the casing to form the column up to the required height for geogrid insertion. The geogrid is then placed within the column, which extends to a depth of 5.5 meters below the surface (Lee *et al.,* 2008). This approach combines the load-bearing stability of stone columns with the additional confinement and strength provided by the geogrid, improving the load capacity and reducing settlement in difficult soil conditions.
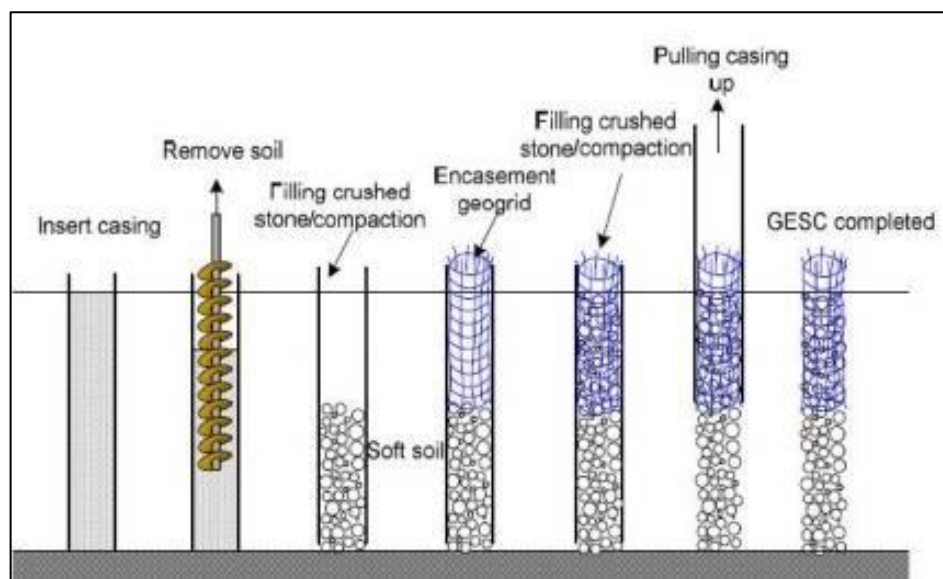
Fig.I.8 Field installation of a partially encased stone column (Lee et al., 2008).

3. Failure Systems

3.1. Isolated column

Barksdale & Bachus (1983) identified three primary failure modes for single stone columns, each illustrated in Fig. I.9 (a, b, c):

- **Bulging Failure:** This occurs when the lateral resistance of the column is insufficient compared to the axial load, leading to ductile deformation. Bulging is more prominent in slender columns, particularly those located near the edge of the footing.

- **Shear Failure:** It happens when the column experiences a high stress ratio and low confinement, resulting in shear failure along the column.

- **Punching Failure (Sinking):** Common in shorter columns, this failure mode is characterized by inadequate skin friction along the column's length and excessive stress at the column's base.

- **Bulging in Deeper Layers:** This type of failure can happen at depths greater than four column diameters when soft soil layers, thicker than two column diameters, allow for the development of bulging, as depicted in Fig. I.9 (d) (Kirsch et al., 2016).
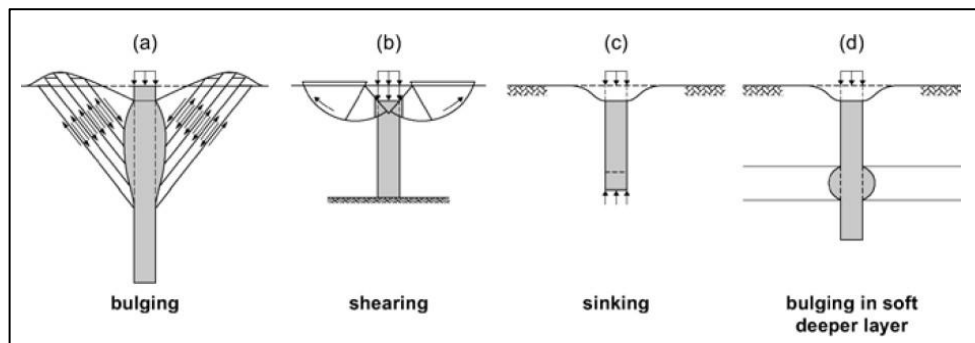
Fig. I. 9 Failure mechanisms of isolated stone columns (Kirsch et al., 2016)

3.1.1. Lateral expansion failure

Three cavity expansion theories, which were originally developed to explain pressuremeter testing, are now used to explain stone column failure. The theory developed by Gibson and Anderson (1961) for a purely coherent soil in undrained condition takes into account the lateral expansion of an infinitely long cylindrical cavity. The theory of Vesic (1972) evolved from the theory of Gibson and Anderson (1961), but was expanded to include cohesive and powdery soils. The theory of Hughes and Withers (1974) is then applied, allowing the lateral expansion of a cylindrical cavity from the center of the column to be modeled using a representative unit cell. All of the relationships require the same fundamental principle of using the passive coefficient of the ballast, which is characterized by the lateral grip of the ground on the column. The most used relation for

the calculation of the ultimate stress by lateral expansion (P$_u$) of an isolated ballasted column has been developed by Greenwood (1970):

$$P_u = tan^2 \left(\frac{\pi}{4} + \frac{\varphi'_c}{2}\right) \times \sigma'_{rup} = K_{pcol} \times \sigma'_{rup}$$

Eq. I. 1

With:

φ'_c: Angle of internal friction of the material constituting the column;

σ'_{rup}: Maximum horizontal stress of the ground.

In the case of the pressuremeter, the limiting soil pressure (P$_l$) and the following relation (Eq.I.2) connects the pore pressure (U) to the maximum horizontal stress:

$$\sigma'_{rup} = pl - u$$

Eq. I. 2

As Datye (1982) demonstrated, failure by lateral expansion in homogeneous soil can occur to a depth of three to four times the diameter of the column, thus the maximum horizontal soil stress should be determined at this depth.

3.1.2. Generalized shear failure

Brauns (1978, 1980) equates the axisymmetric fracture of a volume of composite material ballast-ground, limited by a frustoconical surface centered on the axis of the column placed on a substratum (Fig. I. 10). Relations (Eq.I.3) and (Eq.I.4) define the breaking depth h as well as the limiting vertical stress at the head column:

$$h = 2. R_{col} \times tan\left(\frac{\pi}{4} + \frac{\varphi'_{col}}{2}\right)$$

Eq. I. 3

$$' = \left[(\_) + \left(\frac{2C_u}{}\right)\right] \times \left[1 + \frac{\left(\frac{\pi}{4} + \frac{\varphi'_{col}}{2}\right)}{}\right] \times K_{pcol}$$

Eq. I. 4

With:

σ'_{rup}: The radial confining stress provided by the surrounding soil.

C_u: Undrained cohesion of the soil;

q: overload applied to the ground surface;

δ: Angle made by the generator of the cone with the horizontal, determined by the abacus (Fig.I.10).

19

R_{col}: radius of the column*;*
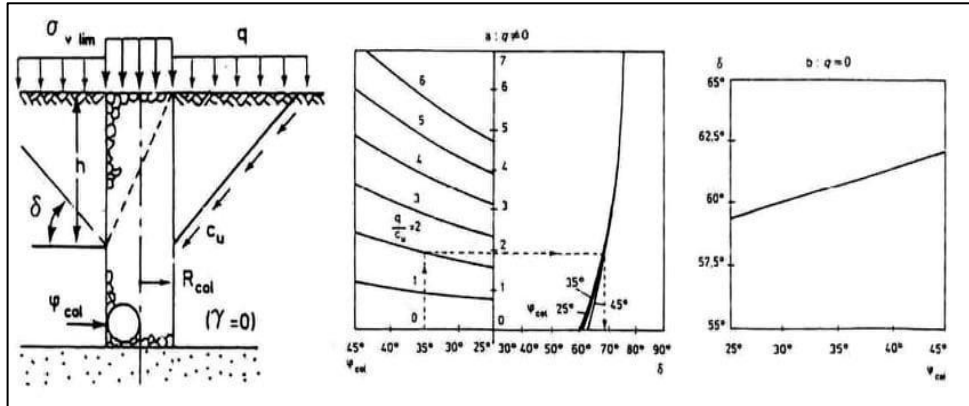
Fig.I.10 Generalized shear failure surface (left) and abacus for determining the angle (straight) (Brauns, 1978).

3.1.3. Punching rupture of a floating column

The limiting load associated with the rupture by punching of a floating column has been defined by Hughes et al. (1975) (Fig.I.11). The column is assumed work as a rigid pile with development of peak force and lateral friction positive. They determined, empirically, a minimum length L_{lim} (Eq.I.6) so that the punching is avoided and a maximum length L_{max} (Eq.I.5) beyond which the treatment is useless:

$$= 0.5 \times R_{col} \; (\tfrac{\sigma_{v,0}}{} - 9) \qquad\qquad Eq.\ I.\ 5$$

$$= 0.5 \times R \quad (\tfrac{-,0}{}) \qquad\qquad Eq.\ I.\ 6$$

With*:*

R_{col}: Radius of the column*;*

$\sigma_{v,0}$: applied vertical stress*;*

Moreover, if the density γ of the column is known, the vertical stress ($\sigma_{v,z}$) at the depth, z can be calculated according to the relation (Eq.I.7) :

$$_, = _{,0} + z[\gamma - \tfrac{2C_u}{}] \qquad\qquad Eq.\ I.\ 7$$
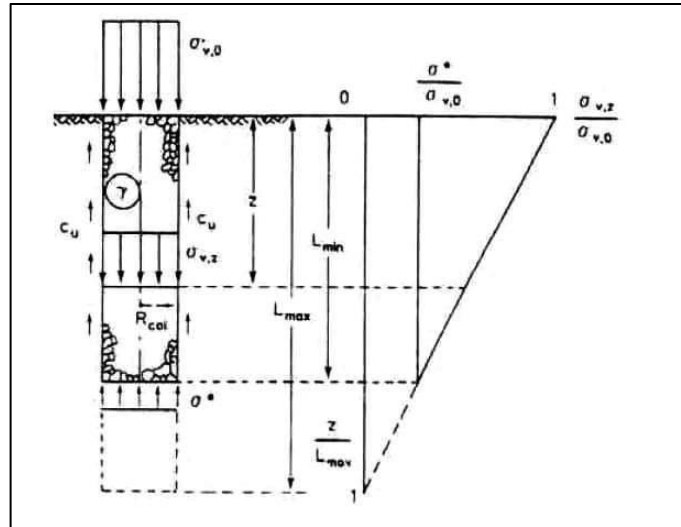
Fig.I.11 Minimum and maximum lengths of a floating column (Brauns, 1980).

3.1.4. Tests on reduced models

- **Cambridge University works**

Hughes and Withers conducted a series of model tests in 1974 in which insulated stone columns with diameters ranging from 1.25 to 3.8 cm were installed in a fixed length of 1.5 cm. These columns were installed in a Cambridge compressible soil sample. Only the head of the stone column (column surface) received evenly distributed loading, and column and soil settlements were measured at several points throughout the column.
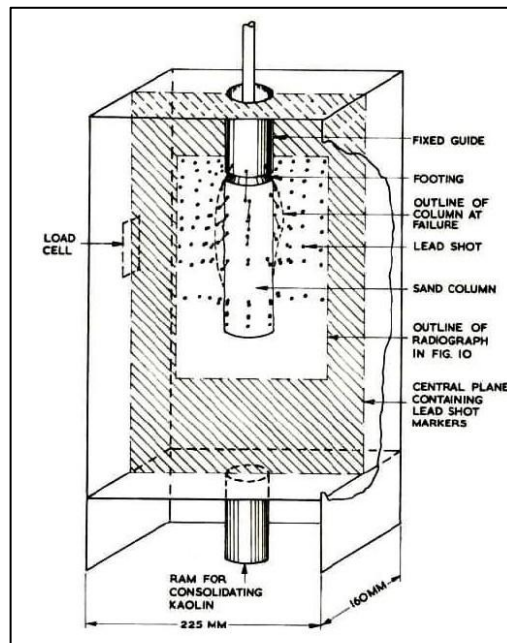
Fig. I. 12 consolidomerter for testing single column (Hughes et Withers, 1974).

A lateral expansion was observed at the head of the stone column under a load evenly distributed on the surface. Beyond four times the diameter of the column, the observed expansion becomes negligible (Fig.I.12). The ultimate strength of stone columns is determined by the lateral embrace provided by the column soil surrounding it in the area of lateral expansion. According to the authors, the behavior of stone columns is similar to that of the pressure-meter probe.
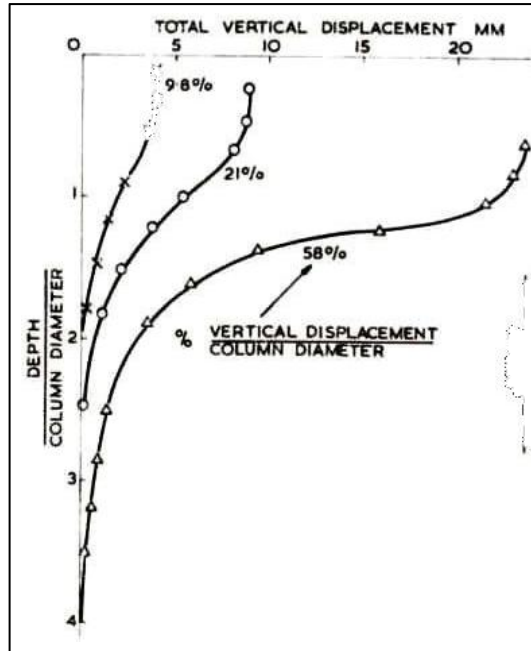
Fig.I.13 Radial displacement at the edge of the column / initial column radius against depth (Hughes et Withers, 1974).
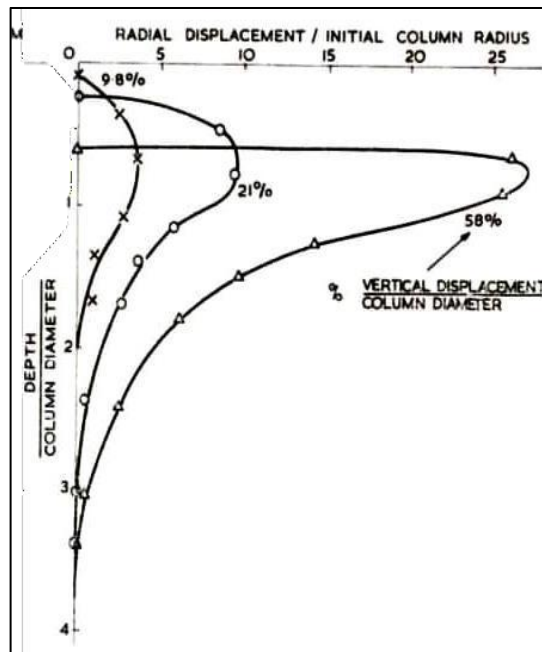
Fig. I. 14 Vertical displacement of the column against depth (Hughes et Withers, 1974).

Hughes and Withers used the cylindrical cavity expansion theory developed in 1961 by Gibson and Anderson to determine the bearing capacity of an isolated ballasted column. For the sake of simplicity, the authors assume that shear stress equals the undrained cohesion of the soil in place along the column walls. Hughes and Withers developed a simple method to determine the distribution of vertical stresses acting throughout the isolated column based on this assumption (Figs.I.13 and I.14). Furthermore, the authors propose a critical length beyond which the columns experienced simultaneous punching and lateral expansion. This critical length is four times the isolated column's initial diameter (diameter before loading the column). This work represents the first understanding of the modes of behavior of isolated stone columns and served as the foundation for several subsequent studies. These studies are still relevant today, especially in terms of practical application.

- **Work of Shivashankar et al. 2011**

Shivashankar et al. (2011) investigated the behavior of a ballasted column installed in a laminate floor, the top layer of which is made of soft clay with low mechanical properties, using a scale model based on the unit cell principle. Because of the symmetry of the uniformly distributed surface load and the geometry, lateral deformations cannot occur at the unit cell's edges, according to Barksdale and Bachus 1983. Shear stresses on the unit cell's boundaries are zero.

In their test on a scale model, Shivashankar et al. (2011) used this concept of the composite cell to predict the behavior of a stone column installed in a large group of columns. The experimental layout of the scale model used in this series of tests is depicted in Fig.I.15 below. Two geometric configurations were used:

(a) A total loading uniformly distributed on the surface of the unit cell.

(b) A loading at the top of the column with a reinforcement degree of 100 %.
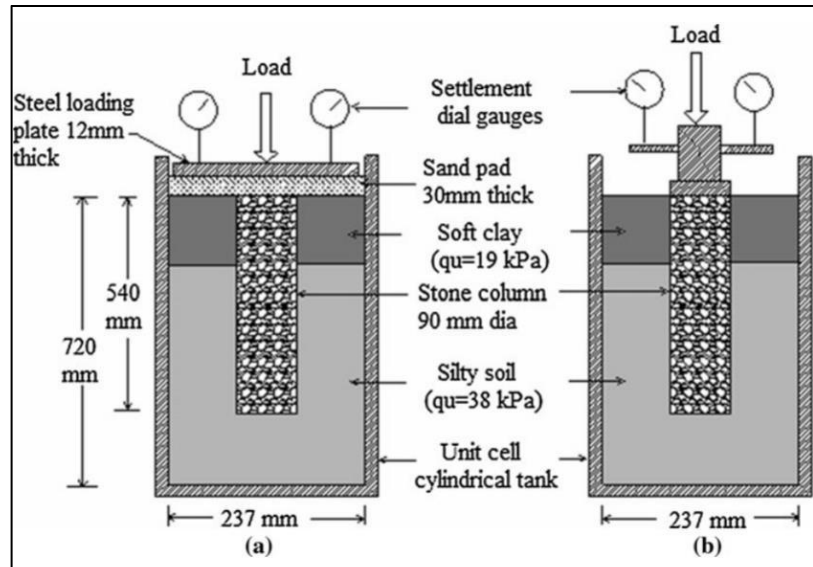
Fig. I. 15 Loading test on a scale model of a stone column: (a) Loading of the unit cell; (b) loading at the head of the column (Shivashankar et al. 2011).

The authors demonstrated that the reduction in settlement caused by the installation of stone columns in laminate flooring, the top layer of which has poor mechanical properties, is not significant (in the order of 20 to 30 percent). This is due to the ballasted column's excessive expansion in the upper layers because of the surrounding soft soil's poor lateral grip. The maximum lateral expansion was observed in the case of homogeneous soil layers to a depth of once the diameter of the column from the top of the column. In addition, the total length of the ballasted column subjected to lateral expansion was 2-3 times the column's diameter. In the case of a ballasted column installed in laminate floors, lateral expansion was observed primarily in the upper layer, which had poor mechanical properties.

3.1.5. Full-scale loading tests

- **Travaux de Hughes, Withers et Greenwood 1975**

Hughes et al. 1975 tested an overhead load on a full-scale ballasted column. The test involves monitoring the vertical displacement of the column's head with tachometers or gauges. The loaded column has a total length of 10m and a final diameter of 73 cm. Fig.I.16 shows the experimental plan established at the Canvey Island site in the United Kingdom.
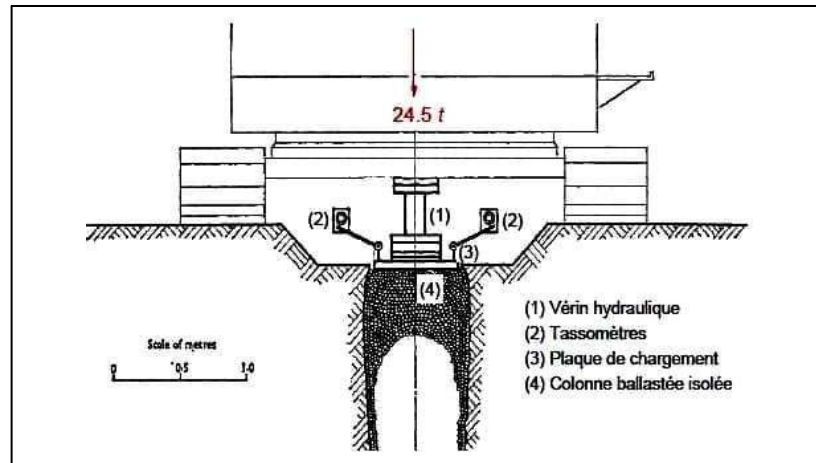
Fig.I.16 Loading test at the head of an insulated stone (Hughes et Withers, 1974).

The goal of this series of prototype tests was to validate the results obtained on laboratory scale models by Hughes and Withers, 1974. The findings of this study confirm the scale model's experience, in which a significant improvement in load-bearing capacity was obtained in the surface layer following the installation of stone columns well compacted in soft clay.

- **Work of Corneille 2007**

Corneille (2007) conducted a series of full-scale loading tests to investigate the failure modes of stone columns. The work was done to investigate the behavior of an isolated ballasted column loaded by a square footing measuring 1.2x1.2x0.5 m. Another footing with the same geometric characteristics resting on natural soil was loaded to compare failure modes between the two cases and to quantify and qualify the improvements made while installing the stone columns in a soil with poor mechanical properties. Fig.I.17 depicts the setup for the full-scale loading test, which was performed on an insulated stone column 8.7 m long and 80 cm in diameter.
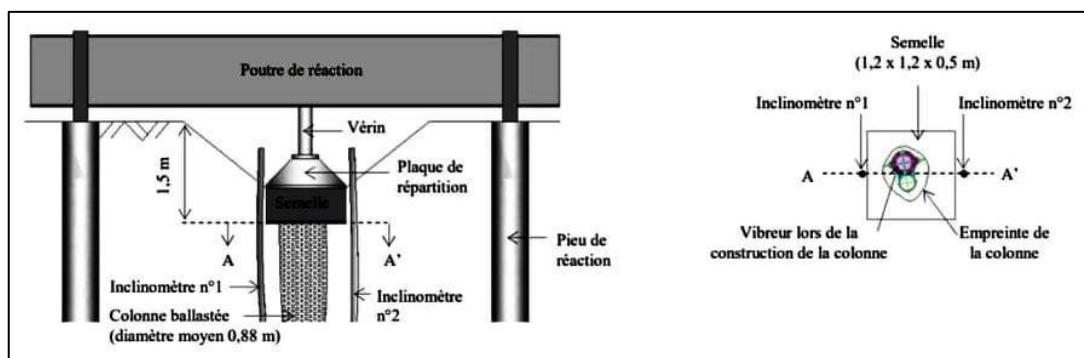
Fig. I. 17 Schematic section of the sole loading test on the stone column (Sébastien Corneille, 2007).

The measured settlement of the sole resting on reinforced soil is 17.3 mm, which is a settlement reduction factor of 5.5 times obtained following the installation of the ballasted column.

3.2. Column group

Column groups exhibit essentially similar failure mechanisms, which are made more complex by the interaction of load application, soil, and columns, as well as their geometrical parameters. Fig.I.18 illustrates the failure mechanisms that can occur in column groups with rigid concrete foundations.
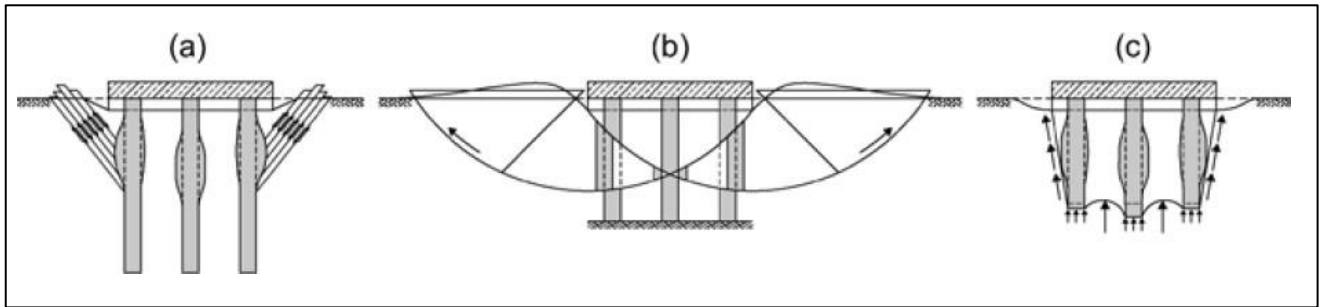
Fig.I.18 Failure mechanisms for column groups (Kirsch *et al.,* 2016).

3.2.1. Tests on reduced models

- **Works of the University of Belfast, United Kingdom**

Mc Kelvey et al. (2004) studied the behavior of small groups of sand piles loaded by isolated, stringy, and circular foundations in a series of laboratory tests in 2004. The flexible columns were suspended in lengths ranging from 6 to 10 times their diameter. Lateral deformations were observed following the loading applied to the surface. The columns at the edges deform by lateral buckling, and a slight lateral expansion of the central columns was observed, most likely due to the confinement imposed by the edge columns (Fig.I.19).
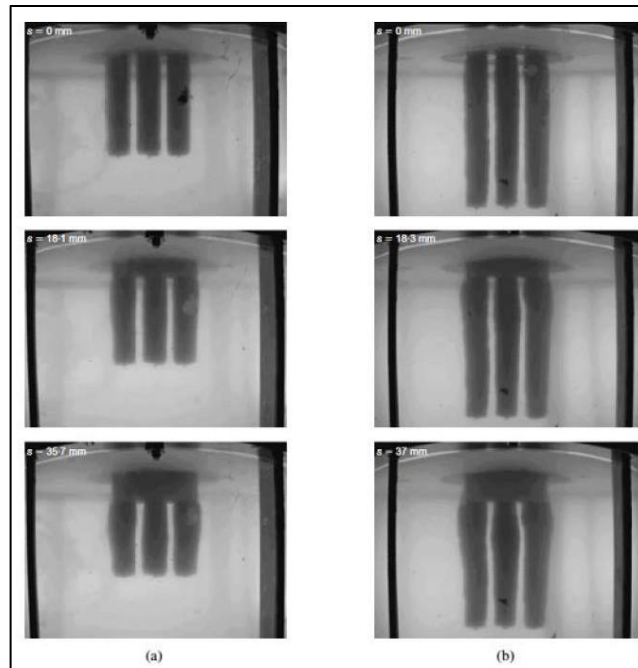
Fig. I. 19 Lateral deformations of sand piles following loading by a circular foundation at the start, middle and end of the loading process: a) L / D = 6; b) L / D = 10 (Mc Kelvey *et al.,* 2004).

The photographs prove that lateral expansion occurs along the entire length of the short columns (L = 6D). While only at the top of the longer columns (L = 10D) will it be more significant. The authors recommend a critical length that is six times the diameter of stone columns. Beyond that point, there will be no increase in bearing capacity. Furthermore, any length higher than this optimum length is more likely to be significant in terms of settlement.

- **Work of the Technological Institute of India**

In 2007, Ambily and Ghandi invested in a series of laboratory tests on the behavior of stone columns installed in reconstituted soft clay (kaolinite). The tests were performed in cylindrical tanks while examining the influence of the cohesion of the soil in place, the internal friction angle of the ballast, and the spacing between the columns on the overall behavior of the stone columns (Fig.I.20).
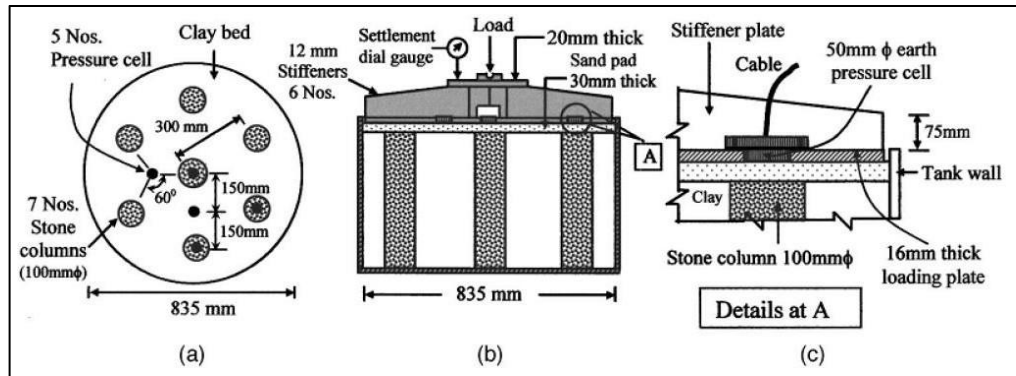
Fig.I.20 Loading tests on a scale model of stone columns: a) plan view; b) cross-section; c) details of the pressure cell (Ambily et Ghandi, 2007).

The authors indicate that the load-bearing capacity decreases while increasing the spacing between the columns. From a spacing equal to three times the diameter of the columns, the change will become negligible. Loading the stone column only, lateral expansion was noticed to a depth of 0.5 column diameter. When the entire surface of the floor-column assembly is loaded, no lateral deformation occurs (Fig.I.21).
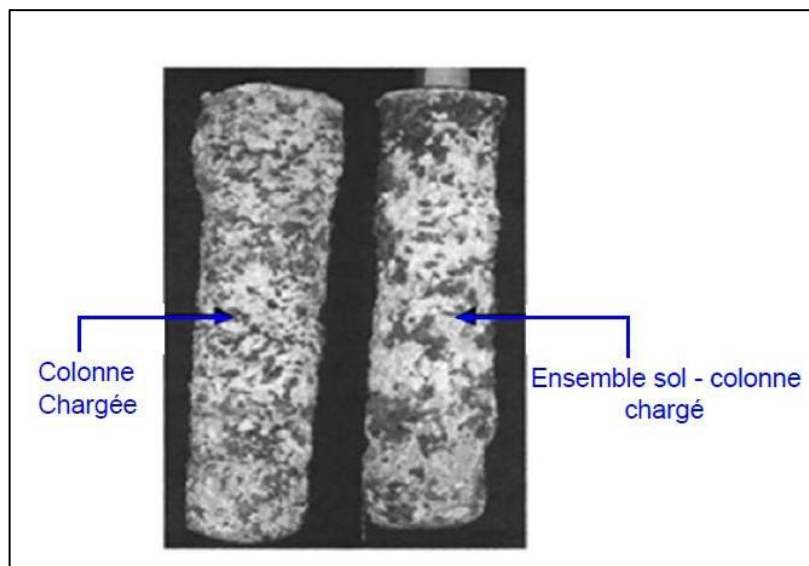
Fig. I. 21 Lateral deformation observed following loading of the columns (Ambily and Ghandi, 2007).

3.2.2. Full-scale loading tests

Han and Ye (1991) presented the findings of full-scale load tests on stone columns reinforced with soft soil in coastal areas. Sixteen stone columns with a length of 14 m and an average diameter of 0.85 m were used in soft soil and arranged in a triangular pattern. Loading was done on both the treated ground with stone columns and the untreated ground. The stone columns were discovered to increase the bearing capacity to twice that of untreated ground.

4. Factors Affecting the Behavior of a Group of Stone Columns

4.1. Spacing

Stone columns should be strategically spaced to ensure that the bearing capacity of the group equals or surpasses the total bearing capacity of the individual columns. The center-to-center distance between two stone columns (S) is typically used as the measurement standard (as depicted in Fig. I.22). It is advisable for this spacing (S) to be at least 2.5 times the diameter of the columns (Al-Mosawe *et al.*, 1985). Moreover, Hughes and Withers (1974) observed that the applied load affects the surrounding clay only within a radius of 2.5 times the stone column's diameter. This spacing configuration optimizes load-bearing efficiency and minimizes settlement, enhancing soil stability and bearing capacity for construction projects on challenging soil types. By adhering to these guidelines, the effectiveness of stone columns in reinforcing soft soils is maximized, ensuring more reliable and durable ground improvement solutions.

4.2. Loading Area

Stone columns used in both small and large group configurations, depending on the size of the area needing reinforcement. For smaller, loaded areas like pads or strip footings, small groups of stone columns are typically used. In contrast, large groups of stone columns are deployed to support extensive loaded areas such as embankments. In smaller groups, the outer columns have a reduced bearing capacity and play a more critical role in supporting the load. Additionally, the vertical stress beneath smaller loaded areas decreases more rapidly with depth compared to the stress beneath larger foundations (Killeen & McCabe, 2014). This distinction highlights the importance of carefully planning the configuration and size of stone column groups to maximize their effectiveness in different applications. Properly designed, stone columns can significantly enhance the load-bearing capacity and stability of foundations in both small-scale and large-scale projects.

5. Unit Cell Concept

Stone columns are employed in various configurations depending on the scale of the loads they need to support. For localized loads such as those from pads or strip footings, stone columns are grouped in smaller numbers. In contrast, larger groups of stone columns are used for more extensive loads, such as those from embankments. Within smaller groups, the outer columns, which typically have lower bearing capacities, are particularly crucial. Additionally, the rate at which vertical stress diminishes with depth is much greater beneath smaller loaded areas compared to larger foundations (Killeen & McCabe, 2014). To model the behavior of an individual stone column within a group, an equivalent diameter (d_e) is used, which represents the combined effect of the column and the surrounding soil under uniform loading conditions. According to Balaam and Poulos (1983), this equivalent diameter is related to the spacing (S) between the columns. Laboratory experiments often use a unit cell approach to simulate this setup, which can be depicted as a

cylindrical chamber with a frictionless, rigid outer wall symmetrically placed around the stone column, as shown in Fig. I.23. This modeling technique facilitates a thorough examination of stone column performance and its interaction with the surrounding soil, offering valuable insights for optimizing design and performance across various loading scenarios and soil conditions.
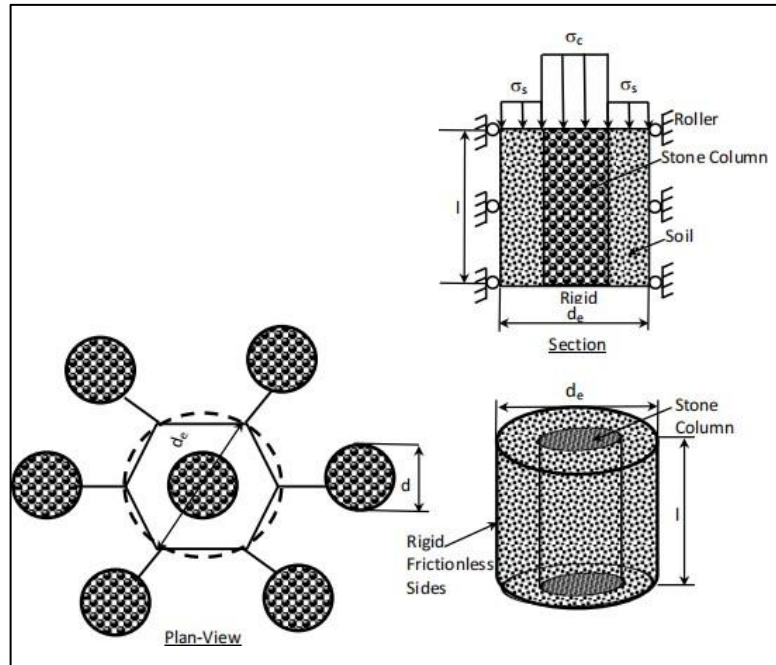
Fig. I. 22 Unit cell idealizations (redrawn from Barksdale and Bachus, 1983).

Where:

d_c: diameter of stone column.

l: length of stone column.

σ_s: Stress acting on soil.

σ_c: Stress acting on the column.

It is very effective for the composite ground with stone columns in reducing the initial excess pore water pressure and keeping the foundation stable. The unit cell's exterior boundary is known as the column (Fig.I.23).

- **Area Replacement Ratio**: The volume of soil replaced by stone columns has an important effect on the performance of the improved ground. To quantify the amount of soil replacement, define the area replacement Ratio, a_s, as the fraction of soil tributary to the stone column replaced by the stone This factor is therefore always less than unity and is written according to the relation:

$$ = \ ^- < 1 \hspace{4cm} Eq.\ I.\ 8$$

Where A_s, is the area of the stone column after compaction and A is the total area within the unit cell (Fig.I.23). Further, the ratio of the area of the soil remaining, A_c to the total area is then it is always greater than unity:

$$= \frac{A_c}{} = 1 - a \ > 1 \qquad\qquad Eq.\ I.\ 9$$

The area replacement ratio,   , can be expressed in terms of the diameter and spacing of the stone columns as follows:

$$= \ _1 \left(\ ^- \right)^2 \qquad\qquad Eq.\ I.$$

10

Where:

S= center-to-center spacing of the stone columns.

C_1 = a constant dependent upon the pattern of stone columns used; for a square pattern C_1 tern $C_1 = \frac{\pi}{4}$ and for an equilateral triangular pattern $C_1 = \frac{\pi}{2\sqrt{3}}$.

For an equilateral triangular pattern of stone columns, the area replacement ratio is then:

$$= 0.907 \left(\ ^- \right)^2 \qquad\qquad Eq.\ I.\ 11$$

These two factors therefore, make it possible to determine the percentage of material incorporated in relation to the natural soil and the resulting improvement (case of an infinite grid of columns) but when the columns are placed under limited surfaces (footings) it is a bit tricky. However, these ratios are also used in the case of footings by considering, no longer the total area of the mesh, but the total area of the foundation.

The soil substitution factor   varies according to the initial soil conditions (before improvement) and according to the improvement objective (reduction in settlements, increase in bearing capacity, reduction in the risks of liquefaction, etc.), this factor varies from 0.05 to 0.5 for uniform loads under an infinite network of columns and from 0.16 to 0.5 for loads on footings (Greenwood, 1991) and (Dhouib et al., 2004, 1998).

6. calculation of the ultimate bearing capacity of an isolated ballasted column

6.1. Theories of the radial expansion of a cylindrical cavity

Gibson and Anderson (1961), Vesic (1972), and Hughes and Withers (1973) developed the three theories presented below(1974) . Gibson and Anderson investigate the radial expansion of an infinitely long cylindrical cavity in an undrained purely coherent medium with elastoplastic behavior.

They calculate the total applied pressure P for a given radius of the cavity using the relation (Eq.I.12):

$$ = {}_0 + \quad (1 + \quad (\quad (1 - \frac{a^2}{}_0))) \qquad\qquad Eq.\ I.\ 12 $$

With:

P_0: Cavity reference pressure;

I_R: Soil stiffness index u G /C_u.

G: ground shear modulus.

C_u: Undrained cohesion of the soil.

a: cavity radius.

a_0: Initial radius of the cavity.

Vesic (1972) developed a general solution to characterize the expansion of an infinitely long cavity cylindrical in coherent soils (as Gibson and Anderson (1961)) and powdery soils. The soil has either an elastic or rigid-plastic constitutive law. The constraint ultimate lateral confinement 3 created by the surrounding soil is expressed as follows (Eq.I.13):

$$ \sigma_3 = (c \times F'_c \times q_m \times F'_q) \qquad\qquad Eq.\ I.\ 13 $$

With:

C: soil cohesion.

q : mean stress $\frac{(\sigma_1 + \sigma_2 + \sigma_3)}{3}$ at the depth of the fracture.

F'_c and F'_q: expansion factors of the cavity.

The expansion factors of the cylindrical cavity, F'_c and F'_q (Fig.I.24), are a function of the angle of friction of the ground as well as the stiffness index noted Ir. The relation (Eq.I.14) gives the latter:

$$ = \frac{}{2(1+u_s)(c+q tan\varphi'_c)} \qquad\qquad Eq.\ I.\ 14 $$

E_s: Young's modulus of the soil.

υ_s: Poisson's ratio of the soil.

q: average stress in the failure zone.

The ultimate vertical stress applied to the column becomes (relation (Eq.I.15)):

$$ {}_{ult} = (c \times F'_c \times q \times F'_q)(\frac{1+sin\varphi_{sc}}{1-sin\varphi_{sc}}) \qquad\qquad Eq.\ I.\ 15 $$
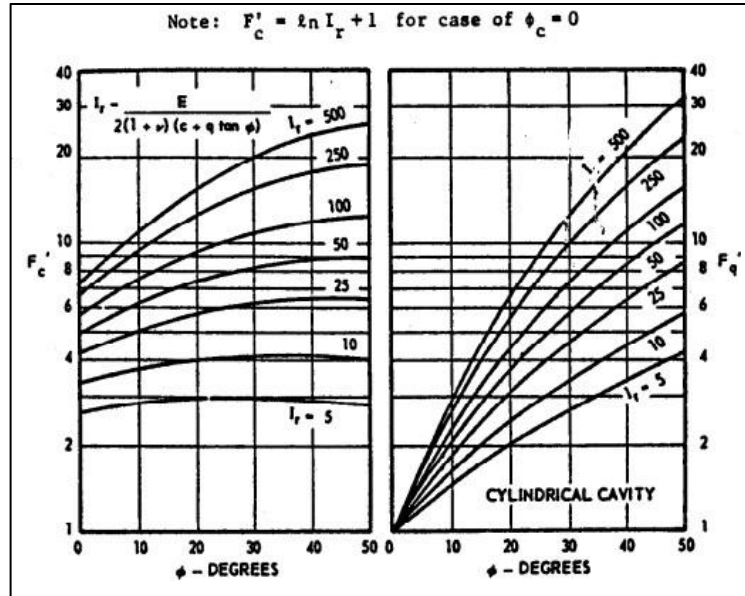
Fig.I.23 Expansion factors, F'$_c$ and F'$_q$, of a cylindrical cavity (Vesic, 1972).

Hughes and Withers (1974) assume that the passive resistance developed by the surrounding soil can be modeled by the infinitely long expansion of a cylinder from its axis of revolution until the ultimate passive resistance of the soil is reached. The lateral expansion of the column in the surrounding soil is simulated by the expansion of this cylindrical cavity. They assume elsewhere Eq. I. 16 that failure due to lateral expansion of a single ballasted column is similar to the formation of a cavity during a pressuremeter test. In their approach, Gibson and Anderson's (1961) theory for a coherent material and an infinitely long cylindrical expanding cavity was used to predict the ultimate lateral stress undrained, of the soil surrounding the column, which is expressed as Relation (Eq.I.16):

$$\sigma_3 = \sigma_0 + \quad(1 + \quad(\frac{\qquad}{2\ (1+\ )})) \qquad\qquad\qquad Eq.\ I.\ 17$$

σ_3: Ultimate undrained horizontal stress of the soil;

σ_0: Total horizontal stress of the soil (in the initial state);

The relation (Eq.I.17) is obtained:

$$= (\sigma_0 + \quad(1+ \quad(\frac{\qquad}{2\ (1+\ )})))(\frac{1\pm\ _\ \ _}{1-sin\varphi_{sc}}) \qquad\qquad Eq.\ I.\ 18$$

A general bearing capacity failure could occur at the surface, where the overburden surcharge effect is the smallest. Madhav and Vitkar (1978), presented a plane strain solution for a general bearing capacity failure of a trench filled with granular material built in a frictionless manner. The solution relies on Drucker and Prager's upper bound 11mit analysis theorem.

33

6.2. The ultimate bearing capacity of an isolated ballasted column according to (D.T.U) 13.2

The D.T.U (Unified Technical Document) 13.2, relating to deep foundations, is still in effect. However, there is also a need to put in place common recommendations for the profession (Dhouib and Blondeau, 2005). Also, this part recalls in a synthetic way this regulation.

The SLS design stress on a theoretical section of a ballasted column must be less than twice the lateral footprint of the surrounding soil but greater than 0.8 MPa. By analogy with the triaxial test, the vertical stress at failure of the column is:

$$q_c = \sigma_h tan^2 \left(\frac{}{4} + \frac{\varphi_c}{2}\right)$$
Eq. I. 19

The admissible stress is calculated from q_c with a safety factor greater than 2 (D.T.U 13.2).

$$= \frac{-}{2}$$
Eq. I. 20

The geotechnical report determines the value of the lateral embraceσ_h. It is determined using laboratory tests or in-place tests such as a pressuremeter, static penetrometer. In the case of the pressuremeter, we can convert the lateral grip p to the limit pressure value.

6.3. Graphical determination of the bearing capacity of an isolated column

Thornburn (1975) developed an abacus (Fig.I.25) to calculate the load-bearing capacity of a column isolated by undrained soil cohesion. The abacus can also be used to group columns together. This abacus, however, is based on knowledge of the diameter of real columns made by vibrators at the time, Cementation or Keller companies. As a result, the practical application of this abacus is limited to these vibrators alone.
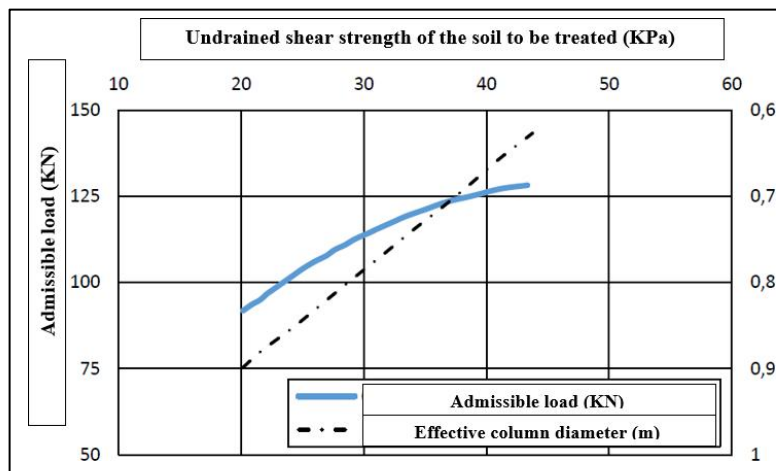
Fig. I. 24 Prediction of the admissible head load and the influencing diameter of an insulated stone column as a function of the undrained shear strength of the soil (Thorburn, 1975).

7. Conclusion

In conclusion, this chapter has provided a comprehensive overview of the techniques used for reinforcing soft soil, underpinned by an examination of notable studies in the field. The performance of these techniques has been summarized, elucidating the characteristics of compressible soil, granular properties pertinent to stone columns, and the role of geosynthetics in enhancing soil stability. Furthermore, we have discussed the three primary execution methods, namely replacement, displacement, and partially encased stone column techniques, along with their respective applications. This exploration has facilitated a deeper understanding of failure mechanisms, as well as insights derived from full-scale load tests and reduced model experiments. Moreover, the factors influencing the behavior of stone column groups, including the unit cell concept and methodologies for calculating ultimate bearing capacity, have been elucidated. Notably, theoretical frameworks such as the radial expansion of a cylindrical cavity and (D.T.U) 13.2 have been employed to assess the performance of isolated ballasted columns. Looking ahead, the subsequent chapter will delve into a bibliographic summary focused on enhancing bearing capacity and reducing settlement in surface.

Chapter 2

Chapter 2

Calculation Approaches for Encased Stone Column Ground Improvement

1. Introduction

Ensuring the structural stability of columns within soil is essential to prevent failure, especially against lateral deformation and settlement. Insufficient reinforcement can lead to severe lateral displacement at the column top and excessive settlement, which may result in structural failure. To address these issues, a new reinforcement method using geosynthetic-encased stone columns has proven to be more effective than conventional stone columns, particularly in very soft soils. Research has examined the performance of geosynthetic-reinforced ballasts with varying densities and configurations, highlighting the advantages of this advanced technique. Additionally, a range of numerical studies utilizing sophisticated stress-strain coupled models have been conducted to simulate the interaction between soft soil and geosynthetic materials. These studies offer valuable insights into the behavior of encased stone columns and support parametric analyses to understand the impact of various factors, many of which have been experimentally validated. This chapter provides an extensive review of the literature on the use of encased stone columns for soil improvement in road embankment and foundation construction. It also explores current calculation methods and offers an in-depth understanding of the mechanisms and benefits of this innovative reinforcement strategy.

2. The existing calculation approaches

2.1 Analytical calculation

In the case of stone columns used in very soft soils, the encased stone column technique has been developed in recent years (ESC). Several analytical methods have recently been developed for the design of this improvement technique, which will be discussed in this section.

2.1.1. Raithel & Kempfert (2000) method

The analytical model proposed by Raithel (1999) and further developed by Raithel and Kempfert (2000) utilizes the unit cell concept to tackle the issue under conditions of axial symmetry, depicted in Figure II.1. This model focuses on a single encased column and its adjacent soil, facilitating the analysis of vertical stress equilibrium.
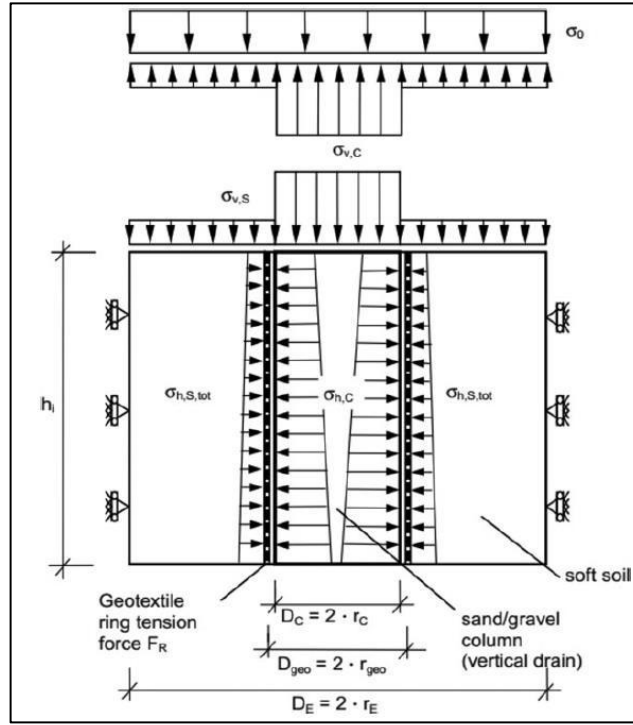
Fig. II. 1 Unit cell model of encased granular column (Raithel and Kempfert,2000)

The deformation of soft soil at the foundation's base can be easily found using standard methods, assuming that the pressure at the foundation's base has been reduced by the installation of GESC. The same method can be used to calculate GESC deformation. In the same way that soft soil is divided into layers, GESC is divided into layers. Furthermore, the vertical deformation of each layer can be calculated using the following relation, which is based on the volume constancy assumption (EBGEO, 2012):

a. Equilibrium: "stresses and forces involved"

Equation (II.1) describes the total stress equilibrium between the embankment load $\Delta\sigma_0$and the vertical stresses acting on the column $\Delta\sigma_{v,c}$and the soil $\Delta\sigma_{v,s}$as follows:

$$\Delta\sigma_0 A_E = \Delta\sigma_{v,c} A_c + \Delta\sigma_{v,s}(A_E - A_c) \hspace{3cm} Eq.\ II.\ 1$$

Where:

$\Delta\sigma_0$ = embankment total vertical stress.

$\Delta\sigma_{v,c}$: Vertical stress applied to the top of the column.

$\Delta\sigma_{v,s}$: Vertical stress at the surface of the surrounding soil.

It has been observed that utilizing an increased coefficient of thrust $K^*_{0,s}$ (ranging from 2 to 3 times $K_{0,s}$) can effectively reduce tension to zero on the geosynthetic encasement (Eq. II.2):

$$\Delta\sigma_{h,c} = \Delta\sigma_{v,c} K_{a,c} + \Delta\sigma_{v,0,c} K_{a,c} \hspace{3cm} Eq.\ II.\ 2$$

$$\Delta\sigma_{h,s} = \Delta\sigma_{v,s} K_{0,s} + \Delta\sigma_{v,0,s} K^*_{0,s} \hspace{3cm} Eq.\ II.\ 3$$

$K_{a,c}$: Active earth pressure of column material.

$K_{0,s}$: The at-rest coefficient pressure.

The hoop force ( ) developed on the geosynthetic encasement is determined using the hoop strain and the tensile stiffness modulus ( ), which is supplied by the manufacturer (as described in Equation (II.4)). Equation (II.4) outlines how to calculate the hoop strain, and this circumferential force can be converted into the horizontal (radial) stress$\Delta\sigma_{h,geo}$ acting on the geosynthetic encasement, as illustrated in Equation (II.5). This conversion is crucial for understanding the stresses involved and ensuring the structural integrity of the encased stone columns over time. Where, (Δr_{geo}) and (r_{geo}) are lateral bulging and initial radius of geotextile, respectively.

$$= .\quad -\; -$$ *Eq. II. 4*

$$\Delta\sigma_{h,geo} = \underline{\quad\quad}$$ *Eq. II. 5*

The value of $\Delta\sigma_{h,diff}$ is defined by equation (II.5),

$$\Delta\sigma_{h,diff} = \Delta\sigma_{h,c} - (\Delta\sigma_{h,s} + \Delta\sigma_{h,geo})$$ *Eq. II. 6*

The column expands due to the stress difference$\Delta\sigma_{h,diff}$. The radial horizontal deformation r_c and the settlement on soil S_s can be calculated using Equations (II.6) and (II.7), respectively.

$$= \frac{\Delta\sigma_{h,diff}}{E^*}\,(\;^{\underline{1}} - 1)\,r$$ *Eq. II. 7*

Where:

$$E^* = (\frac{1}{(1-v_s)} + \frac{1}{(1+v_s)} \times \frac{1}{a_E})\,(\frac{(1+v_s)(1-2v_s)}{(1-v_s)})\,E_{oed,s}$$

v_s : Poisson's ratio of soft soil.

$E_{oed,s}$: constrained modulus of soft soil

$$S_s = (\frac{\Delta\sigma_{v,s}}{E_{oed,s}} - \frac{2}{E^*} \times \frac{v_s}{1-v_s}\,\Delta\sigma_{h,diff})\,h_0$$ *Eq. II. 8*

h_0 : Initial column's length.

$$\Delta r_c = \Delta r_{geo} + (r_{geo-}r_c)$$ *Eq. II. 9*

r_0 : Initial radius of the column.

Equation (II.9) is derived from a purely geometric correlation. As a result, the incremental calculation of the settlement must be performed by updating the values of h_0 and r_0.The variation of the radius of the column, Δr_c, is given by Equation (II.10) as follows:

$$,\; =\quad ,\quad (\frac{(P^*+c'\cot\varphi)}{})^m$$ *Eq. II. 10*

According to the method's inherent hypothesis, the settlement at the top of the column equals the settlement in the surrounding soil, Equation (II.11):

$$=$$ *Eq. II. 11*

According to the assumption given by Equation (II.10), Equation (II.11) is obtained with the variable Δr_c given by Equation (II.12).

$$\{\frac{\Delta\sigma_{v,s}}{,} - \frac{2}{E^*} \times \frac{\nu_s}{1-\nu_s}[\frac{K_{a,c}(\frac{\Delta\sigma_v}{,} - \frac{1-a_E}{,} \times \Delta\sigma_{v,s} + \Delta\sigma_{v,0,s})}{-K^*_{0,}\Delta\sigma_{,,} - K_{0,}\Delta\sigma_{,,} + \frac{J(r_{geo}-r_c)}{2} - \frac{J\Delta r_c}{2}]\} \times h = \lceil 1 - \frac{c^2}{(r_c+\Delta r_c)^2}\rceil \times h \qquad Eq.\ II.\ 12$$

$$\Delta r_c = \frac{K_{a,c}(\frac{\Delta\sigma_v}{a_F} - \frac{1-a_E}{a_F} \times \Delta\sigma_{v,s} + \Delta\sigma_{v,0,s}) - K^*_{0,s}\Delta\sigma_{v,,s} - K_{0,s}\Delta\sigma_{v,,s} + \frac{J(r_{geo}-r_c)}{r_{geo}2} \frac{J\Delta r_c}{r_{geo}2}}{\frac{E^*}{(\frac{1}{}-1)r}+\frac{}{2}} \qquad Eq.\ II.\ 13$$

When Equation (II.12) is substituted in Equation (II.11), only the value of $\Delta\sigma_{v,s}$ is indeterminate; Equation (II.11) must then be solved iteratively. The value of J in Equations (II.11) and (II.12) is the (time-dependent) "ring" tensile stiffness modulus of the geosynthetic encasement. For design purposes, $r_c = r_{geo}$ can be used in Equations (II.9), (II.11), and (II.12), assuming the radius of the encasement is equal to the radius of the column.

b. Soil constrained modulus Eoed,s

As shown in Equation (II.13), the value of the soil constrained modulus ($E_{oed,s}$) can be calculated as a function of the vertical effective stress level in the middle of the soil layer, P^*.

$$\frac{}{,} = \frac{}{,}(\frac{P^*}{})^m \qquad Eq.\ II.\ 14$$

Where:

$E_{oed,ref}$ = reference constrained modulus of soil (see Fig. II.2).

P^* = effective vertical stress in middle of soft soil layer (see Equations (II.14) and (II.15)).

P_{ref}= reference effective vertical stress (see Fig. II.2).

m = exponent coefficient.

Equation (II.15) or Equation (II.16) can be used to calculate P^* (II.16). The net loading obtained by Equation (II.15) is preferred.

$$P^* = \frac{(P^*_2-P^*_1)}{ln(\frac{P^*_2}{P^*_2})} \qquad Eq.\ II.\ 15$$

$$P^* = \frac{(P^*_2+P^*_1)}{2} \qquad Eq.\ II.\ 16$$

In order to consider the effective cohesion of the soil c', the value of the constrained soil modulus ($E_{oed,s}$) can also be obtained using Equation (II.17).

$$\frac{}{,} = \frac{}{,}(\frac{P^*+c'\cot\varphi}{})^m \qquad Eq.\ II.\ 17$$

Because of the effective cohesion is usually quite low in very soft soils, $c' = 0$ is a common design hypothesis. In the example shown in Fig.II.2, $E_{oed,s}$ is 600 kPa, P_{ref} is 100 kPa, and m is 0.86.
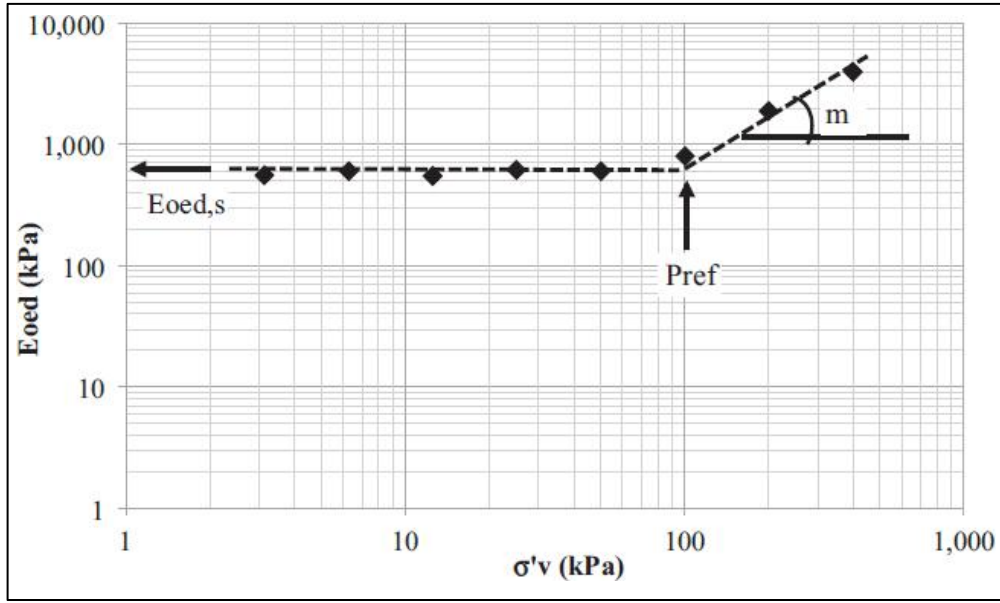
Fig. II. 2 Variation of constrained modulus with vertical stress – values of $E_{oed,s}$, P_{ref}, and m.

2.1.2. Han and Ye (2002)

Han and Ye (2002) developed an analytical method to calculate the degree of consolidation during construction and post-construction periods, originally designed for ordinary stone columns (Barron, 1948) but also applicable to encased columns due to the permeability of the geosynthetic encasement.

Equation (II.19) used to calculate the settlement over time, S (t), as follows:

$$( ) = \quad ( ) \qquad \qquad \textit{Eq. II. 18}$$

Where:

    = settlement on column or on surrounding soil ($S_s = S_c$).

$$U = 1 - e^{-\frac{8}{F'm}} \qquad \qquad \textit{Eq. II. 19}$$

Where:

F'_M = consolidation function (see Equation (II.23));

    = modified time factor.

Equation (II.22) determines the value of the modified time factor ( ).

$$= \quad \frac{\cdot\,-}{2} \qquad \qquad \textit{Eq. II. 20}$$

Where:

    = diameter of the unit cell.

t = time elapsed after application of the load.

$$C \quad = \frac{K_r}{,}.m \quad (1 - a_E) + \frac{m_{vs} \cdot a_E}{(m_{v,s}.m_{v,c}.(1-a_E))} = c \ (1 + \frac{-n_S}{N^2 - 1}) \qquad \textit{Eq. II. 21}$$

Where:

    = soil horizontal (or radial) permeability.

    = specific unit weight of water.

    , = volumetric compressibility coefficient of column.

    , = volumetric compressibility coefficient of surrounding soil.

    = area replacement ratio.

    = coeffiient of horizontal consolidation (due to radial flow).

n_s = stress concentration factor.

$N = d_e/d_c$.

The variable F'_m appearing in Equation (II.23) is determined as follows:

$$F'_m + \frac{2}{N^2-1} \cdot \left(\quad - \quad \cdot \quad_{mr} - \frac{3}{4} \right) + \frac{2}{N^2-1} \frac{(1-\frac{K}{})\cdot(1-\frac{S^2}{})+\cdot}{4^2} \cdot \frac{1}{N^2-1} \cdot (1-\frac{1}{4^2}) \cdot \frac{32}{2}(\_)\cdot(-)^2$$

Eq. II. 22

Where:

K_s = permeability coefficient of soil in the smeared zone.

K_c = permeability coefficient of column material.

H = longest drainage path due vertical flow.

$S_{mr} = d_s/d_c$.

2.1.3. Pulko et al. (2011) method

The method proposed by Pulko et al. (2011) (hereafter referred to by the code PEA) is an extension of the elastic analysis proposed by Balaam & Booker (1985) and Raithel & Kempfert (2000), Stone columns, when arranged uniformly, create a "unit cell" that includes both the column and the surrounding soft soil it influences. This model helps simplify the analysis of soil-column interactions, facilitating predictions of settlement and load distribution. By focusing on this representative unit, engineers can optimize stone column designs to enhance soil stability and bearing capacity effectively, making the method a cost-efficient solution for infrastructure projects involving soil stabilization (Fig. II.3). It takes into account the elastoplastic behavior of the column material while considering confined column yielding based on Rowe's dilatancy theory (1962). The vertical deformations at the top of the column and the surrounding soil are also assumed to be equal in this method. Shear stress at the column/soil interface is ignored. Furthermore, the soil is assumed to be elastic, and the column is assumed to be a perfectly elastoplastic material that meets the Mohr-Coulomb failure criterion. Pulko et al. provide additional information on the method (2011).
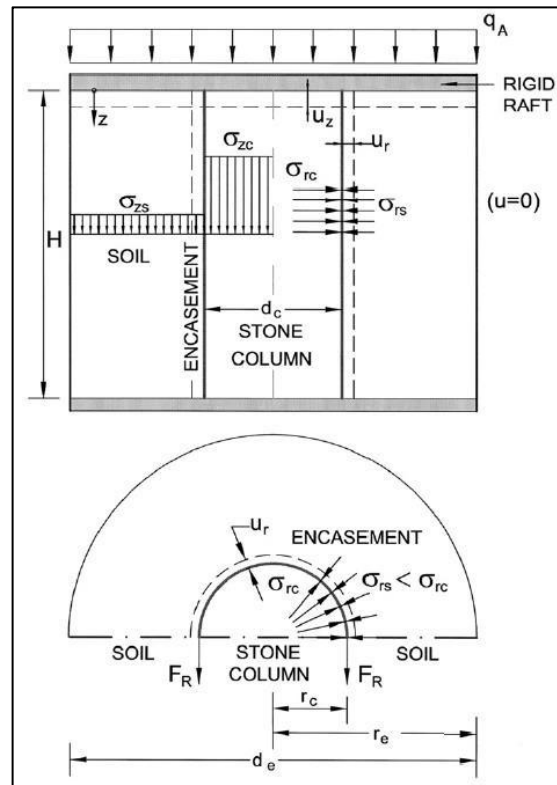
Fig. II. 3 Basic features of the model based on regular patterns of stone columns (Pulko et al. 2011).

2.1.4. Zhang & Zhao (2014) method

Zhang and Zhao (2014) developed an analytical solution using the unit-cell concept to predict the deformation behaviors of geotextile-encased stone columns at various depths below the column's top surface (Fig. II.4). Their solution accounts for shear stress at the soil-column interface, addressing both the vertical shear stress interactions between the columns and the surrounding soil and the deformation characteristics of the stone columns themselves. The objective of Zhang and Zhao's study was to offer an analytical framework that captures the complex deformation behavior of geotextile-encased stone columns by incorporating these shear stress interactions. This approach enhances the understanding of how geotextile-encased stone columns behave under load, especially considering the vertical stress transfer and interaction with the surrounding soil. To validate their method, Zhang and Zhao compared their analytical solution with two other existing analytical solutions, demonstrating its accuracy and applicability in predicting the deformation behavior of geotextile-encased stone columns. This work provides valuable insights for engineers and researchers in geotechnical engineering, particularly in designing and analyzing reinforced soil systems.
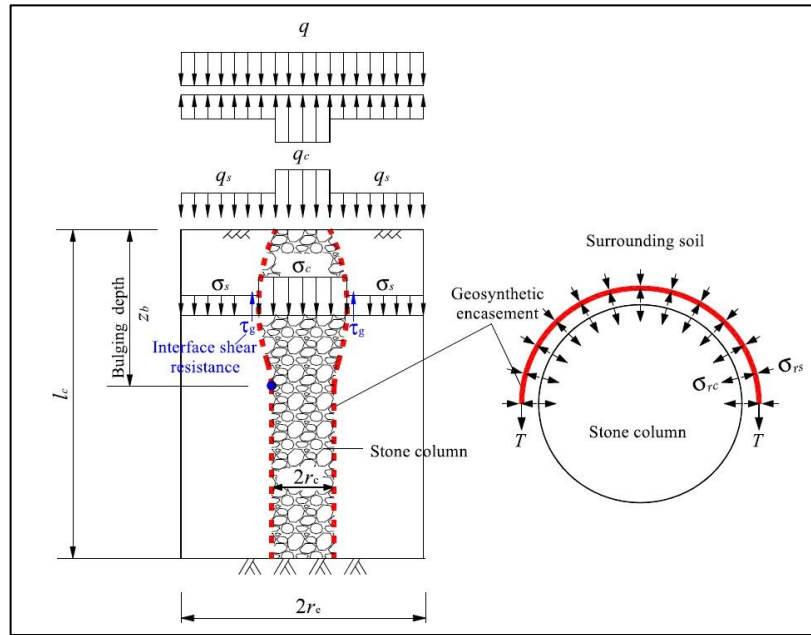
Fig. II. 4 Calculation model of geotextile-encased column (Zhang and Zhao, 2014).

2.1.5. Yang Zhou and Gangqiang Kong (2019) method

The research introduced a mathematical model to predict soil and stone column deformation using cylindrical cavity expansion principles. This approach examines how expansion pressure correlates with radial displacement and calculates vertical stress and settlement through stress equilibrium. Figure II.5 (a) depicts a geosynthetic-encased stone column (GESC), with variables (L), (d_c), and (r_c) representing its length, diameter, and radius, respectively. The study delves into stress and deformation patterns through radial and vertical stress equilibrium, as detailed in Figs. II.5 (b) and II.5 (c). Validation of this method was achieved by comparing results with established literature.
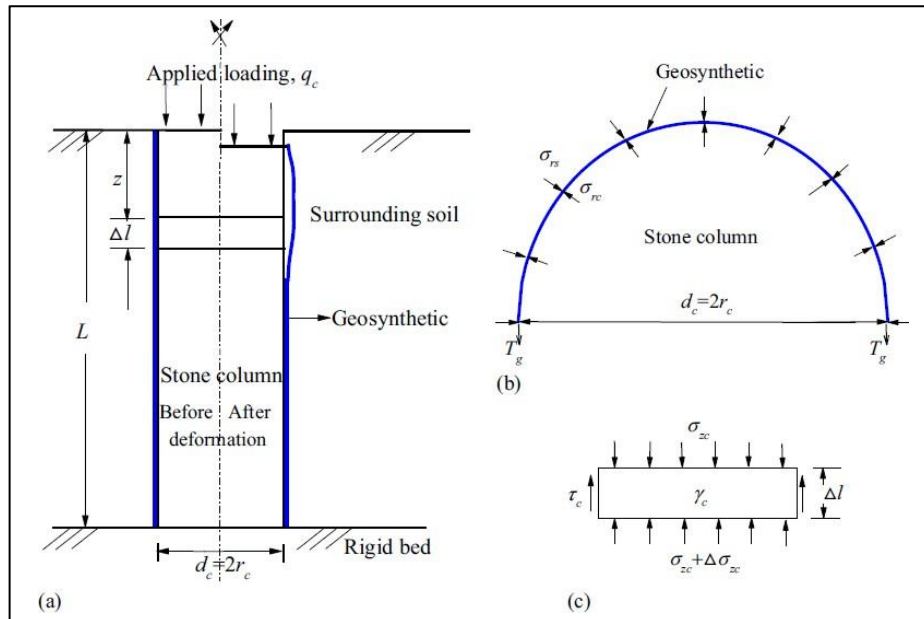
Fig. II. 5 (a) Diagram of the GESC; **(b)** radial stress equilibrium; **(c)** vertical stress equilibrium (Yang Zhou and Gangqiang Kong, 2019).

2.2. Empirical and numerical calculation

2.2.1. Review of the literature on improving the performance of foundation reinforced with coated granular columns

- **Roman Shenkman and Andrey Ponomarev (2016) work**

Roman Shenkman and Andrey Ponomarev (2016) conducted an extensive series of investigations to assess the efficacy of GESC technology in the soil conditions prevalent in the Perm Region. Their research encompassed numerical simulations, full-scale and small-scale experimental studies, as well as analytical analyses. Numerical simulations served as the primary tool for analyzing the stress-strain state of the soil mass and evaluating the technology's effectiveness in mitigating settlements of foundations situated on soft soil reinforced by encased stone columns. Furthermore, they identified the optimal geometric parameters of GESC, including depth, diameter, spacing, and the stiffness of the geotextile cover, utilizing Plaxis 3D software for design purposes. Figure II.6 illustrates the numerical 3D model utilized in their research.

The research also included semi-natural experimental studies, field tests of small-scale GESC models in soft water-saturated clay soils were conducted at one of the construction sites. The loading of small-scale models was accomplished through the use of a plate test consisting of a support frame, an anchoring system, a pneumatic loading device and a deformation locking system. Fig.II.7 show a general overview of the experimental setup and GESC model. These studies were later supplemented by the triaxle test of large-scale GESC models as show in Fig.II.8.
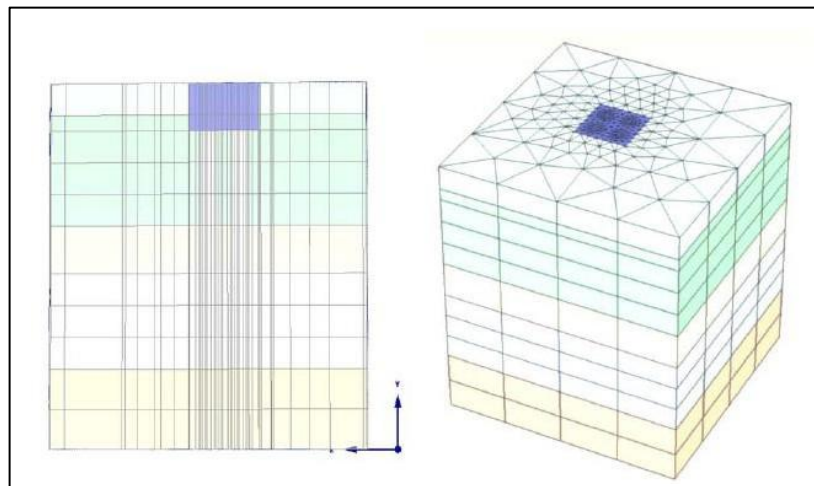
Fig. II. 6 Example of numerical 3D model (Roman Shenkman and Andrey Ponomarev, 2016).

Fig. II. 7 General view of experimental set up and model of GESC (Roman Shenkman and Andrey Ponomarev, 2016).
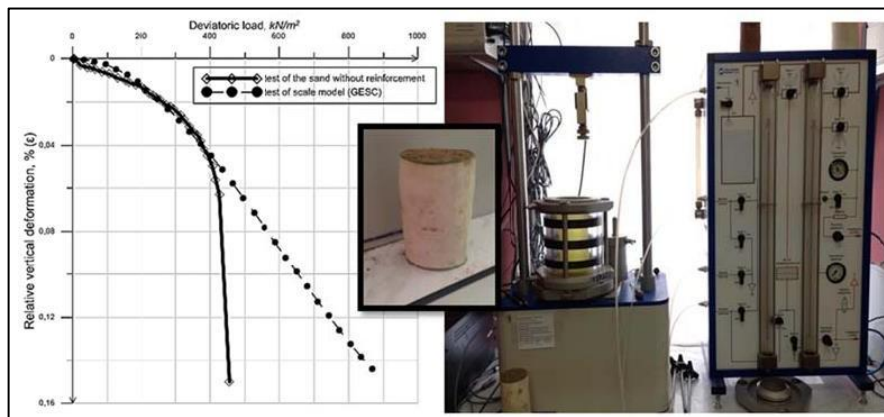
Fig. II. 8 General view of the triaxial equipment, and GESC scale model by this graph (Roman Shenkman and Andrey Ponomarev, 2016).

This graph shows that geosynthetic casing begins to function only after the filling material has lost its load-bearing capacity or has become significantly deformed in the horizontal direction. Roman Shenkman and Andrey Ponomarev (2016) propose also an algorithm for the analytic calculation of foundation deformation based on the following assumptions:

- The drained (final) state is the determining factor for calculation because it provides the maximum deformation and maximum radial tensile stresses in the geosynthetic shell.

- Foundation of the building is absolutely rigid body;

- Shell material is linearly elastic material.

- Inside the column is taken coefficient of active earth pressure: $K_a = tg^2 (45 - \frac{\varphi}{2})$.

- In the soft soil accepted the coefficient of lateral earth pressure: $K_p = 1 - \sin\varphi$.

- The basis of a methodology set out in the rules EBGEO in conjunction with the applicable regulations of the Russian Federation and research in this area.

Numerical modeling of test tasks was performed to determine the effectiveness of this method of calculation. The test tasks are numerically simulated using the Plaxis 3D software package. Fig. II.9 show a graph of vertical foundation deformation.
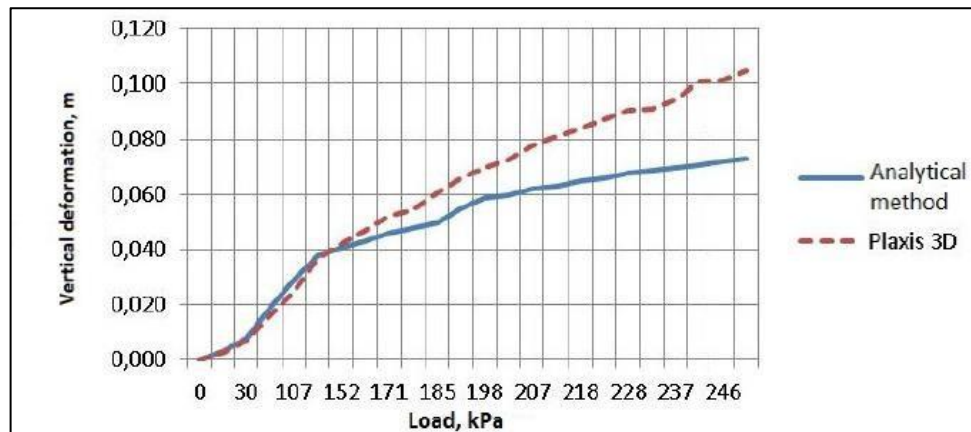
Fig. II. 9 Deformation on the results of numerical simulation and calculation of proposed method (Roman Shenkman and Andrey Ponomarev, 2016).

The results show that the provided calculation methodology, can show results similar to the results of numerical simulations, which can be used for the calculation of shallow foundations on the improved soil base by GESC. This method does not provide a rigorous analytical solution, but it does allow for calculations in accordance with existing regulatory norms and standards.

- **Ahmet Demir and Talha Sarici (2017) work**

Ahmet Demir and Talha Sarici (2017) used the 2D FE program PLAXIS and physical laboratory modeling to investigate the performance of stone columns encased in geogrid reinforcement. Experiments are conducted by only loading the column area in the unit cell area. Loading tests were performed on two different models of rigid circular footings (footing diameters of 5 cm and 10 cm) made of 15 mm thick mild steel. In all tests, the stone column area was the only one that was loaded. The tests were carried out in a circular steel tank with dimensions of 60 cm (diameter) and 60 cm (height) (depth). Fig.II.10 show a schematic diagram of the test setup. The numerical analysis was validated by the load settlement behavior obtained from the experimental tests. To quantify the effect of confinement and the mechanism for improved load capacity due to encasement, numerical analysis results based on various parameters such as the effect of stone column diameter, crushed stone friction angle, geogrid rigidity, and length of geogrid reinforcement are presented. Finite element model used in analysis is shown in Fig. II. 10.
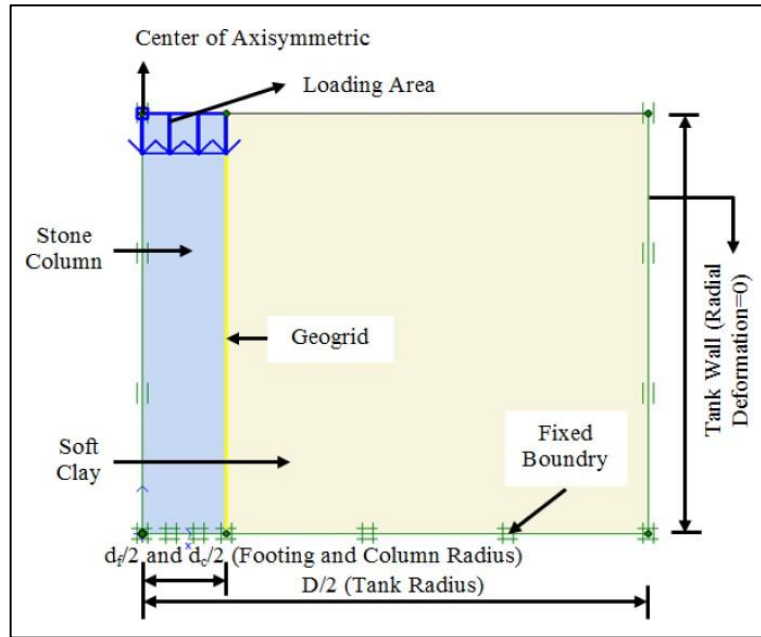
Fig. II. 10 Finite element model (Ahmet Demir and Talha Sarici, 2017).

Through experimental and numerical studies, bearing capacity-settlement ratio curves for rigid circular footings resting on soft clay soil with and without improved bearing capacity were obtained, and the experimental and numerical results for the same condition were compared. As a result, the finite element model's accuracy has been validated. Fig.II.11 depicts the numerical and experimental bearing capacities (q)-settlement ratio curves. Bearing capacities and settlement ratios are represented by the horizontal and vertical axes, respectively. The settlement ratio (s/d_f) is defined as the percentage of footing settlement (s) to footing diameter (d_f). The figures show that the numerically predicted vertical displacements agree very well with the experimental results.
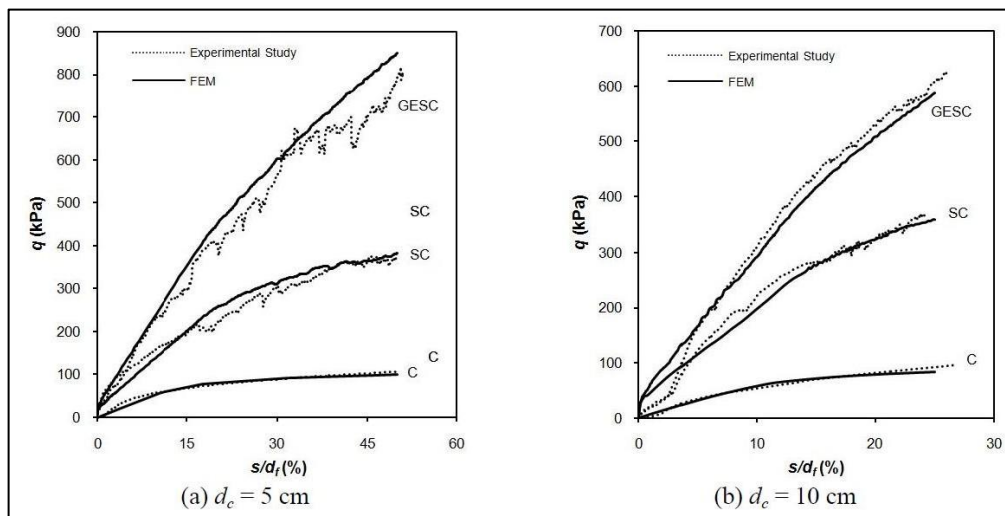
Fig. II. 11 Comparison between numerical analysis and experimental study for different conditions (Ahmet Demir and TalhaSarici, 2017).

As seen from the figures that by using a stone column, the bearing capacity of clay deposits can be increased. Furthermore, the performance of the stone column can be improved further by encasing it with geogrid. The geogrid encasement is found to increase the bearing capacity of the stone column while minimizing lateral bulging.

- **Hassan Kardgar (2018) study**

Hassan Kardgar (2018) investigated the bearing capacity of shallow foundations on geotextile-encased stone columns in two dimensions in this study. PLAXIS, a finite-element program, was used to simulate the soil. The proposed model was validated against small-scale testing results. A parametric study was conducted to investigate the effect of varying stone column diameter, length, and number, encasement stiffness, and foundation breadth. Due to the symmetry constraint, only half of the system was modeled. The finite element mesh used in this study, as well as the foundation on top of a series of encased stone columns, are depicted in Figure II. 12 (Kardgar, 2018).
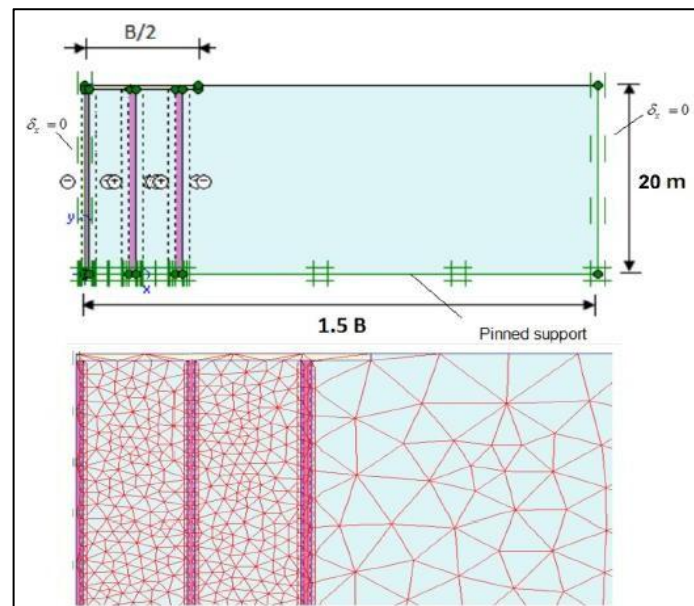
Fig. II. 12 Finite element mesh and boundary condition (Kardgar, 2018).

According to the findings, the foundation breadth, diameter, and number of stone columns increase the foundation's bearing capacity, while their length and encasement stiffness have a more pronounced effect, which can be considered an important factor in the analysis of shallow foundations on reinforced soils.

- **P. and Dey, A. K. (2017) work**

Debnath and Dey (2017) carried out laboratory model tests and numerical analyses on both unreinforced sand beds (USB) and geogrid-reinforced sand beds (GRSB) situated over a cluster of vertically encased stone columns (VESC) within soft clay. The clay served as the foundation bed for constructing the stone columns. The three-dimensional numerical analyses were conducted using the ABAQUS 6.12 finite element software.

Figure II.13 (a) illustrates the layout of the VESC group arrangement, while Fig. II.13 (b) provides a visual representation of the experimental setup.
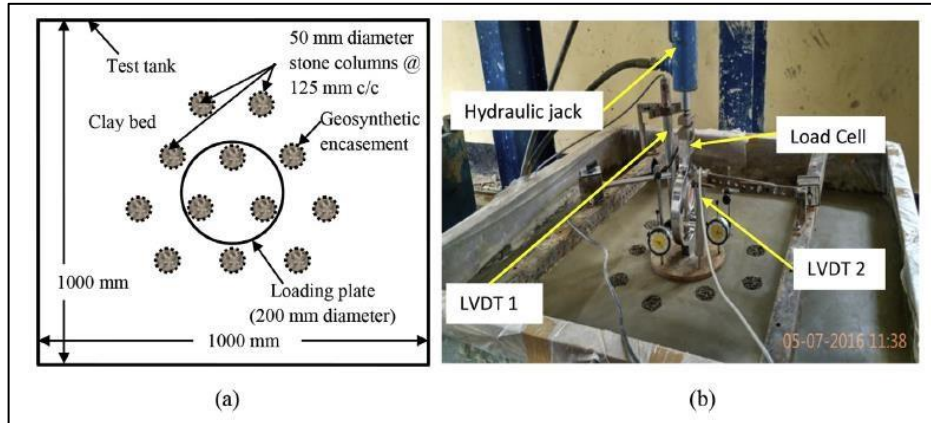
Fig. II. 13 Experimental Load Testing of Stone Column Groups: **a)** Diagrammatic Plan of Vertically Encased Stone Column Arrangement; **b)** Visual Representation of the Testing Setup (Debnath and Dey, 2017).

Fig.II.14 shows a photograph illustrating how the central stone columns exhibit bulging and lateral deflection under different reinforcement scenarios. It can be observed that the columns primarily deflect outward from the edge of the plate. This behavior is attributed to the fact that the central three columns were not aligned in the center of the loading plate, as shown in Fig.II.14 (a). As radial stress diminishes with distance from the plate edge, the columns tend to shift outward. Consequently, the deformation of the stone columns involves both bulging and lateral outward deflection.
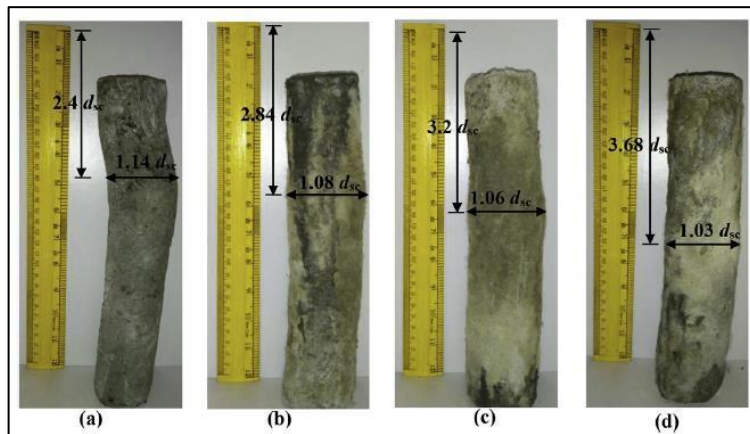
Fig. II. 14 Pictorial view of the deformation patterns of the stone columns when soft clay is improved with **(a)** OSC, **(b)** VESC, **(c)** VESC with 40 mm USB, **(d)** VESC with 30 mm GRSB (Debnath and Dey, 2017).

Table II.1 illustrates how maximum bulging and the depth at which bulging occurs change across different reinforcement setups. With the enhancement of the clay bed using VESC in combination with GRSB, there is a 78.57% decrease in the maximum bulging diameter and a 53.33% increase in bulging depth compared to

ordinary stone columns (OSC). In the case of OSC, a substantial stress concentration near the top of the columns leads to significant bulging. However, placing USB or GRSB over the stone columns significantly reduces this stress concentration, leading to decreased bulging.

Table. II. 1 Influence of Reinforcement Variations on Maximum Bulging and Bulging Depth (Debnath and Dey, 2017).

Parameters	OSC	VESC	VESC with USB	VESC with GRSB
Maximum bulging (mm)	7.00	4.00	3.00	1.50
Depth of maximum bulging (mm)	120.00	142.00	160.00	184.00
Maximum bulging depth (mm)	2.4dsc	2.84dsc	3.2dsc	3.68dsc
Reduction of maximum bulging as compared to OSC (%)	-	42.86	57.14	78.57
Increase in maximum bulging depth as compared to OSC (%)	-	18.33	33.33	53.33

The analysis was conducted using three-dimensional finite element models that replicate the laboratory tests shown in Fig. II. 15 (a) and (c). These models were developed and analyzed with the ABAQUS 6.12 software. The Mohr-Coulomb elasto-plastic failure criterion, along with a non-associated flow rule, was applied in the analysis. Consequently, an elasto-plastic constitutive model was employed to represent the behavior of the geogrid and geotextiles.
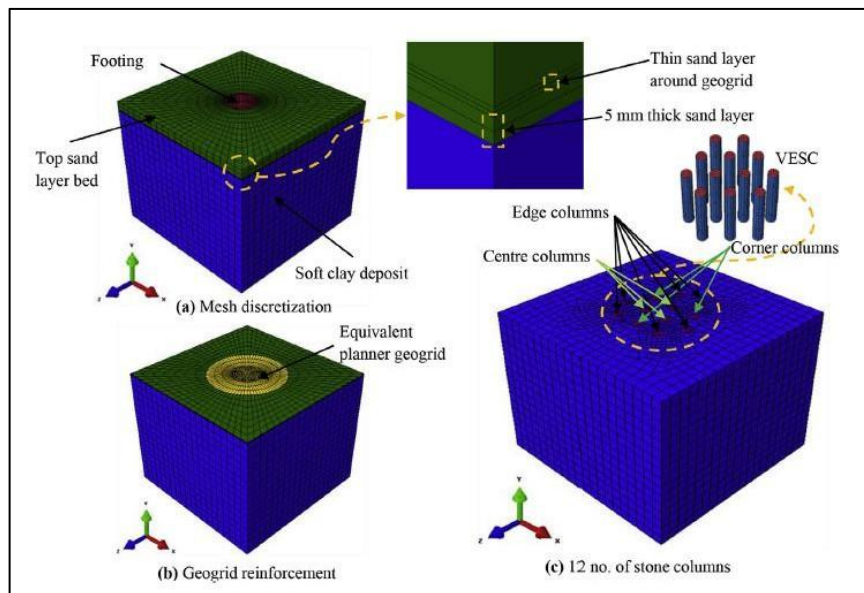
Fig. II. 15 Comprehensive 3D Mesh Design of the Finite Element Model (Debnath and Dey, 2017).

Laboratory tests explored the impact of changing the thickness of Uniform Sand Bed (USB) and Geosynthetic Reinforced Sand Bed (GRSB) on the pressure-settlement characteristics of stone columns. The experiments considered five thickness variations for the USB and three for the GRSB. Figures II.16 and II.17 show the pressure-settlement responses for USB and GRSB with varying thicknesses placed over groups of floating Vertically Encased Stone Columns (VESC) in clay.
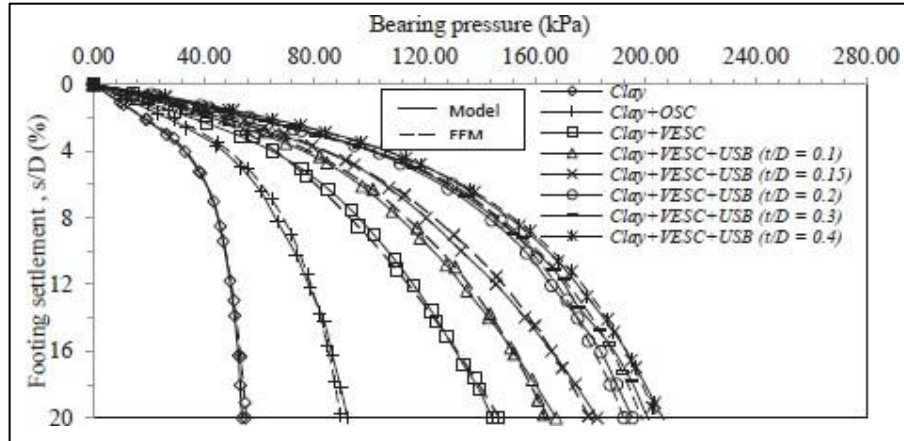
Fig. II. 16 Effects of Uniform Sand Bed Thickness on Footing Pressure-Settlement Behavior (Debnath and Dey, 2017).
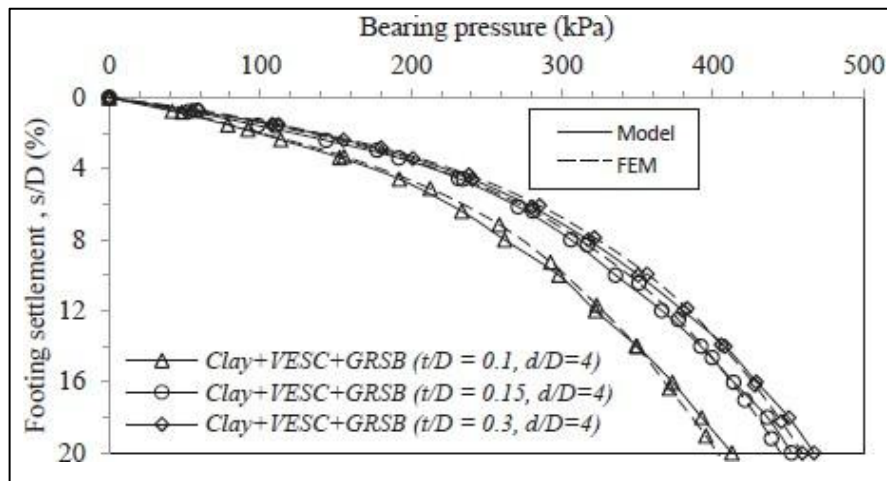
Fig. II. 17 Pressure-Settlement Behavior of Footings on Geosynthetic-Reinforced Sand Beds with Varying Thicknesses (Debnath and Dey, 2017).

Results show that the bearing capacity of a soft clay bed can be increased by 1.72 times with OSC, and by 2.68 times with VESC. When VESC and USB or GRSB are coupled, the bearing capacity increases by 3.63 and 8.45-fold, respectively. While the optimum thickness of USB and GRSB can be taken to be 0.2 times and 0.15 times the diameter of the footing, based on the maximum percentage improvement in load carrying capacity as shown in Fig.II.18.
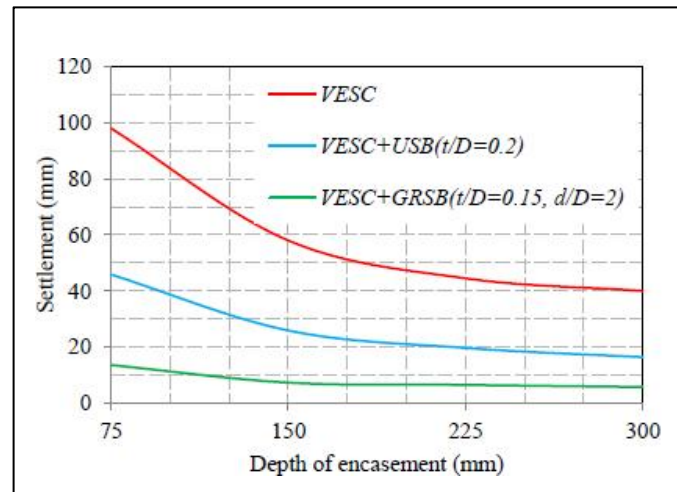
Fig. II. 18 Variation of the settlement against the depth of encasement (Debnath and Dey, 2017).

2.2.2. Review of the literature on improving the performance of embankments reinforced with coated granular columns

- **Chen et al. (2015) work**

Chen et al. (2015) conducted numerical simulations and laboratory tests on geosynthetic-encased stone column (GEC)-reinforced embankments (see Figs. II.19 and II.20). Their study found that bending of the columns led to the failure of the encased stone columns. They used both 2D and 3D simulations to evaluate the embankment's stability. The results indicated that 3D simulations provided more accurate predictions compared to 2D simulations, aligning with the observed bending failure mechanism of GECs. The study recommends adding an additional row of columns to enhance lateral resistance in the soil at the embankment toe, thereby improving overall stability. Figs.II.19 and II.20 display the 2D and 3D finite element meshes utilized in their analysis.
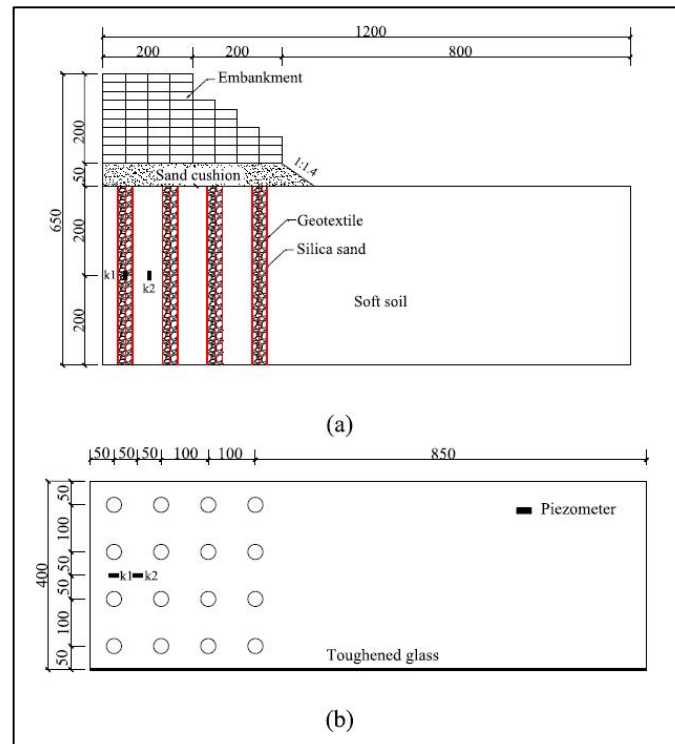
Fig. II. 19 Measurements of the Laboratory Model Embankment Reinforced with GECs in Soft Soils (Units in mm): (**a**) Cross-Section View; (**b**) Top-Down View (Chen et al., 2015).
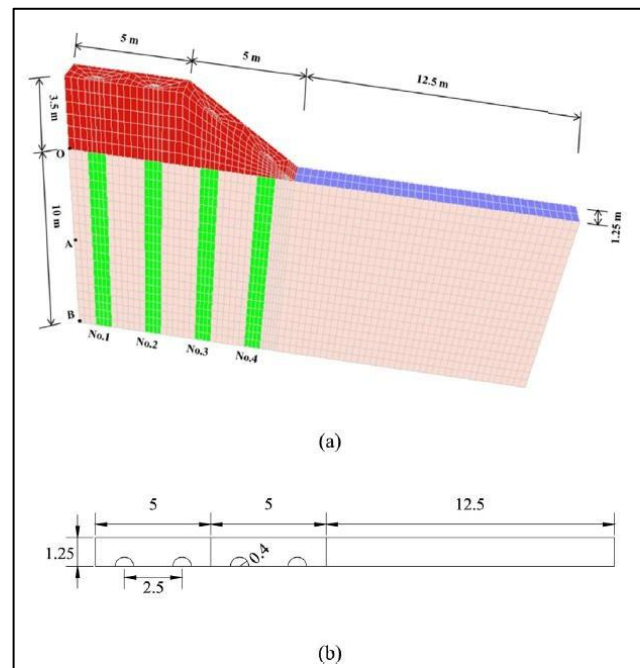
Fig. II. 20 The numerical model of the GECs-supported embankment (units are in meters) three-dimensional view; (**b**) top view (Chen et al., 2015).

- **Alkhorshid et al. (2018) study**

Alkhorshid et al. (2018) utilized both numerical and analytical approaches to assess the impact of encasement on stone columns reinforced with geosynthetics, arranged in a square pattern beneath an embankment. The study employed the Finite Element Method (FEM), with a numerical model detailed in Fig. II.21. It examined

how factors such as geosynthetic stiffness, column spacing, friction angle of the column material, and Stress Concentration Ratio (SCR) affect column performance through parametric studies. The performance of embankments reinforced with Geosynthetic Encased Columns (GECS) was analyzed by comparing results from four methods: Finite Element, R&K, PEA, and Z&Z. Among these, the R&K method generally showed better alignment with FEM results compared to PEA and Z&Z methods (Alkhorshid et al., 2018; Pulko et al., 2011; Raithel and Kempfert, 2000; Zhang and Zhao, 2014).
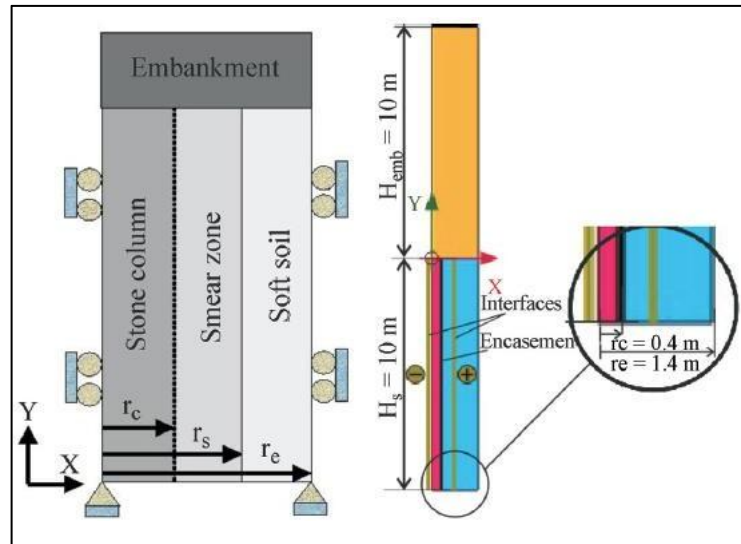
Fig. II. 21 Axisymmetric unit cell model and boundary condition. (Alkhorshid et al., 2018)

- **Debbabi et al. (2020) study**

Debbabi et al. (2020) explored the effectiveness of embankments supported by encased stone columns in regions with locally weak zones (LWZ). The study used various numerical simulations to evaluate how LWZ affects column performance, focusing on aspects like lateral deformation, settlement behavior, and stress distribution between the columns and the surrounding soil. The research specifically looked at road embankments in Algeria, built on Sabkha soil, which is known for its softness and high moisture content during flooding seasons, as well as frequent patches of very soft soil identified by Benmebarek et al. (2015) as LWZs. These zones have a low strength-to-compressibility ratio. The study modeled LWZ properties with dimensions similar to those of Sabkha soil, aligning with the values provided by Benmebarek et al. (2015)specifically a width (B) of 0.6 meters and a depth (DEP) of 3 meters, as depicted in Fig.II.22.
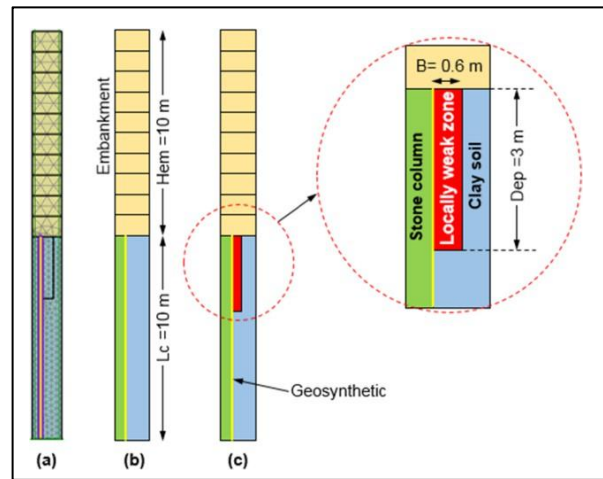
Fig. II. 22 Finite-Element Axisymmetric Simulation of Geosynthetic-Encased Columns in a Unit Cell Concept: **(a)** Boundary Conditions and Finite-Element Mesh, **(b)** ESC Scheme Without Locally Weak Zone, **(c)** ESC Scheme with Locally Weak Zone (Debbabi et al., 2020).

According to Figs. II. 23 and II. 24, when compared to a stone column without geotextile encasement (OSC), the use of (OSC) in the locally weak zone (Sabkha soil) can be problematic due to a lack of adequate lateral confining pressure, especially in the upper portion of the column. This is usually the main reason for using the (ESC).
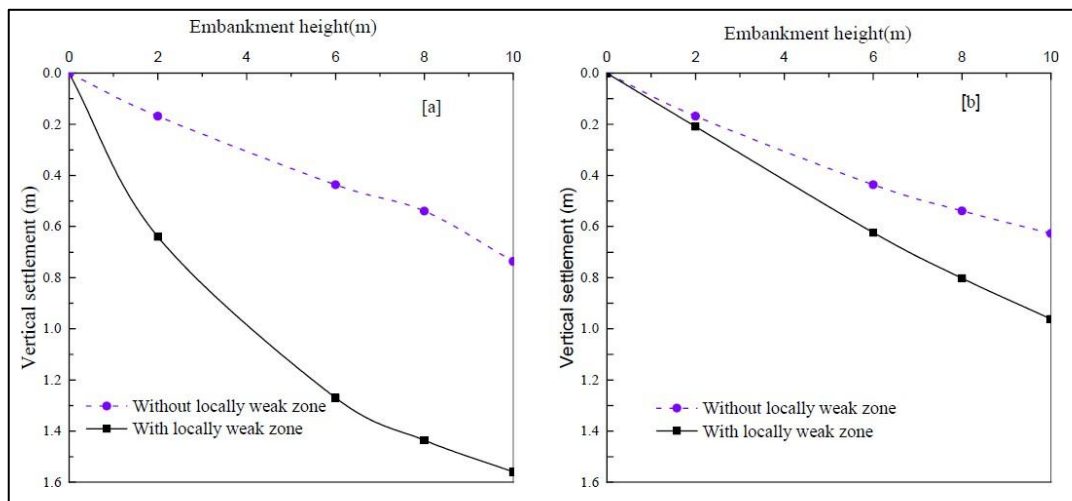
Fig. II. 23 Vertical settlement. **(a)** Ordinary stone column (OSC), **(b)** Encased stone column (ESC) (Debbabi et al., 2020).
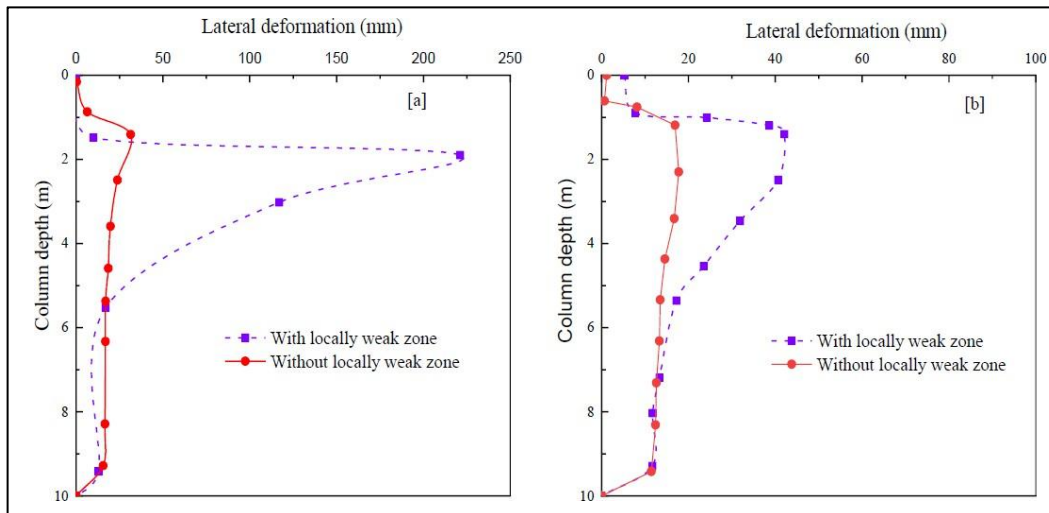
Fig. II. 24 Radius variation. **(a)** Ordinary stone column (OSC), **(b)** Encased stone column (ESC) (Debbabi et al., 2020).

The results indicate that ordinary stone columns (OSC) were inadequate for supporting the embankment due to excessive bulging (221.16 mm) caused by insufficient lateral pressure. In contrast, encased stone columns (ESC) demonstrated much better performance, exhibiting significantly less bulging (42.09 mm) and a more manageable settlement of 0.962 m. This performance of ESCs allows for the construction of stable and higher embankments, in comparison to the 1.560 m settlement observed with OSCs.

3.   Conclusion

In conclusion, this chapter has presented a comprehensive literature review on the application of EGSC reinforcement in the construction of embankments and foundations. This approach stands out as both economically and technically promising. Among the various methods explored, the utilization of geosynthetics emerges as a particularly cost-effective solution, offering advantages in resource conservation, time efficiency, and sustainability. Through thorough investigation, geosynthetic-encased stone columns have been identified as an effective means of enhancing column performance in soft soils, especially very soft soils, through empirical, numerical, and analytical approaches. Notably, geosynthetics contribute to increased safety factors and embankment heights, along with improved performance evidenced by uniform settlements and reduced displacement during construction, leading to material savings. This underscores the significant potential of geosynthetic reinforcement in enhancing the stability and efficiency of embankment and foundation projects.

Chapter 3

Chapter 3

Review of Published Studies on the Effects of Various Parameters on the Performance of Geosynthetic-Encased Stone Columns in Soft and Very Soft Soils

1. Introduction

Encased stone columns play a significant role in geotechnical engineering by enhancing soil stability and strength. The performance of these columns hinges upon various parameters, including column diameter, stone size and grading, encapsulation material, column spacing, and installation technique. Extensive research has delved into the effects of these parameters, yielding invaluable insights.

For instance, augmenting the column diameter enhances load-carrying capacity and reduces settlement, albeit beyond a certain threshold, the incremental benefits become negligible. Larger stone sizes similarly bolster load-carrying capacity while diminishing settlement, yet they introduce the risk of stone crushing and column failure. Likewise, employing thicker and stiffer encapsulation material can elevate capacity and diminish settlement, though excessive stiffness may impede deformation and load distribution, leading to localized failure.

The spacing between columns emerges as another critical factor, with narrower spacing yielding heightened capacity and reduced settlement. However, the proximity between adjacent columns may compromise individual capacity due to interference. Furthermore, the installation technique plays a pivotal role, with the bottom-feed method proving superior in achieving higher capacity and lower settlement compared to the top-feed approach.

In summary, optimizing these parameters holds the key to enhancing the performance of encapsulated stone columns. Nonetheless, the ideal design is contingent upon site-specific considerations and project requirements, underscoring the importance of tailored solutions in geotechnical engineering endeavors.

1. Basic parameters

1.1. The geosynthetic parameters

1.1.1. Influence of geosynthetic encasement length

The influence of encasement length on the behavior of GESC is analyzed by varying normalized encasement length $= \dfrac{}{}$ from 0 and 1; where, (L_{GESC}) and (L_{OSC}) is the length of geosynthetic encasement and ordinary stone column respectively. Xu et al., (2021) carried out a three-dimensional numerical modeling scheme that combines the discrete element method (DEM) and the finite difference method (FDM) to investigate the effects of encasement length and geosynthetic stiffness on the performance of geosynthetic-

encased stone column (GESC) improved ground. Based on the findings, it was concluded that the design of the geosynthetic encasement is crucial for controlling the performance of GESC-improved ground, with encasement length and geosynthetic stiffness being important design factors. The study recommended the use of fully-encased stone columns with high stiffness to enhance the load-bearing capacity and reduce settlement in practical applications (Z. Xu *et al*., 2021). Previously, it was assumed that the encasement length (L_g) of columns is equal to their entire length (L). However, certain researchers have suggested the idea of partially encasing the columns. For instance, Murugesan and Rajagopal (2006) conducted numerical studies and discovered that it was sufficient to encase only the upper $2d_c$ (2 times the column diameter) (Murugesan & Rajagopal, 2006)). Similarly, Muzammil et al. (2018) performed simulations and determined that an optimal encasement length for reducing settlement was 6 times the column diameters. On the other hand, some experts recommend full column encasement, as seen in the works of Gniel and Bouazza (2009), Xu et al. (2021), and Yoo and Abbas (2019). Furthermore, Wu et al. (2009) concluded that the ideal encasement length depends on various factors such as the properties of the soft soil at the construction site and the stiffness of the sleeve. An interesting finding by Dash and Bora (2013) emerged from small-scale laboratory tests on partially encased columns. They observed that some partially encased floating columns outperformed the fully encased ones due to the creation of an enlarged base for the column.

Research paper conducted by Miranda et al., (2017) investigates how geotextile encasement affects the behavior of soft soils that have been enhanced with fully penetrating encased columns. The study examines the distribution of stress, pore pressures, and soil deformation during the consolidation process. Small-scale laboratory tests were conducted using a large instrumented Rowe-Barden oedometric cell, representing a representative "unit cell." The findings suggest that encased columns achieve a settlement reduction factor of approximately 0.6 compared to untreated soft soil, while non-encased columns exhibit a reduction factor of around 0.8 (see Fig.1).
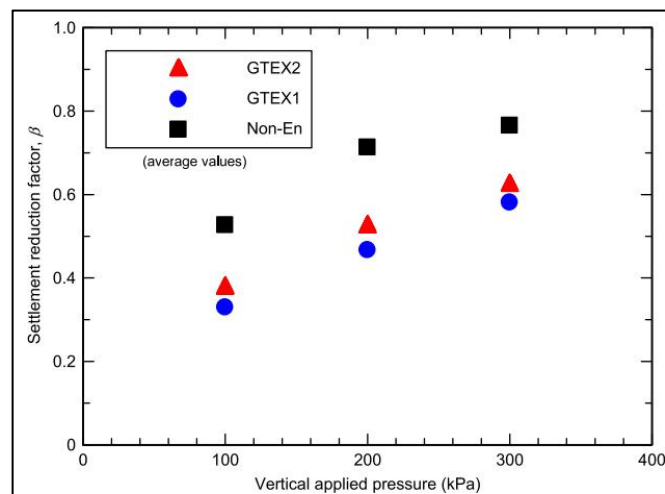
Fig. III. 1 Settlement reduction factor at the end of each load step(Miranda et al., 2017).

1.1.2. Effect of encasement stiffness (EA)

The mechanical properties of geosynthetics used in the encapsulation of ballasted columns include tensile strength, stiffness, deformation modulus, and thickness. Geosynthetics are typically modeled as continuous elements exhibiting linear elastic behavior, with their Young's modulus (E) derived from the relationship $= E \times t$, where J represents the stiffness of the geosynthetic and t denotes its thickness. In practical applications, reinforcement sleeves for vertically encasing ballasted columns are manufactured with diameters ranging from 40 cm to 100 cm, tensile strengths reaching up to 400 kN/m, and stiffness values ranging from 1000 to 4000 kN/m (Araújo *et al.*, 2009).

The study evaluates the impact of the axial stiffness of geogrid encasement on the performance of geosynthetic-encased stone columns (GESC) supporting soft ground under embankment loading by varying the axial stiffness (*EA*). Table III.1 lists the different types of geosynthetics used for encasement in the simulations, including both woven and non-woven varieties. To ensure proper installation, these geosynthetics were either glued or sewn together. The simulations utilized models of varying scales, from medium to large, incorporating different area replacement ratios (a_r) and length-to-diameter (*l/d*) ratios.

The selection criteria for the geosynthetic materials focused on their stiffness and filtration capabilities. The encasement material needed to provide adequate stiffness to effectively support the structure and function as a filter, facilitating water drainage while preventing soil infiltration. Studies have shown that geogrids or geotextiles with higher stiffness perform better in these roles (Gniel and Bouazza, 2010; di Prisco and Galli, 2011). The findings presented by Bathurst & Naftchali (2021) have significant relevance for research inquiries focusing on the impact of reinforcement stiffness on the operational performance of reinforced soil walls and pile-supported embankments (Bathurst and Hatami, 2015; Bathurst and Naftchali, 2021; Van Eekelen and Han, 2020; Rowe and Ho, 1997, 2011; Zhuang *et al.*, 2020). By establishing the relationship between isochronous stiffness and ultimate tensile strength of reinforcement geosynthetics, this research enables modelers to accurately match reinforcement stiffness and strength. Additionally, the provided stiffness approximations are valuable for selecting appropriately scaled model geosynthetic materials in reduced-scale 1g reinforced soil models and centrifuge modeling and (Almeida *et al.*, 2020; Shen *et al.*, 2020; Viswanadham and König, 2004). Furthermore, the two-component hyperbolic creep stiffness model introduced in this study can be directly applied as the constitutive model for geosynthetics in advanced numerical FEM and FDM models of reinforced soil structures. This allows for the capture of changes in reinforcement stiffness over time and strain during and after construction. Although beyond the scope of the current study, have demonstrated this application (Huang *et al.*, 2009; Yu and Bathurst, 2016, 2017)

A numerical study was conducted to investigate the time-dependent behavior of geosynthetic-encased stone columns (GESC) in comparison to conventional stone columns. Parametric analyses were performed to examine the influence of geosynthetic encasement, encasement stiffness, and column length on the

deformation behavior of GESC. The performance of fully penetrated and partially penetrated GESC was evaluated based on parameters such as surface settlement, lateral displacement, hoop tension in the geosynthetic material, and dissipation of excess pore water pressure over time(Rajesh, 2017). Fig .III. 2 shows the settlement evolution and the excess pore water pressure with time for different values of geosynthetic stiffness.
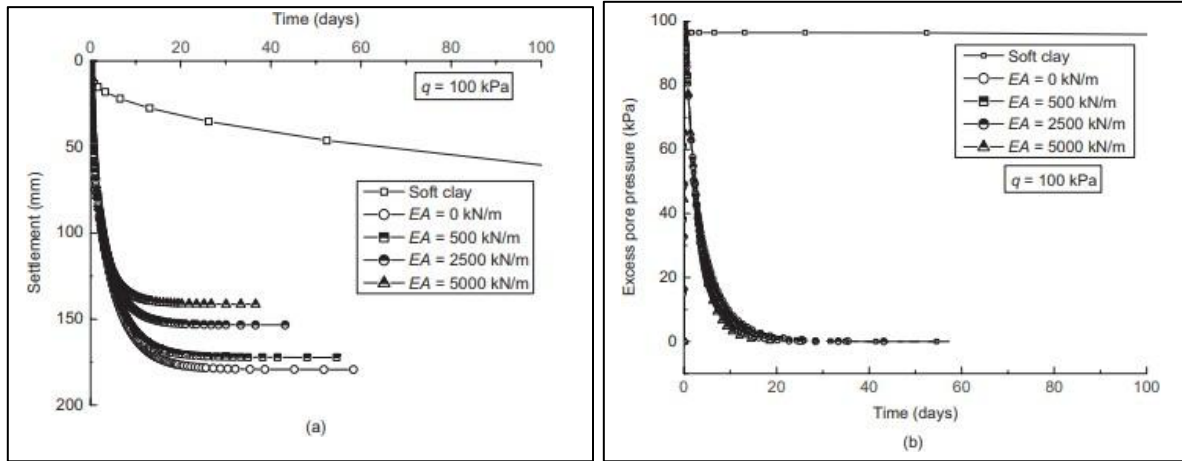
Fig. III. 2 Variation of **(a)** settlement and **(b)** dissipation of excess pore water pressure with time for various values of geosynthetic stiffness.

Based on the numerical analyses conducted by Rajesh (2017), the following conclusions were drawn. First, when the stone column was encased with a geosynthetic material with a stiffness of 5000 kN/m, it led to a reduction of approximately 42% and 21% in total ultimate settlement compared to soft clay and conventional stone columns, respectively. This indicates that the geosynthetic encasement significantly improved the overall settlement performance. Second, the total time required for excess pore pressure dissipation varied among the different systems. In soft clay, it took approximately 7000 days, while for conventional stone columns, it was 52 days. In contrast, the geosynthetic-encased stone columns (GESC) demonstrated a faster dissipation, with a total time of around 30 days. These findings highlight the effectiveness of GESC in accelerating pore pressure dissipation and reducing settlement duration compared to other systems.

1.2. The stone column parameters

1.2.1. Factors Affecting the Behavior of a Single Stone Column

1.2.1.1. Properties and Type of Soil

According to Hughes et al. (2015), the effect of soil on stone columns is dependent on a number of variables, such as the soil's radial pressure deformation properties, the in situ lateral stress inside the soil, and the moistness of the soil. Granular columns, for example, could not be able to support large loads if they are placed in soft soil because of inadequate lateral confinement. The viability of the treatment is assessed using the undrained shear strength of the surrounding soil as a guide. While Wehr (2006) suggested a minimum C_u vary from five to 15 kPa, most studies indicate that a C_u value higher than 15 kPa is necessary to ensure

adequate lateral support. However, stone columns are not suitable when cu exceeds approximately 50 kPa or more because the resistance encountered during column formation becomes excessively high (Barksdale *et al.*, 1983)

There is increasing interest in a specific type of soil known as collapsible soils, which can undergo sudden settlement when they lose lateral support upon saturation (Mitchell & Jardine, 2002). A literature review by Jefferson et al. (2000) indicated that stone columns could be effectively used to treat collapsible loess deposits with depths ranging from 1.5 m to 10 m. They highlighted stone columns as a cost-efficient alternative to traditional piles, though they stressed the importance of meticulous site assessment and management. In a laboratory study, Ayadat (1990) enhanced the performance of ordinary stone columns in collapsible soils by encasing them in geotextile, effectively mitigating the issue of losing lateral support from the surrounding soil. However, the degree of improvement achieved by this method, especially in fine soils, is still not fully understood.

A study conducted by Farah et al., (2020), investigate the behavior of floating stone columns with and without encasement in both single-layered soft soil and layered soil conditions through small-scale laboratory tests were conducted to assess the bearing capacity improvement. the study revealed that the use of geotextiles contributed to improved bearing capacity by distributing induced stresses over larger areas. However, in single-layered soft soil, the maximum bulging of non-encased stone columns was observed at a depth of 1.5 times the original diameter of the column, whereas encased stone columns transferred the maximum bulging to a depth of 3.0 times the original diameter (Farah & Nalbantoglu, 2020).

However, detailed information regarding the impact of soil collapsibility on stone column performance has not been extensively reported.

1.2.1.2. Stone Column Geometry

The geometry of stone columns has a considerable influence on their failure mode. When the length-to-diameter ratio (l/d) is below four, the stone column is more likely to experience end-bearing failure rather than bulging failure, according to the findings of Hughes and Withers (1974). To ensure that, the column receives maximum axial stress restraint, McKelvey et al. (2004) recommend a minimum l/d ratio of six (McKelvey *et al.*, 2015).

- **The infill material**

Several experimental studies have been conducted to explore the influence of different infill materials on column behavior. Naeini et al. (2019) investigated the impact of various aggregates as infill materials, while Kadhim et al. (2018). Specifically studied the use of sand as the infill material. Farah et al. (2020) conducted research using crushed aggregates as the infill material, whereas Fattah et al. (2016) and Ghazavi et al. (2013) used crushed stone. In another study, Ali et al. (2015) and Farah et al. (2020) utilized a combination of sand and stone chips as the infill material. These studies contribute to our understanding of how different infill

materials affect column performance and provide valuable insights for optimizing column design and construction (Table. III. 1).

- **Stone column length and diameter (L_{sc} and D)**

The size of the stone column is a significant factor in enhancing its load-bearing capacity and minimizing the settlement associated with it, as stated by (Greenwood Da, 1975). Similarly, the extent of improvement achieved is greatly influenced by the amount of soil replaced by the granular columns. This can be quantified using the area replacement ratio (a_r), which represents the ratio of the stone column's area to the combined area of the stone column and the surrounding soil,(Shahu *et al.*, 2000).

The critical length, also known as the optimal length (L_c), of a column plays a significant role in determining the bearing capacity and settlement behavior of a group of columns. Hughes et al. (1975) introduced the concept of critical length, defining it as the minimum length of a column capable of supporting the maximum load without any further improvement in bearing capacity, regardless of settlement.

Najjar (2013) corroborated the existence of this critical length (L_c) through a comprehensive analysis of laboratory tests, in situ investigations, and numerical simulations. These studies consistently show that beyond the critical length (L_c), the bearing capacity remains relatively constant, while the stiffness of the column continues to increase, leading to increased settlements until another critical length (L_c) is reached, beyond which further increases in settlement become insignificant. These findings indicate that the critical length for bearing capacity is typically smaller than the critical length associated with settlement.

This research suggests that relatively shorter columns are more effective in improving bearing capacity, while longer columns are better suited to resist settlements. The specific values of the critical column length depend on factors such as column diameter (D), foundation width, and other soil and column parameters (Babu et al., 2013). Previous studies (Wood et al., 2000; Fatah et al., 2017) have reported an increase in the critical length (L_c) with higher surface replacement ratios (A_s), facilitating stress transfer to greater depths. Additionally, Castro (2017) emphasized the significant influence of foundation width on the critical length, as it directly governs the intensity of loads transmitted through the foundation.

1.2.1.3. Properties of Stone Column Material

- **The effect of elastic modulus and the friction angle of the stone column's material**

The material used to fill the stone column needs to have sufficient resistance to shearing forces in order to withstand stress concentrations (Jefferson et al., 2010)(Jefferson *et al.*, 2015). The properties of the fill material, such as the internal angle of shearing resistance (φ'_c) and the modulus of elasticity (E_c), are important factors that influence the performance of the stone columns. These properties determine how the stone columns behave under load and impact their overall effectiveness. The load applied to a soil and stone column system is distributed between them based on their respective stiffness values. As a result, the stone column carries a larger proportion of the applied load due to its higher stiffness. The modular ratio, which is the ratio

between the modulus of elasticity of the stone column (E_c) and the modulus of elasticity of the soil (E_s), represents the stiffness ratio between them. This ratio determines the stress concentration ratio in the system, assuming lateral confinement and elastic behavior of the stone column. However, this theoretical expectation contradicts practical experience. In real cases, the modular ratio is typically in the range of 10-50, while the measured stress concentration ratio is considerably lower, falling within the range of 2-10. This contradiction arises because the stone column is not fully confined, and it undergoes lateral displacement. Furthermore, the behavior of the column is elastoplastic, meaning that it experiences both elastic and plastic deformation. The lateral bulging of the column is a result of its yielding, which contributes to the observed lower stress concentration ratio in practice. The material constituting the column has an internal friction angle (φ'_c) ranging between 30 and 46 degrees. In France, a commonly adopted value for the column friction angle is 38°, while in Germany; it is typically set at 42 degrees.

The design chart (Fig. III.3), which was published by Priebe (1995), shows the relationship between the area ratio (A/A_c) and the improvement factor (F_{imp}) for a typical soil type with a Poisson's ratio (μ_s) of 1/3, taking into account the angle of internal friction (φ'_c).
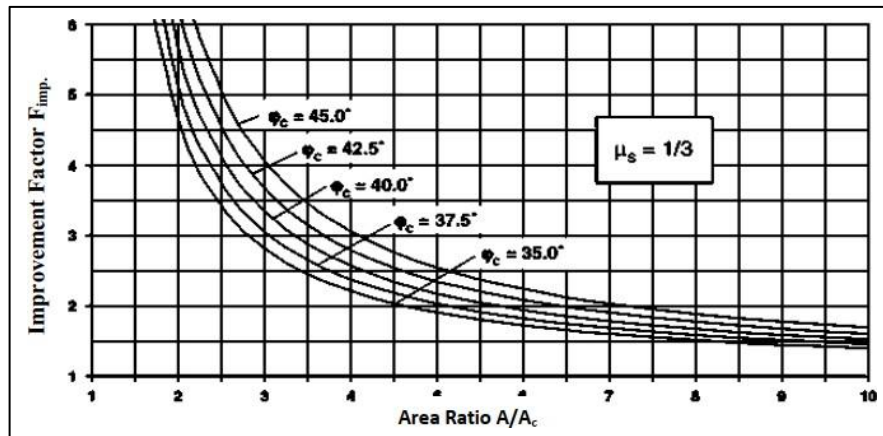
Fig. III. 3 The relationship between the improvement factor (F_{imp}) and the area ratio (A/A_c) for various angles of internal friction (φ'_c). (Priebe, 1995)

1.2.2.   Factors Affecting the Behavior of a Group of Stone Columns

1.2.2.1. Stone column spacing (S)

A rigid foundation will result in a higher stress concentration ratio at the ground surface than a flexible foundation, according to Barksdale and Bachus (1983). This ratio shows how much stress is on the soil relative to the total stress on the column and the surrounding soil. Stone column-soil modular ratio, or the ratio of the column material's modulus of elasticity to the soil's modulus of elasticity, accelerates consolidation under a rigid raft; under a flexible raft, however, the effect is not as great. Balaam and Booker (1981) observed this. It has been demonstrated that the use of stone columns can effectively increase the capacity to transport loads and decrease the compressibility of soil under static loads. Less research has been done on how they behave

when subjected to cyclic loads, as occurs in railway infrastructure. Ashour (2015) discovered that by promoting drainage, stone columns in clayey soil subjected to cyclic loading reduced lower threshold stress and pore water pressure (Basack *et al*., 2015 and 2016).

1.2.2.2. Loading Type and Arrangement

When a load is applied via a rigid foundation, the stress concentration ratio at the ground surface is greater than when a flexible foundation is used, affecting consolidation rates (Barksdale *et al.,* 1983; Balaam & Booker, 1981). Stone columns are known to improve load-bearing capacity and decrease soil compressibility under static loads, though their performance under cyclic loading, such as in railway applications, has not been extensively studied. According to Ashour (2015), stone columns in clayey soils undergoing cyclic loading can reduce threshold stress and pore water pressure by facilitating drainage. To overcome the limitations of traditional models, researchers have developed a finite-difference model based on modified Cam clay theory, supported by comprehensive field and lab tests, to assess the performance of stone columns under cyclic loads. In practical scenarios, the load is distributed across the entire composite area of the stone columns and the treated ground, typically arranged in triangular, square, or hexagonal patterns (Balaam & Booker, 1981; Moradi *et al.,* 2018). Triangular footings have been found to provide superior load-bearing capacity (Al

Mosawe et al., 1985), and research by Thakur et al. (2021) has further explored the effects of the distribution of encased columns (see Fig.III.4).
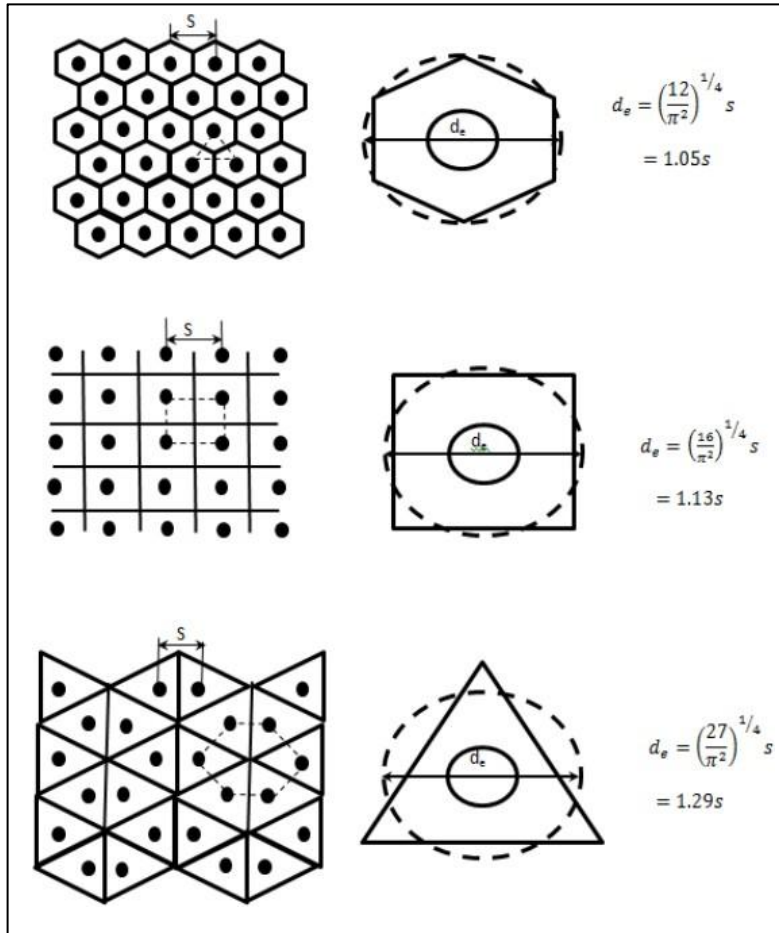
Fig. III. 4 The arrangement of stone columns: **(a)** Triangular Arrangement, **(b)** Square Arrangement, and **(c)** Hexagonal Arrangement. These layouts, redrawn from Balaam and Poulos (1983).

Where:

S: spacing between two stone columns.

The study conducted by Jayarajan et al. (2021) investigated different installation patterns of granular columns and drew several important conclusions. Among the patterns examined, it was found that granular columns installed in a triangular plan arrangement exhibited the highest improvement in bearing capacity and reduction in settlement. This particular pattern proved to be the most effective in enhancing the performance of the granular columns.

In contrast, the hexagonal pattern demonstrated the lowest area replacement ratio and improvement factors compared to both square and triangular patterns. This indicates that the hexagonal pattern alone may not yield significant improvements in terms of bearing capacity and settlement reduction.

However, the study revealed that the performance of granular columns installed in a hexagonal pattern could be enhanced by employing geosynthetic encasement. Geosynthetic encasement played a crucial role in improving the effectiveness of the hexagonal pattern and brought its performance closer to that of more efficient patterns like square and triangular arrangements. Thakur et al. (2021) conducted a laboratory test aimed at examining the application of vertically and horizontally reinforced stone columns as a remedial approach for ordinary unreinforced stone columns. The study focused on two cases of stone column groups: one consisting of three columns arranged in a triangular pattern, and the other comprising four columns arranged in a square pattern as shown in Fig. III.4. The findings show that the vertical encasement of stone columns in a group of 3 led to a significant increase in bearing capacity, with a 76.7% improvement compared to the horizontally reinforced group of 3 stone columns. Similarly, in the case of a set of 4 stone columns, the vertical encasement resulted in an 81.9% increase in load-carrying capacity, slightly lower than the 83.6% increase observed with horizontal reinforcement. These findings demonstrate the effectiveness of both vertical and horizontal reinforcement methods in enhancing the bearing capacity of stone columns. However, when considering floating columns in weak sandy soil, the study suggests that the horizontal reinforcement method may be more favorable. Although the percentage increase in bearing capacity was slightly higher with vertical encasement, the difference was minimal, indicating that both methods can effectively improve the load-carrying capacity of stone columns in such soil conditions.
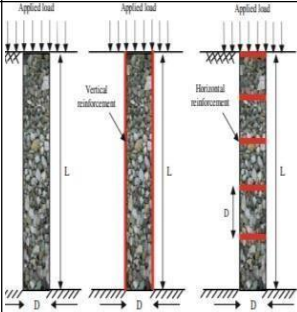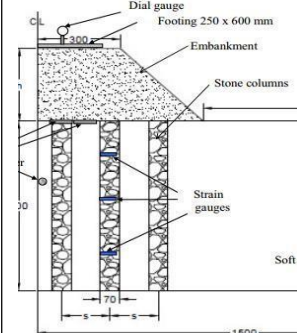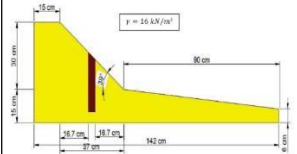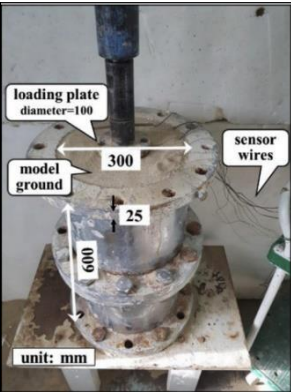
Fig. III. 5 a. Group of 3 stone columns. **b.** Group of 4 stone columns
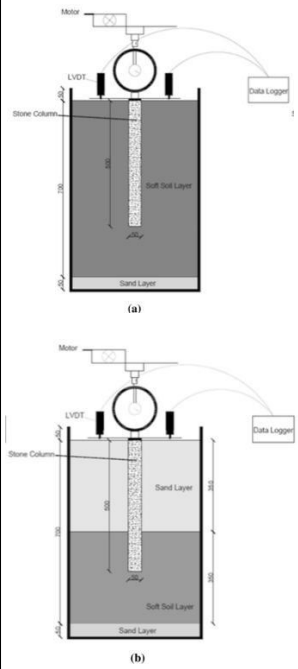
1.2.2.3. Loading Area
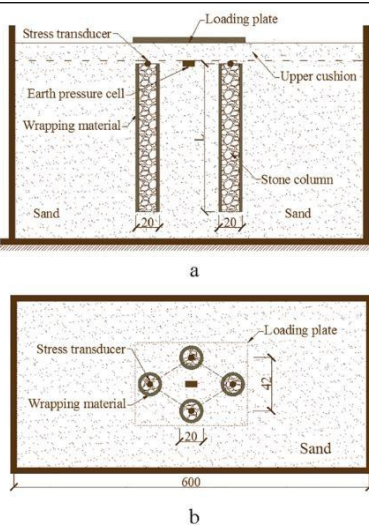
Small groups of stone columns are frequently used to strengthen restricted loaded areas, like pads or strip footings. Larger clusters of stone columns are used, however, for more expansive laden regions, such as embankments. Because of their comparatively lesser bearing capacity, the periphery columns are especially significant in smaller clusters. Furthermore, the performance and design concerns for these systems may be impacted by the fact that the vertical stress beneath a small loaded area drops more quickly with depth than the stress beneath a broader foundation (Killeen and McCabe, 2014).

Table. III. 1 Previous laboratory studies on encased stone columns

References	Soil type	Fill materials	Geosynth-tics used	Dimensions of tank or boxused	Soil bed formation	Method of installation	Loading arrangement	D	Ar	l/d ratio	Setup sketch	Main conclusions
Afshar & Ghazavi 2014) (Nazari Afshar & Ghazavi, 2014)	Clay	Crushed stone	Nonwoven polypropylene geotextile	Large test boxwith plan dimensions of 1,200 mm x 1,200 mm	Compaction	Replacement	Rigid steel loading plate with a diameter of 200 mm and a thickness of 30 mm	60, 80, and 100	0.300, 0.400, and 0.500	5.00		The study demonstrated the effectiveness of columns reinforced with a cage constructed from geotextile or geocell discs. Nevertheless, the researchers advised conducting additional tests to evaluate the load-carrying performance of columns with equal area ratios of replacement.
Fattah et al. (2016)(Fattah *et al.*, 2016)	Clayey siltysoil	Crushed stone	Pars mesh polymer type SQ12	Steel container of 1,500 mm length, 800 mm width, and 1,000 mm depth	Putting in the wet soil in 11 layers by light tamping	Replacement	Footing-type foundation under embankment resting on grouped stone column; load is applied by a hydraulic system	70	Varying spacing between columns 2.5d, 3d, and 4d	5.0 and 8.0		In testing an embankment model constructed on soft soil reinforced with a group of encased stone columns, it was observed that the bearing capacity of the system increased with the reduction in spacing between the stone columns, particularly at a given embankment height.
(Nasiri & Hajiazizi, 2019)	Kermanshah sand)	The stone particles	Non-woven geotextile	Test box, Size of box is 20 cm (width) × 55 cm (height) × 142 cm (length).	Sandy embankment	A plastic encase with a diameter of 3.6 cm was used for constructing the OSC.	In each step of loading after 10 min 1 kg was applied on the crown of slope.	36	-	Various		The optimal placement for stone columns is at the middle of the slope, where shear displacements are most pronounced. Experimental and numerical analyses consistently show that Geosynthetic-Encased Stone Columns (GESC) significantly enhance both the safety factor and bearing capacity compared to Ordinary Stone Columns (OSC).

| (Yoo & Abbas, 2020) | Sand | aggregates | 3 types of nonwoven polypropylene | Test cell of 300 mm diameter and 600 mm height was used | Sand in four lifts by tamping to a target relative density of 50% | Replacement | The load (monotonic, cyclic loads on the GESC) was applied by hydraulic system A 100 mm diameter circular loading plate was placed over the GESC with its center in line with the center of the GESC. Each test was comprised of three loading phases: pre-cyclic monotonic, cyclic, and post cyclic monotonic loading. | 50 | 0.5 | 12 | | The geosynthetic encasement significantly improves the performance of stone columns under cyclic loading, surpassing its benefits under static conditions. It reduces load transfer and achieves a 25% reduction in the stress concentration ratio. For optimal performance, full encasement is recommended, as it extends the lateral bulging zone beyond the critical encasement length seen under static loading. This finding has important implications for engineering design and application. |

Reference	Soil	Stone	Geosynthetic	Tank size	Soil configuration		Construction	Loading				Image	Remarks
(Farah & Nalbantoglu, 2020)	35-cm-soft soil +5-cm-thickness of sand at the bottom	The crushed stone aggregate	Non-woven geotextile	test tank a size of 750 × 750 × mm (Length, width, and thickness).	single-layered soft soil: 50 mm of sand +700 mm soft soil. (a) Layered soil: 50 mm of sand + 350 mm of soft soil+ 350-mm- of sand. (b)	-	The steel pipe at the center was filled with stones into batches.	The load was applied via a 50-mm-diameter circular steel plate with 38 mm thickness	50	1	100		Geotextiles enhanced bearing capacity by effectively distributing induced stresses over a larger area. In single-layer soft soil, non-encased stone columns exhibited maximum bulging at a depth of 1.5 times their original diameter. In contrast, encased stone columns managed to transfer the maximum bulging to a depth of 3.0 times their original diameter.
(Xu, Moayedi, et al., 2021)	Poorly graded clayey sand (SP-SC)	Poorly graded gravel (GP) Stone aggregate	2 types pf Polypropylene and steel	square tank with a size of 0.75 × 0.75 × 0.75 m (Length, width, and thickness).	Poorly graded clayey sand (SP-SC)	-	The steel pipe at the center was filled with stones into batches	Load was applied on square steel plate of 300 × 300 × 8 mm (length, width, and thickness).	10	0.03	1.5, 3,4.5, 6.		Short stone columns often tend to punch into soft soil under minimal stresses, resulting in stress concentration along the columns. However, well-designed stone columns can significantly enhance the bearing capacity of soft soils and minimize settlements, even when they are short. To achieve optimal performance and avoid problems such as stress concentration and punching into the soil, it is crucial to consider factors such as depth, length, and encasement properties during the design process.

(Gao *et al.*, 2021)	Sand	crushed stone	Three types of geogrids: - single-ribbed geogrid (GG1), - Double-ribbed geogrid (GG2) -Fine metal mesh (GG3).	, the inner dimensions of the model box (length × width × height) are 600 mm × 290 mm × 400 mm, a	The sand used to fill the soil in layers of 50 mm.	The steel pipe at the center was filled with stones into batches	The cyclic loading	20	0.3	150, 200, 250		Cyclic loading impacts the distribution of load between the soil and the stone column, with the stone column bearing a greater portion of the load compared to the soil. The performance characteristics of Geosynthetic-Enclosed Stone Columns (GESCs) are significantly influenced by the strength of the wrapping material. Additionally, increasing the length-to-diameter ratio of the columns effectively enhances their performance.

2.   Conclusion

The literature review on the general characteristics of reinforcing soft soils using geosynthetic encased stone columns has demonstrated the effectiveness of this technique and the advantages it offers compared to other reinforcement methods. The study also highlighted that encased stone columns and the surrounding soil form a composite system composed of two materials with significantly different properties and their behavior is determined by considering the properties of both the encased column material and the soil.

Based on this foundation, the essential parameters influencing the behavior of the soil-column system have been identified and presented in this chapter. These parameters include the diameter and length of the columns, as well as the size and quality of the aggregate materials used in the columns (friction angle, cohesion, etc.). Additionally, factors such as the installation technique of the columns and the geometric configuration of the column group (triangular, square, etc.) significantly influence the behavior mode of the columns and their bearing capacity improvement. These influences manifest through various properties of the group, such as column spacing, replacement ratio, stress concentration factor, and critical column length.

PART TWO: NUMERICAL MODELING

Chapter 04

Chapter 4
3D Numerical Modeling of Encased Stone Columns for Soft Clay Stabilization

1. Introduction

Soft soils, with their inherently low shear strength and high compressibility, present substantial construction impediments, particularly due to their poor load-bearing capabilities and tendency to undergo significant deformation under applied stresses. Addressing these challenges requires effective soil improvement techniques, and stone columns have emerged as a highly recognized and viable solution. Originating in Germany during the mid-1930s as an enhancement of seismic consolidation methods for cohesive soils, stone columns have proven to be a robust, cost-effective, and environmentally sustainable method for improving advancements in soil stability and strength over the last thirty years (Hosseinpour et al., 2019). Despite their effectiveness, traditional stone columns face limitations in extreme soil conditions such as peat and very soft soils, where their performance is constrained by inadequate lateral confinement provided by the surrounding soil. To address these limitations, the use of geosynthetic encasement has been introduced, significantly enhancing the lateral confinement and load-carrying capacity of stone columns in challenging environments. The interaction among soil, geosynthetic materials, and stone columns play a critical role in the performance of geosynthetic-encased stone columns (GESC), and this relationship has been extensively explored in recent studies (Yoo and Abbas, 2019; Xu *et al*., 2021; Gao *et al.,* 2021). The accurate simulation of construction conditions and prediction of lateral stress development around these columns necessitate advanced numerical and experimental methods. This is crucial for refining the design and understanding the mechanical behavior of geosynthetic-reinforced stone columns (Alkhorshid et al., 2018; Ghazavi and Nazari Afshar, 2013; Xu *et al.,* 2021). Recent research underscores the need for continued investigation in this field (Nav et al., 2020; Thakur *et al*., 2021; Dar and Shah, 2021; Kahyaoğlu and Doğan, 2022). Installation effects, which encompass the changes in soil properties resulting from the insertion of stone columns, are often overlooked in conventional design practices. These effects can include increases in pore pressures and horizontal stresses, as well as significant remolding of the surrounding soil (Castro and Sagaseta, 2015; Gäb *et al.,* 2007; WATTS *et al*., 2001; Watts *et al*., 2015). Physical modelling techniques like centrifuge testing have been used in an attempt to comprehend these installation impacts, although the soils used in these trials are often artificially created rather than being typical of the environment. There are further difficulties in theoretically modelling installation impacts. Although the idea of cavity expansion has been well-studied (Carter *et al*., 1979), extensive numerical studies that particularly address the effect of installing stone columns are scarce (Guetif *et al*., 2007). By using complex soil models to mimic the behaviour of naturally structured soft soils, recent developments have attempted to close this gap (Castro and Karstunen, 2010). Understanding how installation

effects influence soil improvement is complex but critical. For example, Schweiger's research demonstrated that incorporating installation effects into models can lead to a significant reduction in settlement for circular footings under high loads by increasing mean stress in the clay and enhancing lateral support for the columns. Schweiger's approach, which used a volumetric strain field to approximate installation effects, underscores the importance of accurate modeling. Similarly, Kirsch (Kirsch et al., 2016) investigated the effects of installation on settlement reduction for floating column groups in sandy silt, differentiating between localized installation effects and broader global effects. Kirsch's study, which included field measurements, highlights the practical implications of these effects and their impact on settlement reduction, achieving reductions of up to 40% and 5–25%, respectively.

leterature reviw

Introduction

Numerical modelling

numerical model and material definition

Scope and aims of the present investigation.

Geometry and boundary condition

Initial conditions and material properties

Analysis procedures

validation of the model

results and descusions

performance evaluation

comparative analysis

Installation phase

Reduction settlement ratio

Horizontal displacement

Vertical displacement

short column

float column

OSC

GESC

conclusion

Fig. IV. 1 R e s e a r c h M e t h o d o l o g y O v e r v i e w

1.1. Overview of numerical modelling techniques and major findings

To effectively model the effects of stone column installation, three main approaches have been utilized. To take into consideration the increased stiffness that the columns give, the first method entails raising the initial earth pressure coefficient (K_o). This technique, often used in numerical simulations, adjusts the soil's mechanical properties to reflect a uniform increase in stiffness around the stone columns (Kareem Al Ammari *et al.*, 2018; Kelesoglu *et al.*, 2022). However, this method may oversimplify the distribution of stiffness, as it doesn't account for variations in column diameter, length, or the non-uniformity of stiffness with depth (Elshazly *et al.*, 2008; Al Ammari and Clarke, 2016; Benmebarek *et al.*, 2018). The second approach involves applying a preload to the column and modeling it as an elastic material with a much higher modulus compared to the surrounding soil. This method considers soil stiffening and the interaction between the column and soil but assumes linear elastic behavior of the stone column, which might not fully capture its non-linear response under load (Guetif *et al.*, 2003; Ellouze *et al.*, 2017; Remadna *et al.*, 2020). While this method is straightforward, it may introduce inaccuracies if the column's behavior deviates from the linear assumption. The third approach utilizes the radial expansion technique, which simulates the growth of the stone column by applying a radial displacement proportional to the column's diameter. This method is particularly effective for evaluating columns in soft soils where lateral expansion plays a significant role in the performance of the reinforced soil system (Nguyen *et al.*, 2007). This approach provides several benefits, such as a more accurate depiction of column behavior through non-linear deformation and an effective enhancement of horizontal stresses and soil stiffness (Elshazly *et al.*, 2008). However, pinpointing exact radial displacement values is a complex task that is crucial for replicating real-world conditions accurately. Research indicates that installing stone columns elevates effective horizontal stresses in the adjacent soil, leading to a higher lateral earth pressure coefficient (K) compared to the original value (K_0). The radial expansion technique, known for boosting horizontal stresses and soil stiffness, has been shown to improve these parameters significantly (Guetif *et al.*, 2003, 2007). Observations have revealed that lateral expansions of up to 10% result in (K/K_0) ratios ranging from 1.5 to two. Short columns typically show K values between K_0 and K_p, whereas floating columns present values from 0.7 to 1.5 (Watts *et al.*, 2000; Kirsch, 2006; Sexton and McCabe, 2015). More recent studies have reported K values ranging from 1.6 to 2.0 (Benmebarek *et al.*, 2018; Remadna *et al.*, 2020), underscoring the significant effect of column installation on the lateral earth pressure coefficient. The zone of improvement around stone columns extends approximately eight times the column's diameter from its center, with post-installation K values generally exceeding the initial K_0 of the surrounding soil.

1.2. Scope and aims of the present investigation.

The purpose of this project is to investigate in detail the combined impacts of erecting stone columns and applying geosynthetic encasement for ground improvement, thereby addressing a key research gap. In the past, research has usually concentrated on installing stone columns or geosynthetic encasing independently.

To provide a thorough grasp of their combined consequences, this research, however, integrates both aspects. The work assesses these impacts under several circumstances, such as varying degrees of radial expansion and particular strain situations, using sophisticated numerical analysis, in particular the radial expansion method.

2. Description of the models employed in this investigation

The study investigates three key constitutive models utilized in soil mechanics: the Linear Elastic (LE) model, the Mohr-Coulomb (MC) model, and the Hardening Soil (HS) model. Each model presents distinct approaches to capturing soil behavior under varying conditions.

2.1. Linear Elastic Model (LE):

The LE model, rooted in Hooke's law of isotropic elasticity, centers on Young's modulus (E) and Poisson's ratio (v). While not directly suited for soil modeling, it finds application in representing rigid elements within soil, such as concrete walls and intact rock formations.

2.2. Mohr-Coulomb Model (MC):

The MC model, a linear elastic perfectly-plastic formulation, requires five parameters: E and v for elasticity, ϕ and c for plasticity, and ψ for dilatancy. Serving as a 'first-order' approximation, it offers a pragmatic approach for initial analysis, employing constant or depth-dependent stiffness estimates for each layer.

2.3. Hardening Soil Model (HS):

In contrast, the HS model provides a more sophisticated portrayal of soil behavior. Similar to the MC model, it relies on ϕ, c, and ψ to delineate stress limits. However, it introduces three distinct stiffness parameters: triaxial loading stiffness (E_{50}), triaxial unloading stiffness (E_{ur}), and oedometer loading stiffness (E_{oed}). This model, accounting for stress-dependent stiffness, reflects the evolving behavior of soil under varying pressures, with initial soil conditions, such as pre-consolidation, factored into stress generation. The comparative analysis of these models sheds light on their respective strengths and limitations, offering insights into their applicability across diverse soil mechanics scenarios.

3. Numerical modelling

3.1. Geometry and boundary condition

A fundamental unit, also known as an elementary cell, can adequately depict the collective behaviour of a large number of stone columns under a distributed vertical stress. This concept, explored by researchers such as Castro (2017), Priebe et al. (1995) and Nav et al. (2020), is pivotal for understanding the performance of geosynthetic-encased stone columns (GESC). By utilizing a unit cell model, researchers can gain insights into with particular emphasis on how geosynthetics improve settlement behaviour, the relationships between the stone column, the geosynthetic material, and the surrounding soil. Several aspects, including as loading conditions and installation methods, and their effects on settlement characteristics, can be thoroughly analysed with this model. Several research have used numerical modelling approaches in 2D and 3D to examine GESC behaviour. Maleki and Mir Mohammad Hosseini (2019), Maleki and Imani (2022) and Rahmani et al. (2022)

have made noteworthy contributions. In the current study, PLAXIS 3D, a sophisticated finite element software (Brinkgreve R.B.J. *et al*., 2016), was used to investigate the effects of stone column installation. The research concentrated on the effects of geosynthetic encasement on important parameters, including the settlement reduction ratio (β), vertical displacement under a rigid foundation, and fluctuations in the earth pressure coefficient surrounding the perimeter of the column. To represent a variety of behaviours, other situations were examined, such as floating columns and short columns. The behaviour of GESC centrally positioned beneath a gravel mattress and a stiff foundation was simulated in this work using a unit cell model a surface load of 50 MPa on cohesive soil was supported by a solid foundation measuring 20 cm wide and a gravel mattress measuring 50 cm broad. The unit cell's heights ranged from 10 to 20 meters, while its dimensions ranged from two to 6 meters by 2 meters. The diameter (d_c) and length (L) of the stone column inside the unit cell were 1 and 10 meters, respectively. In order to capture intricate interactions, a triangular mesh with 10 node elements and a medium mesh size was utilised, with additional refinement underneath the footing and around the column. To provide stability and avoid both vertical and horizontal movement (U_x and U_z), pin supports were applied at the bottom boundary of the model. These supports resisted vertical and horizontal forces but allowed rotations. Roller supports were used on the vertical sides, preventing horizontal movement and rotation while enabling vertical movement, maintaining stability during settling (Fig. IV. 3) This setup effectively minimized boundary effects on the numerical model results, as indicated by displacement and stress contours in the finite element software (Maleki and Nabizadeh, 2021; Maleki and Mir Mohammad Hosseini, 2022; Maleki *et al.,* 2023). To simulate the installation effects, the lateral expansion method was applied. Horizontal lateral expansion values ranging from 0% to 15% were introduced in the x and y directions, with strains defined as $\varepsilon_v = 2\varepsilon_x = 2\varepsilon_y$ and $\varepsilon_z = 0$. This approach effectively captures the installation impact on the surrounding soil and stone column interaction, providing a
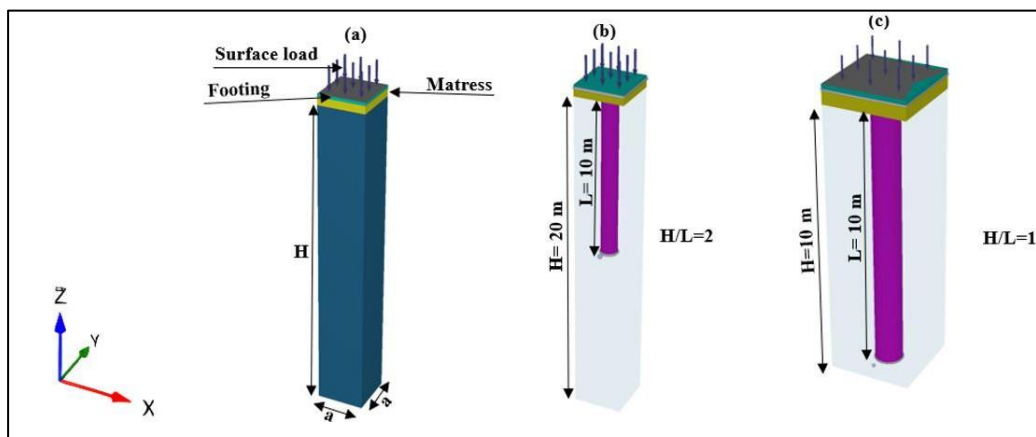
realistic representation of the changes in soil behavior due to the presence of the column.

Fig. IV. 2 a. 3D representation of the unit cell model, **b.** floating column, **c.** short column (Bahi and Houhou, 2024).

3.2. Initial conditions and material properties

In the early stage of this research, an analysis of various unit cell dimensions was conducted, including sizes of 2 m x 2 m, 2.5 m x 2.5 m, 3 m x 3 m, 4 m x 4 m, and 6 m x 6 m. The height-to-length ratio (H/L) was determined to be one for short columns and two for floating columns. A unit cell size of 3 m x 3 m was chosen for detailed analysis because it offers detailed insights into the behavior of geosynthetic-encased stone columns. Throughout the study, the column diameter (d_c) was consistently set at 1 m, with a column length (L) of 10 m. The hardening model criterion was used to accurately predict the behaviour of stone columns and very soft soil, as it efficiently models materials that experience plastic deformation and fluctuations in shear strength under varied loading circumstances. This method is especially important for fitting a wide range of soil types and dynamic loading scenarios, such as seismic occurrences and soil consolidation, which improves forecast accuracy for settlements, deformations, and overall soil behaviour (Tan *et al*., 2013). Numerous numerical studies have supported the use of the Mohr–Coulomb criterion to simulate gravel under drained circumstances (Halder and Manna, 2022; Ghaemi *et al.,* 2021; Jabir *et al.,* 2020; Nafees *et al.,* 2021; Iqbal *et al.,* 2021; Zhao *et al.,* 2023;; Castro, 2014; Gholaminejad *et al*., 2020; Killeen and McCabe, 2014; Sukmak *et al.*, 2021;Tan *et al*., 2014). The axial stiffness (EA) of the geosynthetic materials was chosen based on a typical range of 100 to 4000 MPa, as reported in various literature sources (Zhou *et al.,* 2019; Jamshidi Chenari and Bathurst, 2023). For this analysis, an axial stiffness of 4000 MPa was selected, aligning with the research parameters and objectives to ensure optimal performance of the geosynthetic-encased stone columns. Interface elements were not employed for modelling the Geosynthetic Encased Stone Columns (GESC) in this study. Instead, an interaction parameter R_{inter}=0.85was used between the encased column and the surrounding soil. Detailed information on the properties of the various materials used in the simulation is presented in Tables IV.1 and IV.2. By adjusting the cross-section ratio (A/A_c), the study aimed to evaluate how lateral expansion of the encased stone column affected settlement reduction ratios (β), where A represents the surface area of the unit cell and A_c represents the surface area of the column. Stone columns in actual geotechnical applications can experience lateral expansion of up to 10%, emphasising the need of considering this effect. For a complete understanding of lateral expansion behaviour and to evaluate the performance of stone columns in a variety of scenarios and settings, it is imperative to analyse expansion values above and below 10% (Nguyen *et al*., 2007). This method makes it easier to forecast how enclosed stone columns will behave in terms of reducing settling and improving the ground overall. In this study, the impact of varying radial expansion values, ranging from 0% to 15%, on geosynthetic encased stone columns (GESC) was analysed to understand their effect on the earth pressure coefficient (K) near the column edge and the vertical displacement (U_z) beneath a rigid foundation. Various configurations, including short columns, floating columns, ordinary stone columns (OSC), and GESC, were investigated to evaluate the influence of encasement and radial expansion on these parameters. Fig. IV.4, which presents simulations with various lateral expansion values,

shows the mesh configuration and the overall displacement profile prior to vertical loading. increasing displacement along the column perimeter is positively correlated with increasing lateral expansion, as the data clearly show. The surrounding soil deforms and moves more significantly with increased lateral expansion, suggesting a strong contact between the column and the surrounding soil. This link is consistent with theory, which states that greater lateral expansion amplify the column's impact and interaction with the surrounding soil structure. The examination of earth pressure coefficients showed that increasing lateral expansion values led to significant changes in the earth pressure coefficient (K) near the column edge. This change in pressure reflects how the column exerts force on the surrounding soil, causing it to accommodate the expanded column through deformation. Consequently, the vertical displacement (   ) under the rigid foundation is also affected, demonstrating that lateral expansion plays a critical role in influencing the settlement behavior of stone columns. These findings provide valuable insights into the behavior of stone columns during installation, particularly regarding how lateral expansion affects soil-structure interaction. Understanding this relationship aids in optimizing ground improvement strategies, ensuring that stone column installations are designed to maximize their effectiveness in stabilizing and reinforcing soft soils. By analyzing different scenarios and configurations, this study contributes to a more comprehensive understanding of the mechanical behavior of stone columns, guiding engineers in making informed decisions regarding the implementation of geosynthetic encased stone columns in various geotechnical projects.
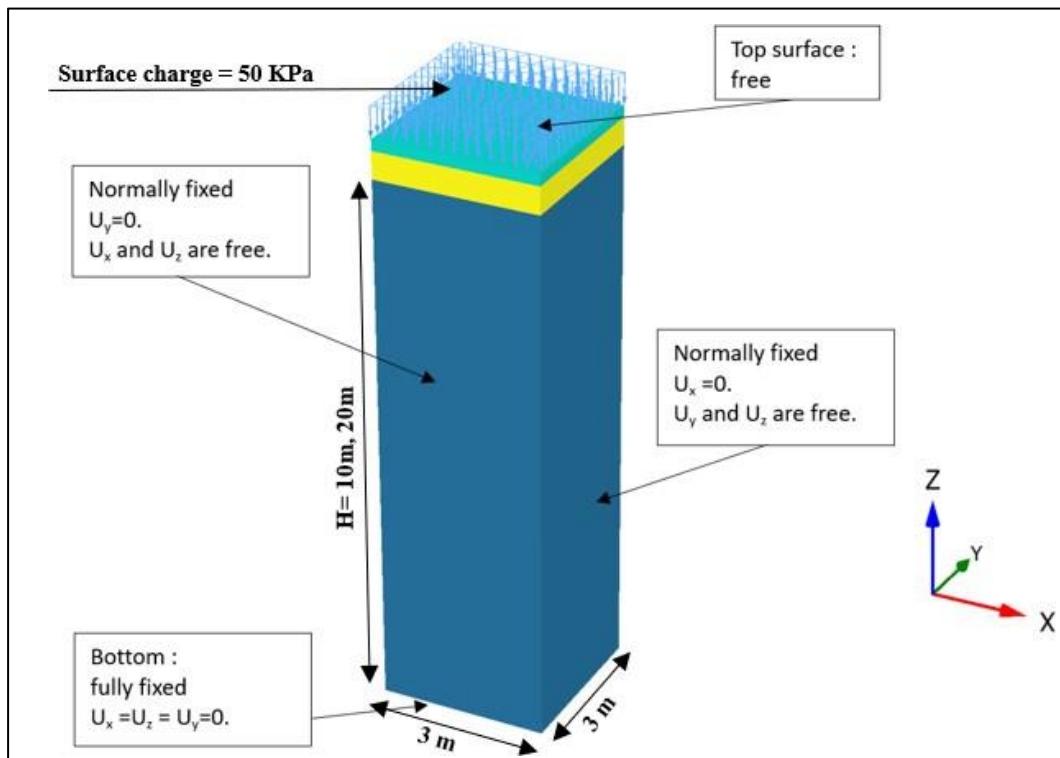
Fig. IV. 3 Unit Cell Geometry and Boundary Conditions (Bahi and Houhou, 2024)

Total displacements |u| (scaled up 5,00 times) Maximum value = 8,617*10⁻³ m (Element 78987 at Node 27896)	**Total displacements |u| (scaled up 5,00 times)** Maximum value = 0,01626 m (Element 51300 at Node 802)
0%	2 %
Total displacements |u| (scaled up 5,00 times) Maximum value = 0,03100 m (Element 55447 at Node 10)	**Total displacements |u| (scaled up 5,00 times)** Maximum value = 0,03996 m (Element 55447 at Node 10)
5.5 %	7.5%
Total displacements |u| (scaled up 5,00 times) Maximum value = 0,05186 m (Element 55447 at Node 10)	**Total displacements |u| (scaled up 5,00 times)** Maximum value = 0,08977 m (Element 56378 at Node 825)
10%	15%
A	

Total displacements |u| (scaled up 5,00 times)

Maximum value = 0,02468 m (Element 622 at Node 4265)

0%

Total displacements |u| (scaled up 5,00 times)

Maximum value = 0,03231 m (Element 3089 at Node 2778)

2 %

Total displacements |u| (scaled up 5,00 times)

Maximum value = 0,04503 m (Element 637 at Node 346)

5.5 %

Total displacements |u| (scaled up 5,00 times)

Maximum value = 0,05114 m (Element 667 at Node 3632)

7.5%

Total displacements |u| (scaled up 5,00 times)

Maximum value = 0,05916 m (Element 667 at Node 3634)

10%

Total displacements |u| (scaled up 5,00 times)

Maximum value = 0,08169 m (Element 622 at Node 9)

15%

$[*10^{-3}$ m$]$

80,00
70,00
60,00
50,00
40,00
30,00
20,00
10,00
0,00

B

Fig. IV. 4 3D mesh visualization of total displacement under varying lateral expansion values: **a.** short column, **b.** Float column (Bahi and Houhou, 2024).

Table. IV. 1 the footing and gravel material parameters (Nguyen et al., 2007).

Name	(KN/m^3)	(KN/m^2)		(KN/m^2)	$\Phi(°)$
Footing	25	30 000	0.2	-	-
Gravel mattress	20	100000	0.25	1	38

Table. IV. 2 Soil and stone column parameters (Tan et al., 2013).

Name	(KN/m^3)	50 (/ ^{2})	(/ ^{2})	(/ ^{2})	C' (/ ^{2})	$\varphi'(°)$	V_{ur}	(/ ^{2})	m
Stone column	20	10000	10000	30000	1	45	0.2	100	0.5
Soil	16	3000	2500	10000	1	25	0.2	100	1

3.3. Analysis procedures

The various calculation stages are detailed in Table IV.3.

Table. IV. 3 Phases of calculation (Bahi and Houhou, 2024)

Phases	Description
1	Establish the initial phase by applying the $_0$ procedure, where $_0$ is calculated using the formula Establish the initial phase using the K_0 procedure: $K_0 = 1 - \sin \varphi'$
2	Installation Phase: Simulate different values of lateral expansion for the column, treating each expansion value as a separate phase. The values to be modeled include 0% (represented as "wished in place"), 2%, 5.5%, 7.5%, 10%, and 15%.
3	Activate the single Geosynthetic Encased Stone Column (GESC), along with the gravel layer and rigid foundation, and apply a surface load of 50 $kN/m²$ to the GESC.
4	A plastic analysis was performed to permit settlement caused by the applied surface load.

4. Model validation

In this study, the validation of the 3D numerical model was rigorously assessed by comparing its results with the findings of renowned researchers such as Poorooshasb and Meyerhof (1997), Priebe (1995), and Pulko and Majes (2005). These previous studies were based on direct observations of a solid foundation subjected to a uniform load, backed by an endless square-shaped grid of ballasted columns.

The curves comparing the settlement reduction ratios obtained from this study at different column lateral expansion levels with findings from earlier studies are shown in Fig. IV.5. Although the validated simulation values from the current study do not incorporate geosynthetic material, the numerical simulation results closely match the data from earlier research. This consistency highlights the robustness and reliability of our

methodology. The model can faithfully reproduce observed settlement patterns, as demonstrated by the alignment of our results with established research. This validates the model's efficacy and suggests that geotechnical engineering may benefit greatly from it. The behaviour of geosynthetic-reinforced stone columns and regular stone columns was thoroughly compared using three-dimensional modelling. Deeper understanding of the performance of stone columns under varied situations was obtained by integrating the installation impacts of the columns utilising the lateral expansion approach in this analysis.

Conditions of the current study: $E_c/E_s = 20$, $L/D = 10$, $H/L = 1$, $E_s = 5000$ kPa.
Pulko et Majes (2005), $E_c/E_s = 40$, a: elasticity analysis.
Pulko et Majes (2005), $E_c/E_s = 40$, b: elasto-plasticity analysis.
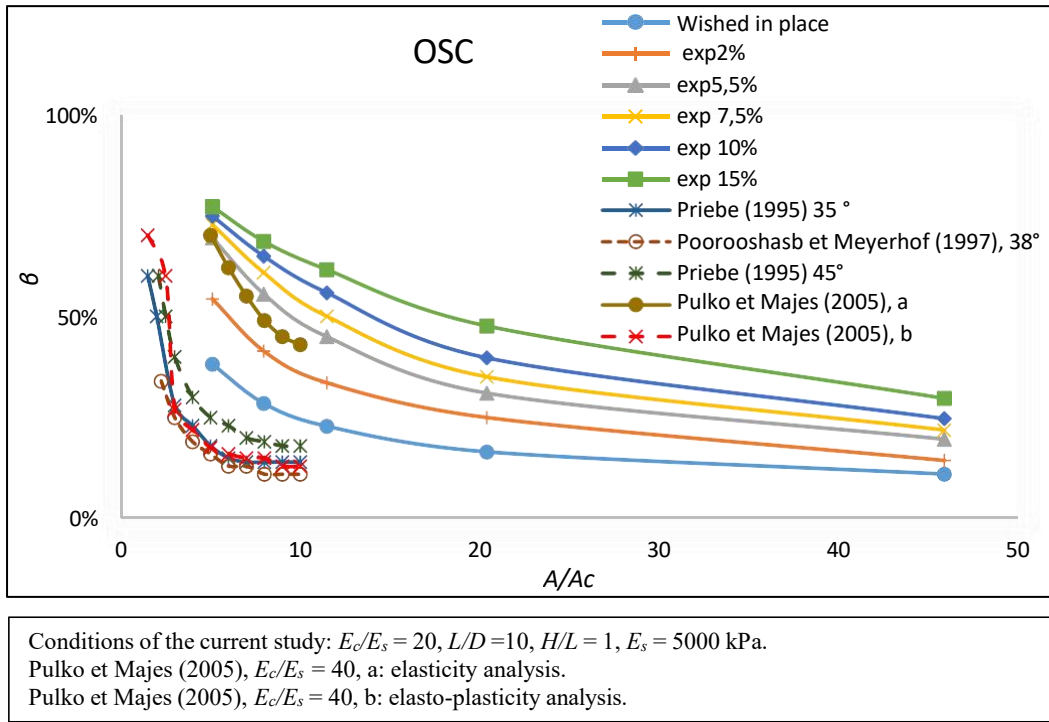
Fig. IV. 5 Settlement reduction ratio evolution (Bahi and Houhou, 2024)

5. Analysis and Interpretation of Results

5.1. Installation phase

To accurately model variations in lateral ground pressure following installation, the lateral expansion approach was employed in this study. Various lateral expansion values were assessed (wished in place (exp 0%), exp 2%, exp 5.5%, exp 7.5%, exp 10%, and exp 15%), as shown in Fig. IV.4. The K_0 was calculated using Jaky's formula ($K_0 = 1 - \sin\varphi'$). Fig. IV.7 illustrates the progression of earth pressure coefficients for both short and long columns near the column edge at cross-section (AA'). The figure highlights three zones: the column edge, the area beyond the column edge, and the cell edge. The K ratio peaks at the column edge for both short and long columns, with short columns exhibiting higher ratios. The ratio declines as it approaches the cell boundary. Beyond the column edge, long columns generally show higher ratios, but at the cell edge, the trend reverses, with long columns displaying lower values than short columns. Notably, without radial expansion (0% expansion), the K/K_0 ratio remains at one. As radial expansion increases, the ground pressure
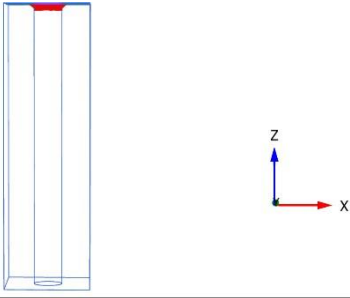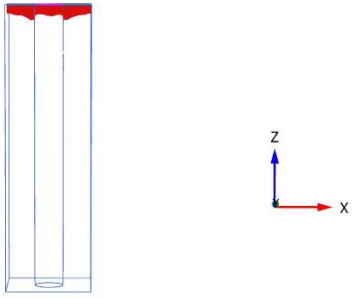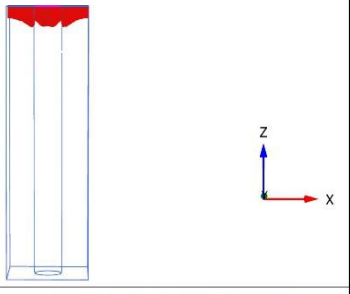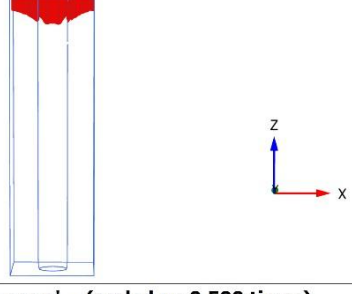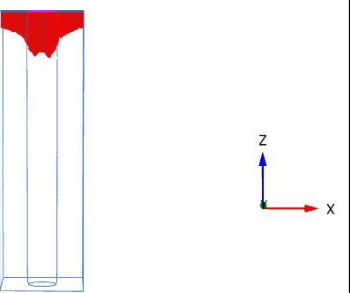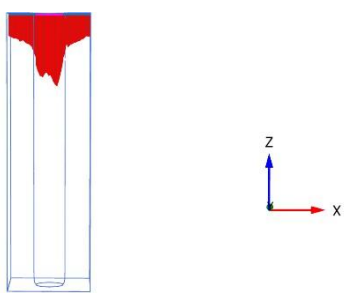
coefficient rises proportionally. For short columns, the earth pressure coefficient at the edge ranges from 2.57 to 3.38, while for long columns, it varies between 1.68 and 3.28 across different radial expansion values (exp 2%, exp 5.5%, exp 7.5%, 10%, 15%). Fig.IV.8 depicts the changes in horizontal stress at a depth of 0.5 m along the same cross-section (*AA'*), emphasizing the critical role of radial expansion in soil behavior and its significance in geotechnical engineering applications.
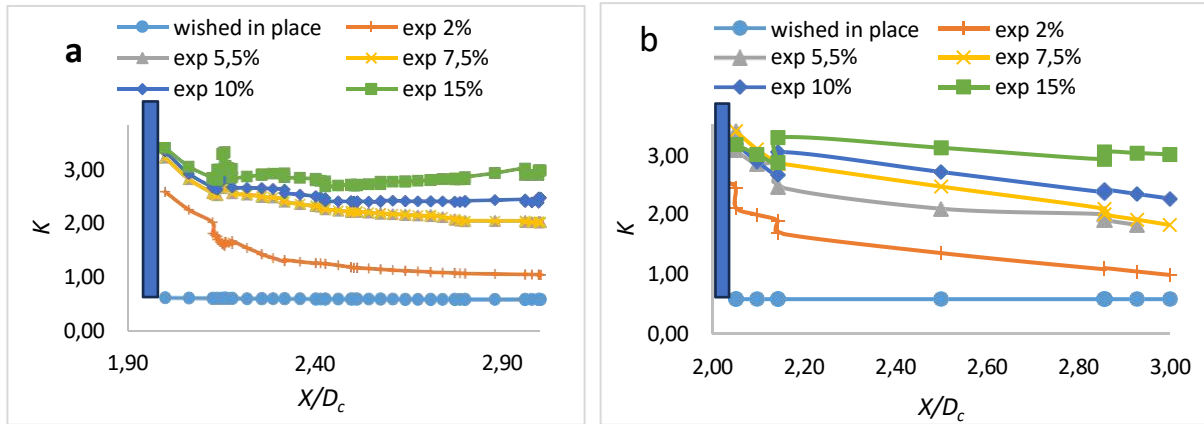
Fig. IV. 6 Normalized effective stress variation following column installation: **a.** short column, **b.** float column (Bahi and Houhou, 2024)
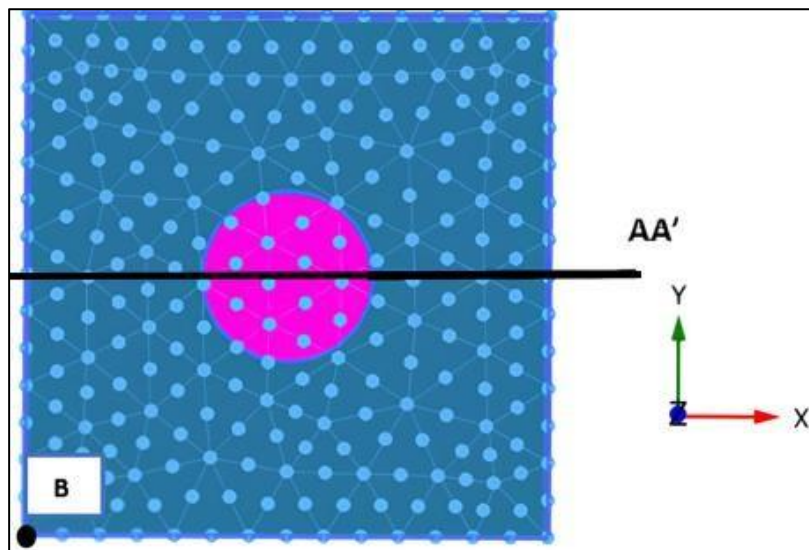
Fig. IV. 7 Position of the studied points and cross-sections (Bahi and Houhou, 2024)

Cartesian effective stress σ'ₓₓ (scaled up 0,500 times) Maximum value = 0,06478 kN/m² Minimum value = -0,5048 kN/m²	**Cartesian effective stress σ'ₓₓ (scaled up 0,500 times)** Maximum value = -0,6165 kN/m² Minimum value = -1,085 kN/m²
0%	2 %
Cartesian effective stress σ'ₓₓ (scaled up 0,500 times) Maximum value = -0,8658 kN/m² Minimum value = -1,547 kN/m²	**Cartesian effective stress σ'ₓₓ (scaled up 0,500 times)** Maximum value = -1,009 kN/m² Minimum value = -2,043 kN/m²
5.5 %	7.5%
Cartesian effective stress σ'ₓₓ (scaled up 0,500 times) Maximum value = -1,178 kN/m² Minimum value = -3,375 kN/m²	**Cartesian effective stress σ'ₓₓ (scaled up 0,500 times)** Maximum value = -1,538 kN/m² Minimum value = -5,260 kN/m²
10%	15%
A	

Fig. IV. 8 Lateral stress distribution for various lateral expansion values: **a.** short column, **b.** float column
(Bahi and Houhou, 2024)

5.2. Reduction settlement ratio

Yoo et al. (2020) describe the reduction settlement ratio (β) as a key metric for evaluating the effectiveness of ground improvement methods. This ratio is calculated by dividing the settlement (S) of the original, unimproved ground by the settlement of the ground after improvement, as outlined by Kirsch (2006). A higher

reduction settlement ratio (*β*) indicates a more effective ground improvement technique, as it demonstrates a significant decrease in settlement.

$$\beta = \frac{S_{without\ reinforcment}}{S_{with\ reinforcement}}$$ *Eq. IV. 1*

A comparative analysis was performed on several types of columns (with the data shown in Figs. IV.6 and IV.7), including short and float columns, and ordinary and geosynthetic encased columns (OSC and GESC). The results indicate that an increase in the section ratio (*A/A_c*) results in the settlement reduction ratio (*β*) falling. This pattern is explained by the soil mass's greater cross-sectional area, which requires more soil compression and displacement by the stone columns. Either larger or more columns are required to obtain the same level of settlement decreaseIn particular, a settlement reduction factor that was considerably lower was obtained with a greater section ratio (*A/A_c* > 20) compared to a settlement reduction factor that increased quickly with a smaller section ratio (*A/A_c* < 10). Approximately three times the column diameter (*3d_c*) is the column spacing in real-world circumstances, meaning that a section ratio of about 10 is normalWith a radial expansion of roughly 7.5% for the ordinary stone column (OSC), the short column succeeded in reducing settlement by 50%, as shown in Fig. IV.9. In contrast, the geosynthetic encased stone column (GESC) achieved the same settlement reduction ratio with a radial expansion of around 5%, indicating that the GESC required less expansion to achieve the same reduction as the OSC. In comparison to short columns, floating stone columns achieved settlement reductions of 47% and 50% for OSC and GESC, respectively, with a 15% radial expansion. These results are shown in Fig. IV.10. These results highlight the significance of the research, offering insightful information about how well geosynthetic encasement and lateral expansion might reduce settlement.
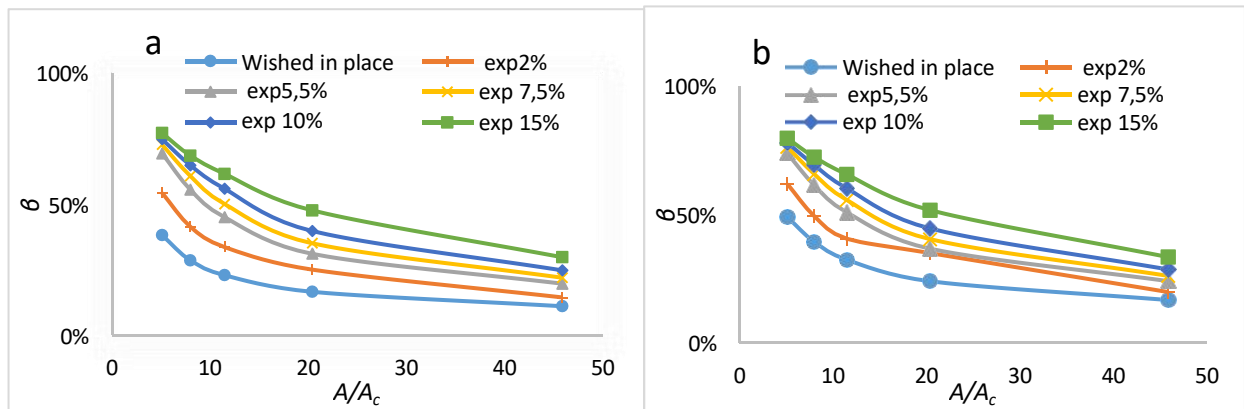
Fig. IV. 9 Settlement reduction ratio for the short column scenario (H/L=1): **a.** OSC, b. GESC (Bahi and Houhou, 2024)
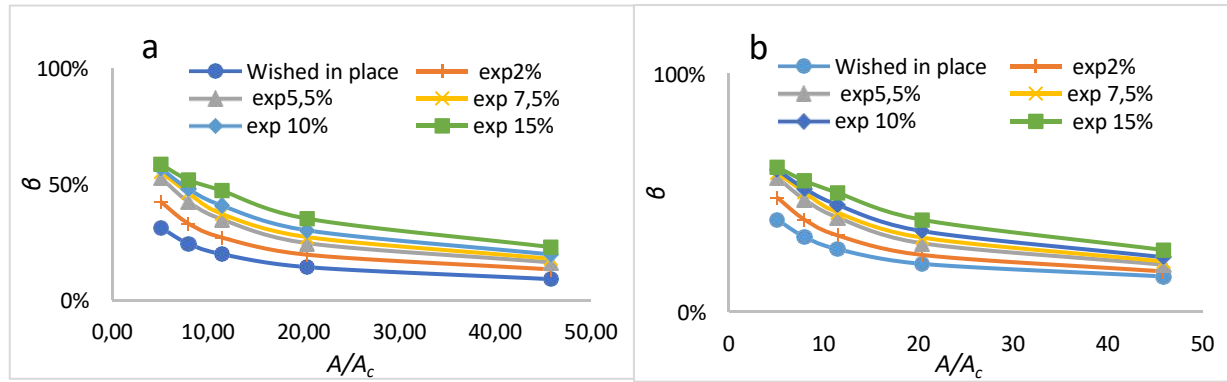
Fig. IV. 10 Settlement reduction ratio for the floating column scenario (H/L=2): **a**. OSC, **b.** GESC (Bahi and Houhou, 2024)

5.3. Horizontal displacement

This section examines the effects of installation on the deformation of stone columns, specifically focusing on horizantal displacement at the column-soil contact. The study includes both short and floating columns, with and without geosynthetic encasement, using a unit cell of dimensions 3 m x 3 m and a column length (L) of 10 meters. The height (H) of the columns was varied to achieve height-to-length ratios (*H/L*) of 1 and 2. The investigation, illustrated in Figs. IV. 11 and 12, explores how different values of lateral expansion impact the column's edge's horizontal displacement (U_x) in relation to depth. The results reveal a notable difference between ordinary columns and geosynthetic encased columns (GESC). The ordinary columns exhibited significantly greater lateral displacement compared to the encased columns, with the geosynthetic encasement reducing lateral displacement to approximately one-fifth of that observed in the ordinary columns. Both column types experienced an increase in lateral displacement up to a specific depth—1 meter for short columns and 2 meters for floating columns—where maximum bulging was observed. Beyond this depth, the displacement gradually decreased. For short columns, displacement slightly reduced near the column base, while for floating columns, it increased, resulting in lateral bending due to soil confinement. Contrary to McCabe and Killen's (2016) findings, which identified punching as the predominant deformation mode at the upper section of the column, this study found that significant lateral bulging and deformation also occurred at lower depths. The experimental results of McKelvey *et al.* (2004) show that floating columns showed punching into the underlying clay and bulging along their length. This combination of punching and bulging is consistent with those findings. The analysis demonstrates that increasing lateral expansion significantly mitigates lateral displacement, with the most substantial reductions occurring close to the base of the column and at the depth of maximal bulging. Enhanced lateral expansion results in increased effective horizontal stress within the surrounding soil, improving confinement and reducing both lateral and vertical soil displacement. This effect leads to decreased footing settlement. However, It is important to remember that in some circumstances, abnormally high K_0 values may be harmful. Figs. IV. 11 and 12 illustrate that while the general shape of the displacement curves remains consistent with increasing lateral earth pressure coefficients, higher

lateral expansion effectively reduces maximum column bulging. For instance, at various expansion levels (0%, 2%, 5.5%, 7.5%, 10%, and 15%), the maximum bulging for short columns ranges from approximately 1.88 cm to 1.21 cm for ordinary stone columns (OSC) and from 0.40 cm to 0.32 cm for GESC. For floating columns, the maximum bulging values range from 1.52 cm to 1.01 cm for OSC and from 0.423 cm to 0.283 cm for GESC. Increasing lateral expansion up to 15% effectively reduces lateral displacement to zero at a depth of 4 meters in various scenarios. Figures IV. 13 and 14 provide visual representations of the lateral displacement shading and deformation characteristics, further illustrating the study's findings.
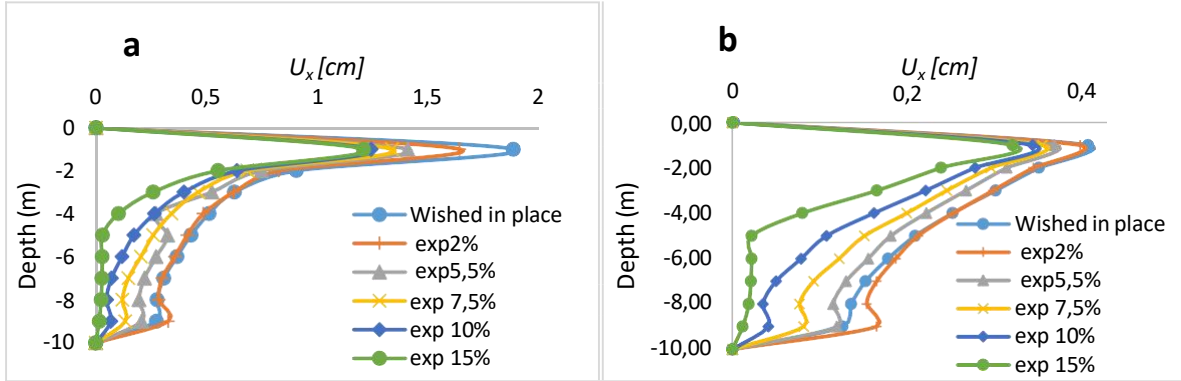
Fig. IV. 11 The lateral displacement observed in the case of short columns (H/L=1): **a.** OSC, **b.** GESC (Bahi and Houhou, 2024)
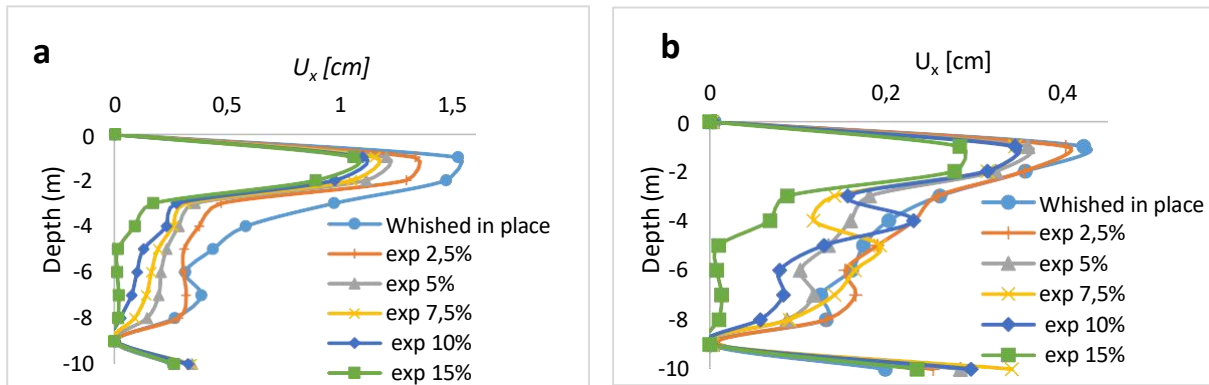
Fig. IV. 12 The lateral displacement observed in the case of float column (H/L=2): **a.** OSC, **b.** GESC (Bahi and Houhou, 2024)
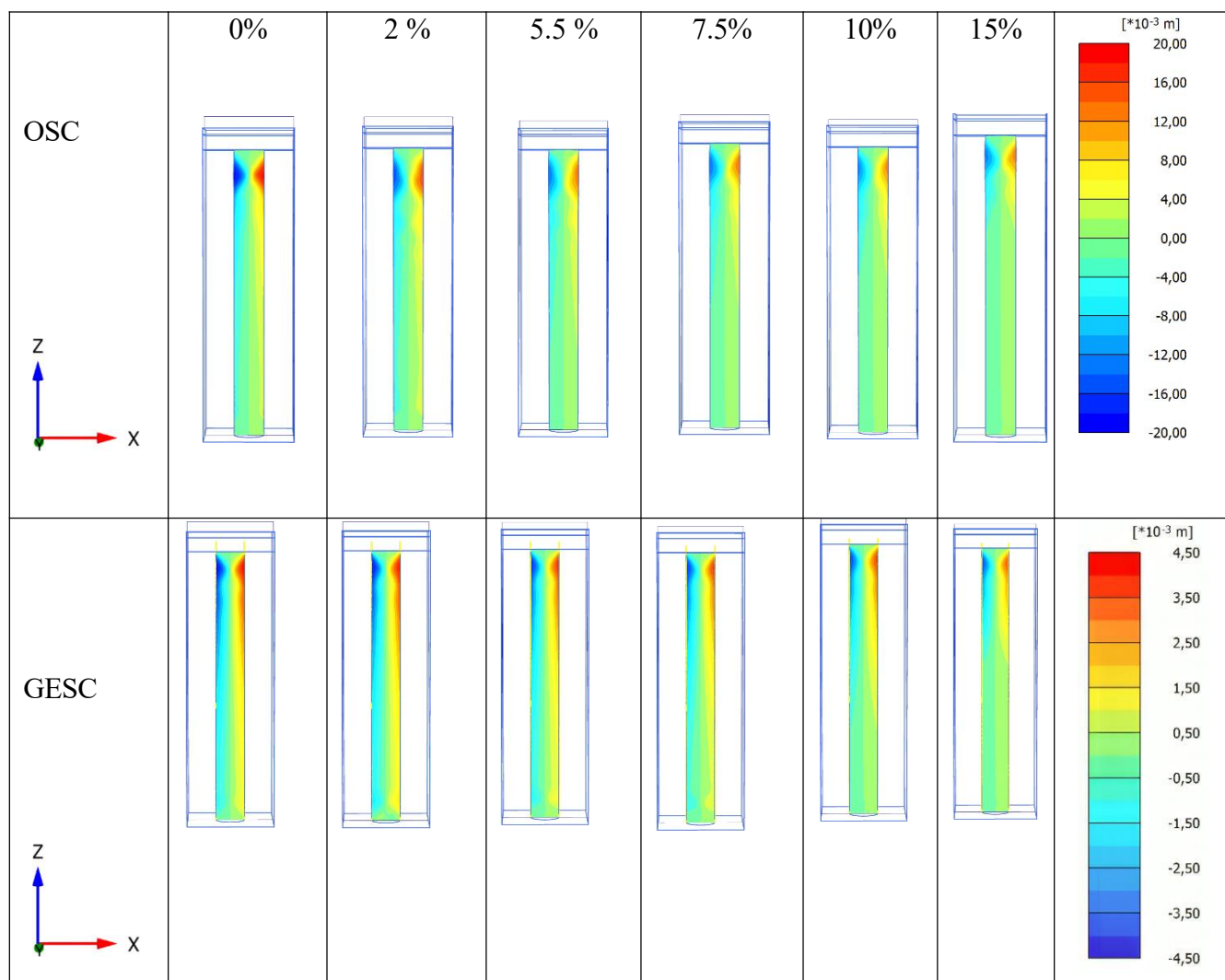
Fig. IV. 13 The horizontal displacement shading of the short stone column for the different values of lateral expansion (Bahi and Houhou, 2024)
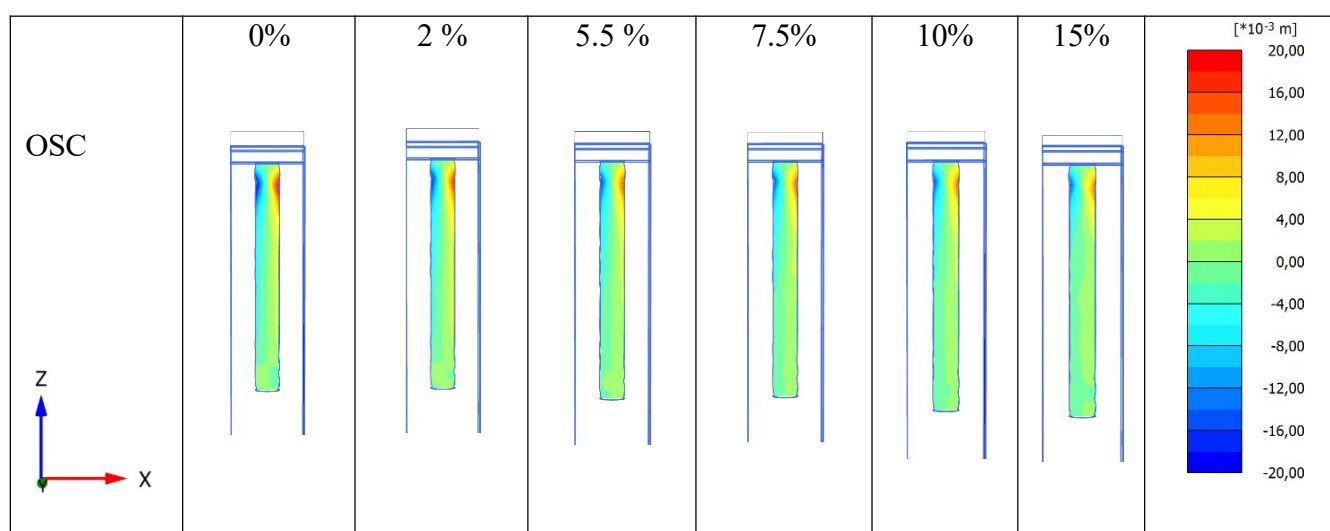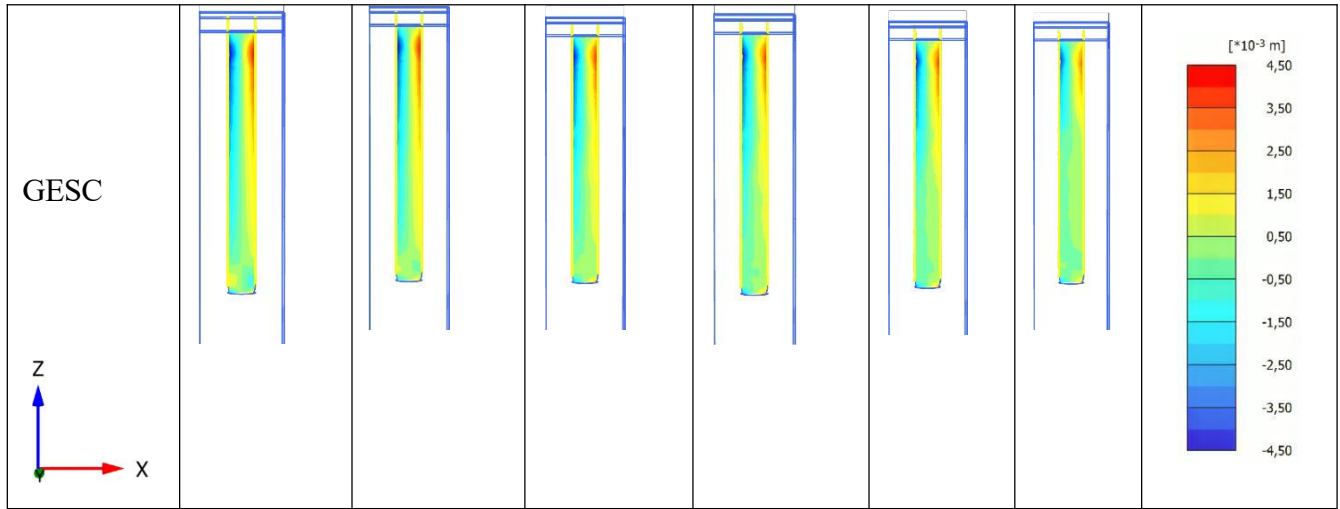
Fig. IV. 14 The horizontal displacement shading of the float stone column for the different values of lateral expansion (Bahi and Houhou, 2024).

5.4. Vertical displacement

According to numerous studies (Xu et al., 2021; Bazzazian Bonab et al., 2020; Miranda and Da Costa, 2016; Farah and Nalbantoglu, 2020;; Jayarajan and Karpurapu, 2021) lateral expansion has a major effect on the settling behaviour of very soft soils along with stone columns. Figures IV. 15 and 16 show how different lateral expansion rates—that is, 2%, 5.5%, 7.5%, 10%, and 15%—affect the extremely soft soil's vertical displacement (U_z) at point B (see Fig. IV. 6).These figures compare scenarios with and without geosynthetic reinforcement for both short and floating columns. The results indicate that lateral expansion has a more pronounced effect on vertical displacement for short columns than for floating columns. This effect is further amplified in Geosynthetic-Encased Stone Columns (GESC) compared to Ordinary Stone Columns (OSC), due to the superior confinement provided by the geosynthetic encasement. In the case of short columns, as depicted in Fig. IV. 15, the vertical displacement under a rigid foundation decreases from 42 cm to 21 cm for OSC and from 39 cm to 18 cm for GESC with increasing radial expansion. Similarly, Fig. IV. 16 shows a reduction in vertical displacement from 62 cm to 41 cm for OSC and from 57 cm to 39 cm for GESC with increasing radial expansion. These reductions in displacement are consistent across all expansion levels. Overall, the data demonstrate that increasing the lateral expansion coefficient effectively reduces vertical displacement. The observed trend highlights that as lateral expansion increases, vertical displacement decreases, reaching zero at the unit cell depth for all cases analyzed. This demonstrates how well lateral expansion and geosynthetic encasement work to reduce settlement and provides important information for enhancing ground stabilisation methods.
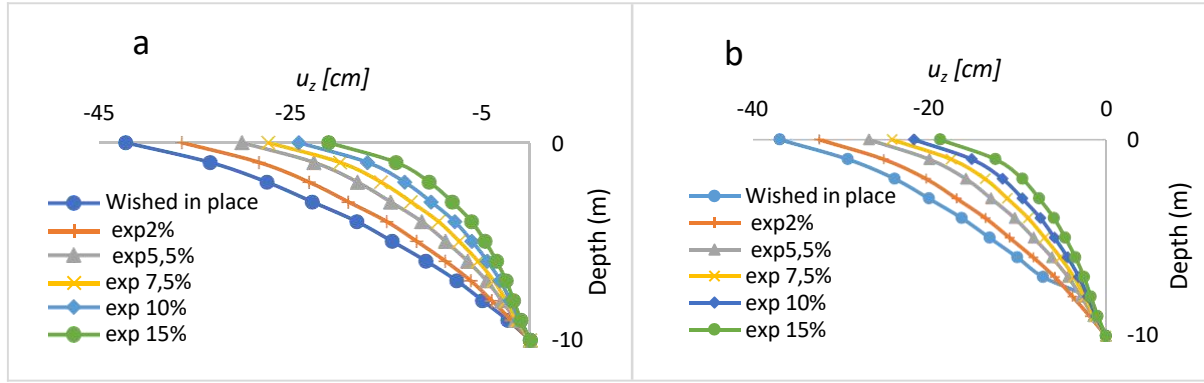
Fig. IV. 15 Vertical displacement beneath the foundation for the case of a short column (H/L=1): **a.** OSC, **b.** GESC (Bahi and Houhou, 2024)
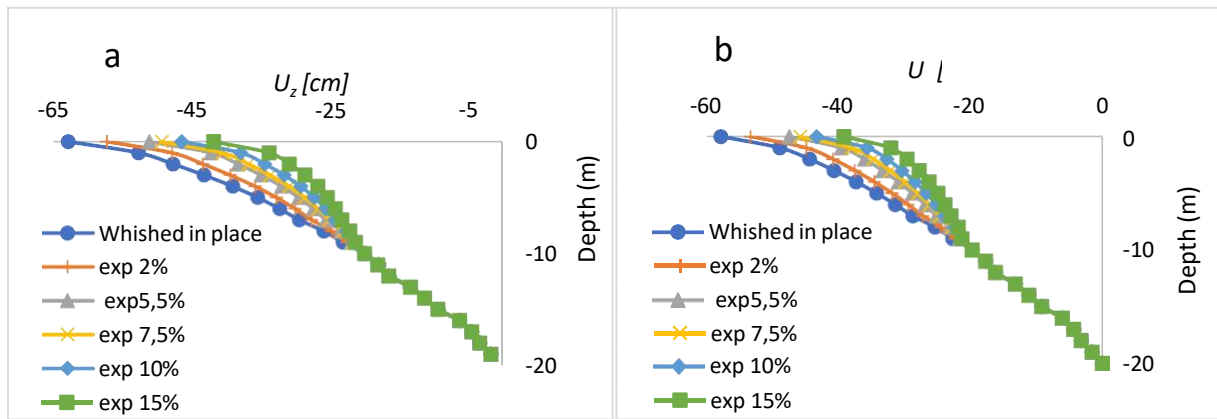
Fig. IV. 16 Vertical displacement beneath the foundation for the case of a floating colum (H/L=2): **a.** OSC, **b.** GESC (Bahi and Houhou, 2024)

Figs. 17 and 18 depict vertical cross-sections showing variations in vertical displacement shading for short stone columns as well as floating ones. The analysis emphasises how crucial it is to take installation effects into account as well as how advantageous geosynthetic encasement is for minimising settlement in extremely soft soils. For ordinary stone columns, as illustrated in Figs. IV. 17 and 18, the highest vertical displacement is observed at the top of the unit cell (indicated in red), with displacement decreasing to a minimum at a certain depth (shown in blue). Increasing the column's lateral expansion reduces vertical displacement. Furthermore, Because of the increased load bearing capability provided by geosynthetic encasement, vertical movement is reduced even more. This discovery is consistent with the work of Muzammil et al. (2018) and the experimental findings of Dar and Shah (2021).
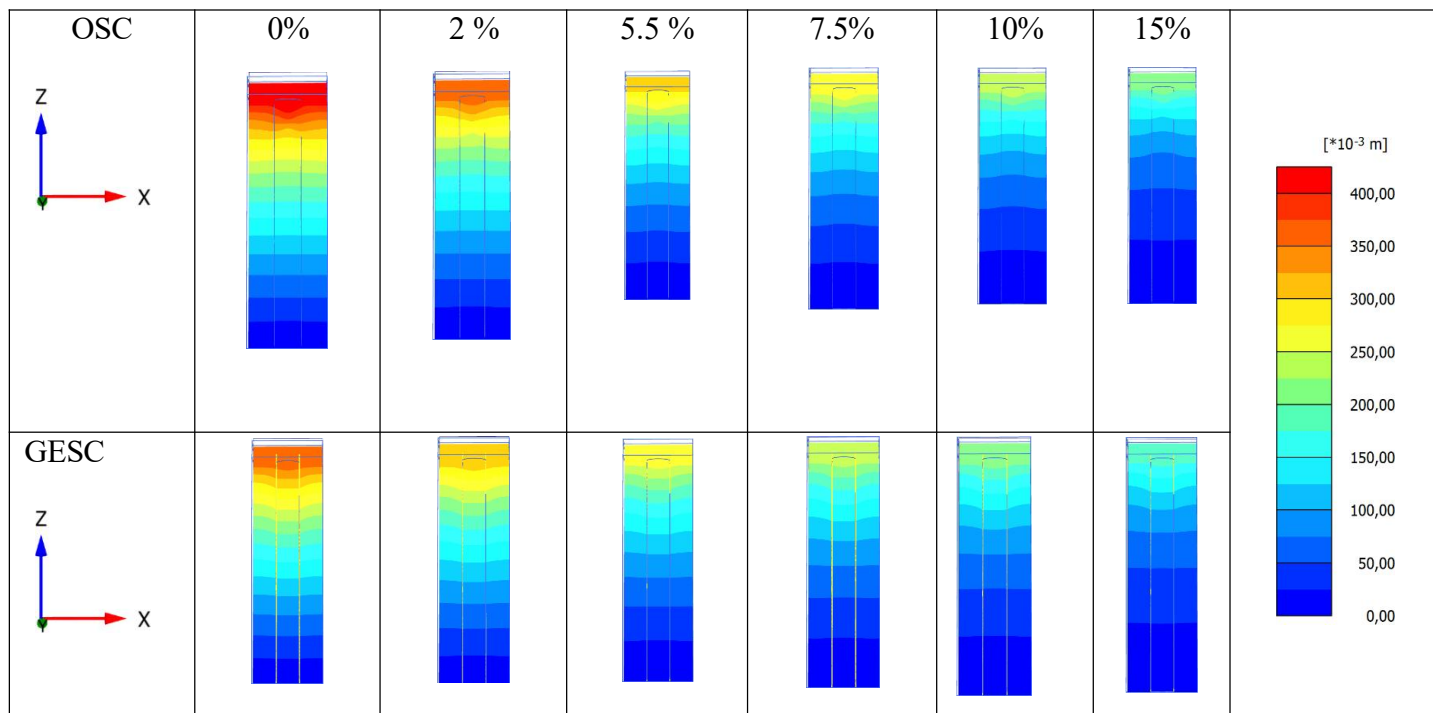
Fig. IV. 17 The vertical displacement shading for the short stone column across various lateral expansion values (Bahi and Houhou, 2024).
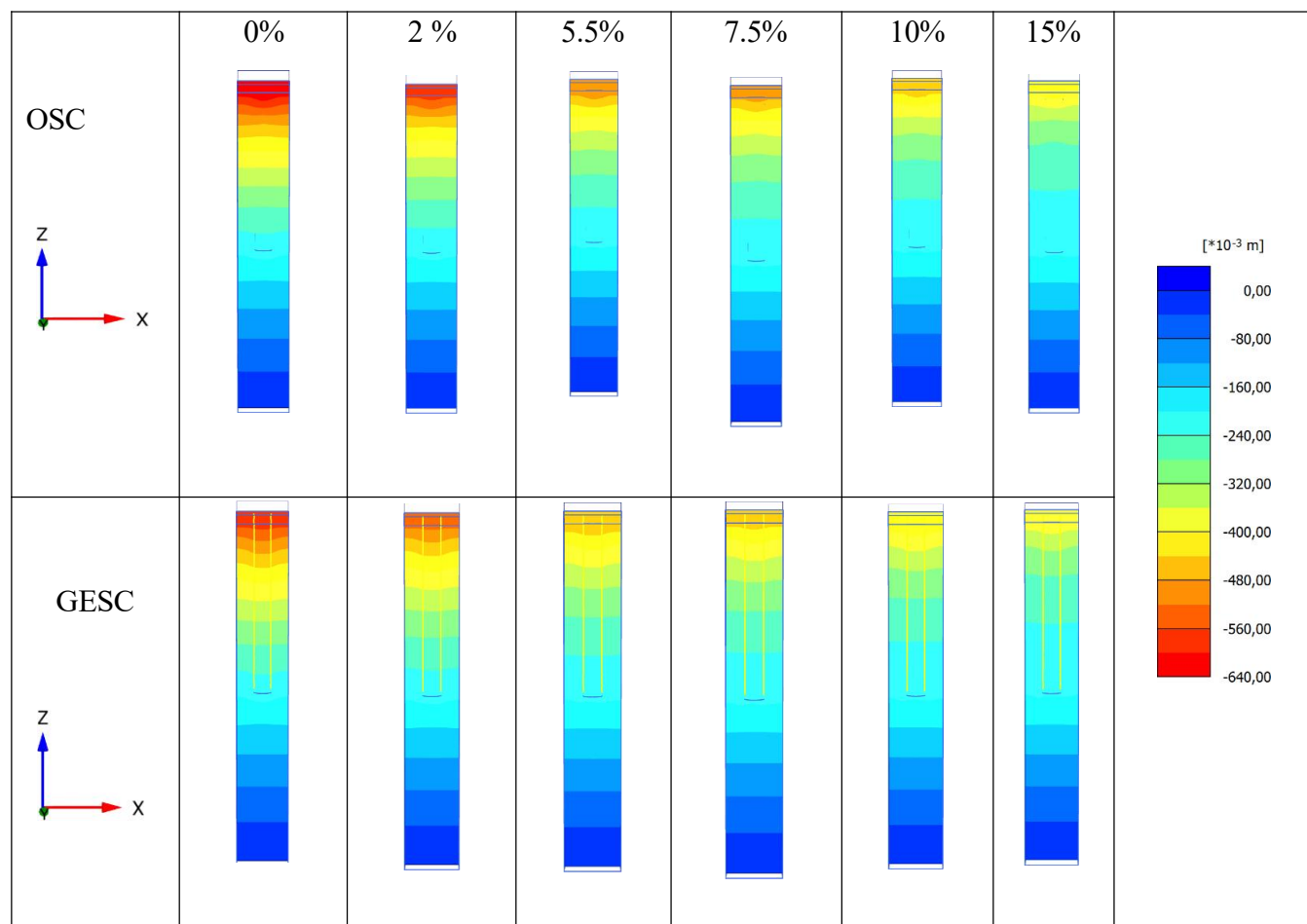
Fig. IV. 18 The vertical displacement shading for the floating stone column at various lateral expansion (Bahi and Houhou, 2024)

6. Conclusion

The study focused on metrics examples include vertical movement, earth pressure coefficient, and settlement decrease. The results highlight the benefits of combining geosynthetic encasement with lateral expansion to enhance stone column performance in very soft clay, demonstrating that shorter geosynthetic encased stone columns significantly improve ground stability over ordinary stone columns. This research provides insights into optimizing stability in difficult soil conditions by addressing issues like settlement, lateral shift, and vertical shift. There are still numerous areas that need to be investigated, even if the study provides a strong foundation for understanding the behaviour of encased stone columns under particular circumstances. In the future, research on various soil types, column diameters, and the impact of erecting many stone columns could be conducted to further our understanding of ground improvement techniques. Although lateral expansions up to 15% are shown to produce the greatest results in simulations, further empirical research is required to establish the optimum expansion for a range various soil kinds and project requirements.

Chapter 05

Chapter 05

Advanced 3D Modeling of Geosynthetic-Encased Stone Column Group Installation and Performance in Soft Clay Beneath Embankment

1. Introduction

Challenges often arise with ordinary stone columns (OSC) in extremely soft soils like peat and marine clays due to inadequate lateral confinement from the surrounding soil. This limitation leads to undesirable column expansion or bulging, particularly in the upper sections, and significantly reduces the load-bearing capacity (Fattah *et al*., 2016; Hosseinpour *et al.,* 2019; Nav *et al*., 2020; Zhang *et al.,* 2020). To overcome these challenges, several methods have been explored to enhance the performance of ordinary stone columns in such conditions. Techniques include reinforcing the top of columns with materials like steel skirts, using the deep mixing method, applying horizontal layers of geogrid, or introducing concrete plugs (Debbabi *et al*., 2021; Jamshidi Chenari and Bathurst, 2023; Rezaei *et al*., 2019; Shamsi *et al.,* 2019). A promising method for enhancing the lateral confining pressure and load-bearing capacity of granular columns involves encasing them with geosynthetic materials. This technique, known as geosynthetic encased stone columns (GESC), improves stiffness through the hoop force provided by the geosynthetics, thereby boosting load-bearing capacity. Furthermore, the geosynthetic encasement prevents the lateral mixing of granular materials with the adjacent soft soil, preserving the drainage capacity of the stone columns (Gholaminejad *et al.,* 2020; Miranda *et al.,* 2021; Z. Xu *et al.,* 2021). Significant research has been carried out to investigate the behavior and performance of encased stone columns through field measurements, small-scale model tests, and laboratory experiments (Miranda *et al.,* 2017; Miranda and Da Costa, 2016; Nasiri and Hajiazizi, 2019; Ouyang *et al*., 2024a; Sadaoui and Bahar, 2019; Thakur *et al.,* 2021; Wang *et al*., 2023; F. Xu *et al*., 2021; Yoo and Abbas, 2020), and analytical solutions (Alkhorshid *et al.,* 2018; Almeida *et al.,* 2020; Bathurst and Naftchali, 2021; Castro *et al.,* 2024; Castro and Sagaseta, 2011; Golait and Padade, 2017; Ouyang *et al.,* 2024b; Pulko *et al*., 2011; Zhuang *et al.,* 2020). Numerical analyses have also been performed to simulate the effects of stone column installation on surrounding soil (Golait and Padade, 2017; Moghadam and Ashtari, 2020; Pulko *et al.,* 2011; Sadaoui and Bahar, 2019; Wang *et al.,* 2023; Zhuang *et al*., 2020).

This study uses PLAXIS 3D software to assess the accuracy of various conversion methods for settlement in embankments reinforced with geosynthetic-reinforced stone columns (GRSC), validated against field data from the Penchala Toll Plaza project. The model covers 40 meters from the embankment center, with a width of 4.8 meters, consisting of 12 layers and a 1:2 slope configuration, constructed in 12 stages followed by consolidation analysis. GRSC, arranged in a square pattern with 2.4 meters spacing, 0.8 m diameter, and 6 m length, were used to enhance stability. The study examines the effects of stone column installation using the lateral expansion method at 0%, 5%, and 10% expansion percentages, along with the influence of geosynthetic wrapping. It also explores the radial expansion method, the most realistic but least explored technique, to assess its impact on settlement reduction. A comprehensive parametric analysis considers factors like geosynthetic strength, the stone column's friction angle, different reinforcement arrangements (square and triangular), and geosynthetic reinforcement methods (horizontal, vertical, and combined). The findings reveal that geosynthetic encasement and stone column installation methods significantly influence settlement reduction, improving stability in soft clay substrates. This research enhances the understanding of GRSC applications in soft soil embankments, offering valuable insights for engineers working on infrastructure projects in challenging geotechnical conditions.

2. Model validation

This study utilized Plaxis 3D software for numerical modeling to evaluate the proposed methods for predicting the settlement of an embankment reinforced with geosynthetic-reinforced stone columns (GRSC) (Brinkgreve RBJ, 2016). The numerical results were validated against field measurements from the Penchala Toll Plaza project. The original study focused on the 2003 embankment construction for the Penchala Toll Plaza project on the New Pantai Expressway, Malaysia. The embankment, filled with sandy material, was 20 meters wide and 1.8 meters high. Stone columns were arranged in a square grid, extending from the embankment base to a depth of 6 meters above a stiff clay layer. A 1-meter-thick layer of hard soil replaced the soft clay surface, creating a stable construction platform and aiding water drainage during consolidation. The groundwater level was one meter below the ground surface. Two settlement plates (SP1 and SP2) were installed to measure settlements at the center of the embankment and 8 meters from its edge, as shown in Fig. V.1. The Penchala Toll Plaza project faced significant challenges due to excessive settlements caused by soft clay deposits under the embankments, critical for heavy transportation utilities. A stone column reinforced foundation was chosen to improve the soft ground conditions.

The numerical results from Plaxis 3D were validated by comparing them with the field measurements from the Penchala Toll Plaza project. This validation is essential for confirming the reliability of numerical models in simulating real-world conditions and ensuring the effectiveness of stone columns in mitigating settlement issues in soft soil environments.
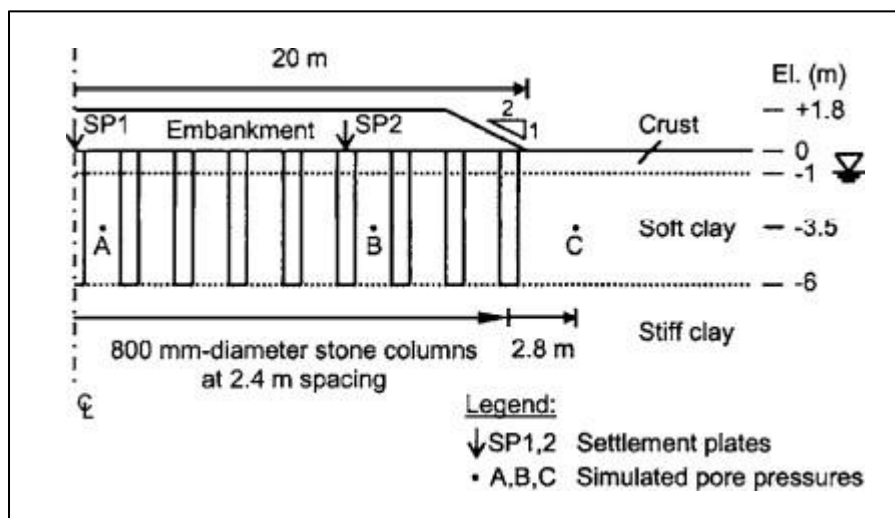
Fig. V. 1 Cross-Sectional View of Embankment for Model Validation (Tan et al., 2008).

Fig.V.2 displays a comparison between the observed and predicted settlements over time at a location beneath the centerline of the embankment (refer to point SP1 in Fig.V.1). The numerical model effectively captured both the trend and the magnitude of the observed settlement, predicting a consolidation settlement of approximately 80 cm over a period of about 100 days. Additionally, Fig.V.3 shows the distribution of pore water pressure at the center of the soft clay layer at point B. The pore water pressure increases during the initial 9 days of embankment construction and subsequently dissipates, with full dissipation occurring over 100 days, indicating complete consolidation. The strong correlation between the numerical predictions and field data validates the model's accuracy in forecasting embankment performance. This model can be employed for further parametric studies to explore various factors influencing embankment behavior.
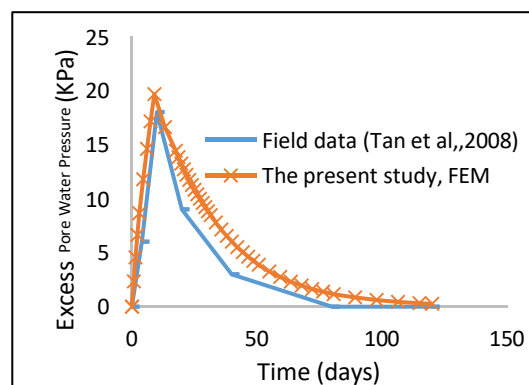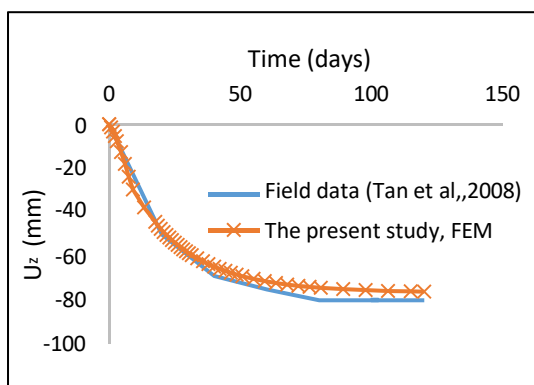
Fig. V. 2 Vertical displacement evolution at SP1.   **Fig. V. 3** Excess pore pressure evolution at the point B.

3. Numerical modeling

3.1. Finite Element Method (FEM) Analysis

In this study, the soft soil was improved using geosynthetic-encased stone columns (GRSC), whereas, in the original study, ordinary stone columns were used. Building on the original study, the current research aims to

scrutinize the influence of the installation effect of a group of stone columns using the lateral expansion method, while considering the reinforcement with geosynthetics (GRSC) on the stability and performance of an embankment constructed on soft clay. The analysis employs a 3D simulation using 10-node elements(Brinkgreve RBJ, 2016). Additionally, a parametric study was conducted to examine the influence of various parameters on the performance of the embankment enhanced by the reinforced stone columns. This included evaluating the impact of different factors such as the strength of the geosynthetic material, the friction angle and strength of the stone columns, the arrangement of columns in square and triangular grids, and the effectiveness of various reinforcement methods (horizontal, vertical, and combined).

3.2. Geometric Model and Construction Sequence

The geometric model spans 40 meters from the center of the embankment and has a width of 4.8 meters. It consists of 12 layers, each 0.6 meters thick, with a slope configuration of 1:2. Due to its symmetrical design, only one half of the embankment is modeled. Construction was performed in 12 stages, with each layer placed over 36 days, reaching a final height of 7.2 meters (see Fig.V.4a). Following construction, a consolidation analysis was conducted until the complete dissipation of excess pore water pressure.

3.3. GESC Installation

To enhance the stability of the soft clay substrate, 18 geosynthetic encased stone columns (GESC)were installed. These columns, each 6 meters long and 0.8 meters in diameter, were arranged in a square pattern with an equidistant spacing of 2.4 meters between them as shown in Fig.V.4b. According to IS 15284 Part-1, the recommended spacing between stone columns is typically 2–3 times the diameter of the columns, allowing for flexibility based on specific site conditions. In this study, a spacing of 2.4 meters was chosen, which is exactly three times the diameter of the columns (0.8 meters x 3 = 2.4 meters). This spacing adheres to the recommended guidelines and is intended to evaluate the effectiveness of stone columns under these conditions. The GRSC were deployed within two 6-meter-deep layers, consisting of a 1-meter crust and 5 meters of soft clay. The groundwater level was set 1 meter below the ground surface to replicate field conditions accurately
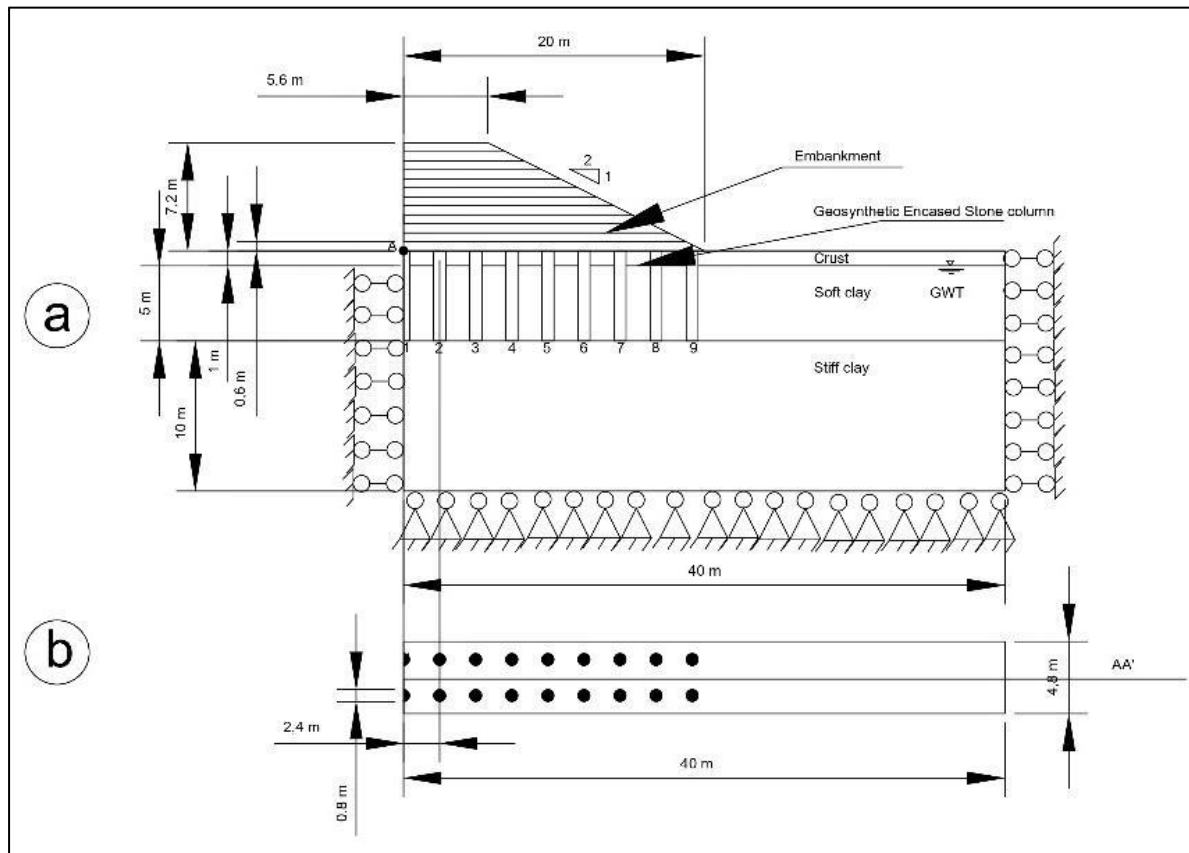
Fig. V. 4 The numerical model studied: **a.** Cross section, **b.** Plan view.

3.4. Finite Element Mesh

The finite element mesh was constructed using 10-node triangular elements, with mesh refinement applied in the geosynthetic-reinforced stone column-treated areas to enhance accuracy (see Fig.V.5). The materials were modeled as Mohr-Coulomb (MC) soils, providing realistic approximations of the actual soil conditions, as presented in Table. V. 1
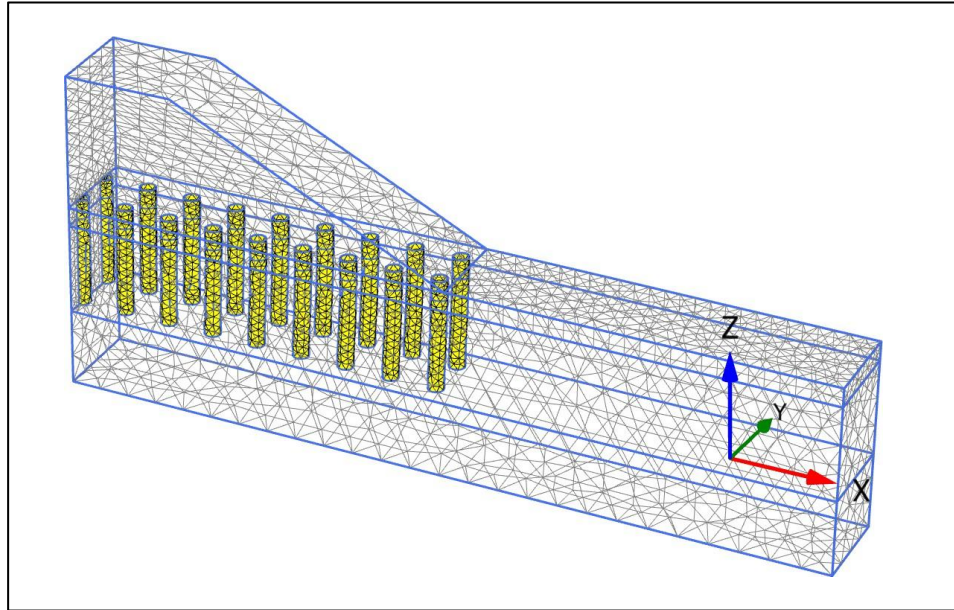
Fig. V. 5 mesh generation.

Table. V. 1 Material parameters (Tan et al., 2008)

Material / Properties	γ_{dry} (kN/m³)	γ_{sat} (kN/m³)		E (MPa)	K_h (m/s)	K_v (m/s)	C' (Kpa)	ϕ' (°)
Soft clay	15	15	0.3	1.1	3.47×10^{-9}	1.16×10^{-9}	1	20
Stiff clay	18	20	0.3	40	3.47×10^{-9}	1.16×10^{-9}	3	30
Embankment fill	18	20	0.3	15	1.16×10^{-5}	1.16×10^{-5}	3	33
Stone column	19	20	0.3	30	1.16×10^{-4}	1.16×10^{-4}	5	40
Crust	17	18	0.3	15	3.47×10^{-7}	1.16×10^{-7}	3	28

3.5. Geogrid Reinforcement

The geogrid reinforcement was modeled as an isotropic element composed of six nodal triangular elements, each with three translational degrees of freedom per node. Characterized by its tensile stiffness, the geogrid element can sustain tensile forces along its length. A perfect bond was assigned along the interface between the geogrid element and the surrounding soil, following the approaches of Hatami and Bathurst (2011) (Hatami and Bathurst, 2011). Using an elastic element ensures that tensile rupture of the geosynthetic will not occur in the parametric study. The geogrid is only capable of sustaining tensile stress, so its tensile stiffness was the primary parameter used to simulate its behavior, with this value varied in the parametric analyses. The geosynthetics were modeled to behave in a linear elastic manner, with an axial stiffness (*EA*) of 4000 MPa, aligning with values reported in the literature (Deshpande et al., 2021; Jamshidi Chenari and Bathurst, 2023;

Zhou et al., 2019). The tensile strength at 2% strain was set at 80 kN, chosen to meet the research objectives optimally.

3.6. Boundary Conditions

The base of the mesh is subject to pin support, assuming no horizontal or vertical displacement. The vertical sides of the mesh are restricted from lateral movement but allowed vertical settlement. A medium mesh was used for the finite-element modeling to balance computational efficiency and accuracy.

4. Installation phase

Numerous numerical analyses have been conducted to evaluate the lateral earth pressure coefficient (K) after column installation, with most studies relying on axisymmetric numerical models. These models assume rotational symmetry around a central axis, simplifying the analysis of single column behavior by reducing computational complexity (Bahi and Houhou, 2024). While useful, axisymmetric models have limitations when applied to more complex configurations involving groups of columns or varying soil conditions. This study employs a three-dimensional ($3D$) numerical model that includes a group of geosynthetic-reinforced stone columns (GESC). The 3D model offers several advantages, such as a more accurate representation of interactions between multiple columns and the surrounding soil, capturing effects that axisymmetric models might miss. This is especially important in real-world applications where stone columns are typically installed in groups. The numerical model in this paper shows consistent results, as illustrated in Fig. V.6. With increasing lateral expansion percentages, K increases at the column edges. Similar trends were observed for columns beneath the embankment, with values reaching 3.55 at 15% expansion and 2.7 at 10% expansion. The earth pressure coefficient K gradually decreases as the distance from the embankment edge increases, stabilizing at 1 at a distance of 20 meters. In scenarios with no lateral expansion (0% expansion), K remains constant at K_0 along the length of section (AA'), calculated using Jaky's formula ($K_0=1-\sin\varphi'$). The installation of geosynthetic-reinforced stone columns (GRSC) significantly impacts the surrounding soil, primarily through lateral expansion, inducing notable displacement and altering pressure distribution. Simulations show that maximum displacement occurs at the column edges, with values of 1 mm, 28.8 mm, and 61.9 mm for lateral expansions of 0%, 10%, and 15%, respectively (Fig. V.7). These values increase with greater lateral expansion, indicating a direct correlation between lateral expansion extent and soil displacement. This displacement diminishes towards the perimeter of the model, emphasizing the concentrated effect at the column edges. Increased lateral expansion enhances soil pressure, leading to improved compaction and shear strength, crucial for stability in soft soil conditions. These effects contribute to better load distribution and reduced settlement risks, essential for infrastructure projects like railway embankments.
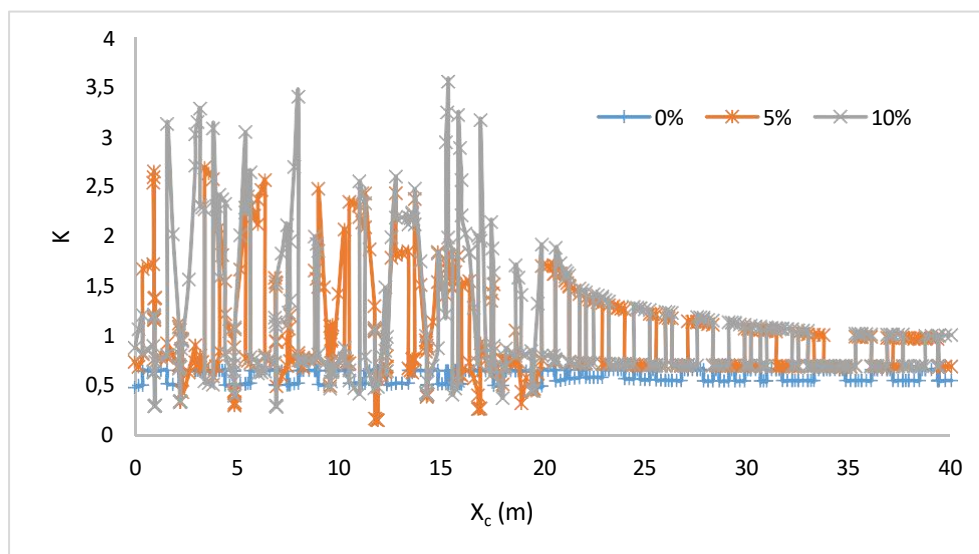
Fig. V. 6 Earth pressure coefficient evolution at section (AA').

Wished in place (exp 0%)

Exp 5%   Exp 10%
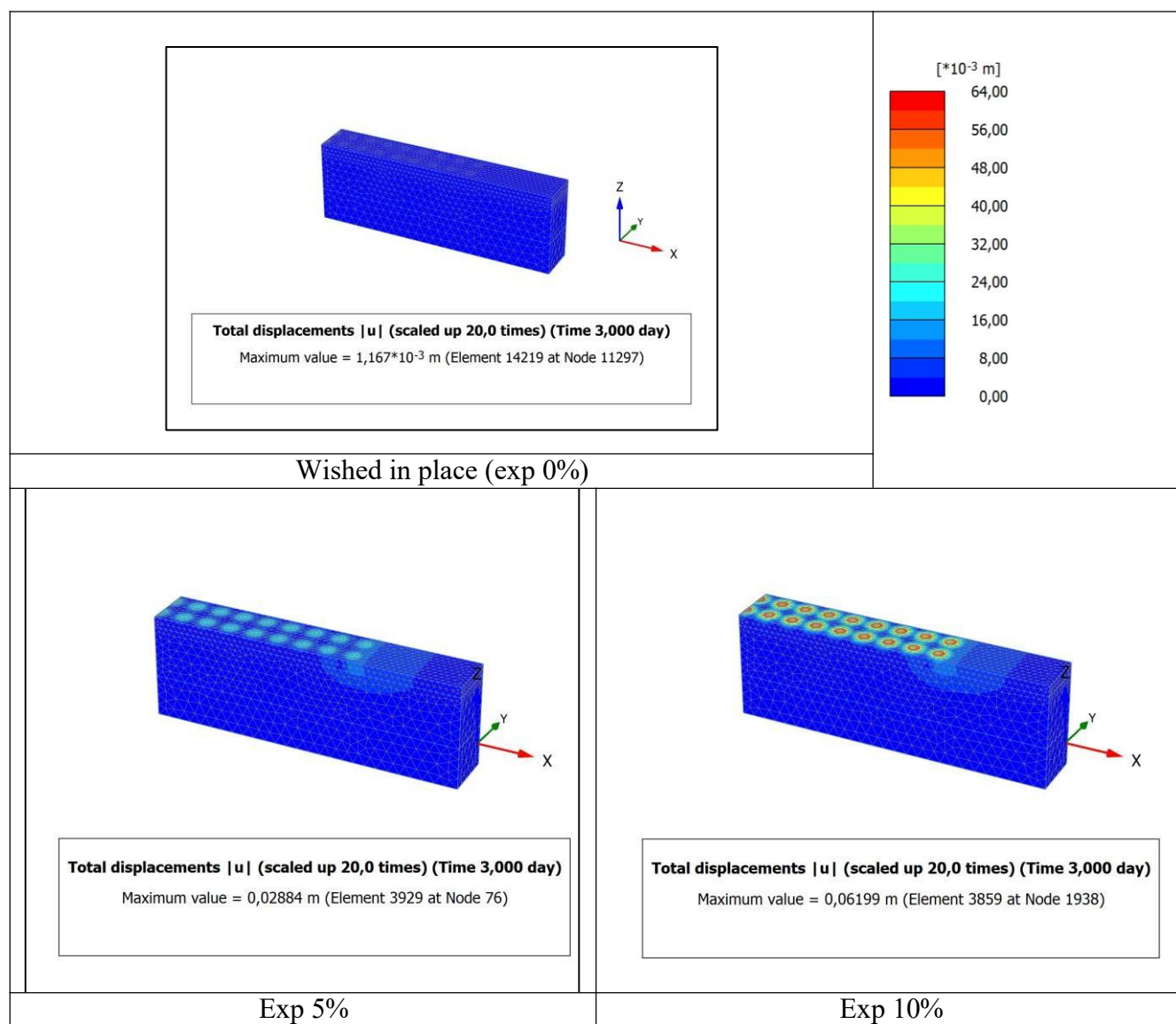
Fig. V. 7 The installation effect on the surrounding soil.

114

5.   Results and discussion

5.1. Installation effect

Figure V.6 illustrates the progression of maximum settlements over time at the central point of model A (0,0,0) under various geosynthetic reinforcement scenarios. Stone columns are a widely used ground improvement method to stabilize structures built on soft clay soils. Consolidation settlement, caused by water loss, results in a time-dependent volume reduction, which increases vertical effective stresses and enhances shear strength (Ghazavi et al., 2018; Singh and Sahu, 2019). This section examines the effect of stone column installation, both with and without geosynthetic encasement, on the vertical displacement (U_z) of an embankment. The analysis focused on settlement patterns along a specified section (*AA'*) of the embankment and settlement at its center (point A) over time. The settlement curves displayed a sinusoidal pattern beneath the structure, regardless of geosynthetic encasement. These oscillations corresponded to the positions of the stone columns, showing reduced settlement in the areas where columns were present (Fig. V.8a). This highlights the importance of strategic column placement in mitigating settlement variations. The study also investigated the impact of different lateral expansion ratios (0-10%) and geosynthetic encasement on settlement behavior. Consistent with previous findings, the maximum settlement occurred at the embankment's center, where the load is highest, and gradually decreased towards the edges. This settlement pattern included an initial uplift at the base, followed by a decrease and eventual stabilization. The study clearly demonstrates the significant benefits of combining stone column installation with geosynthetic reinforcement in reducing vertical settlement in embankments on soft clay soils. Initially, installing stone columns without geosynthetic encasement reduced settlement from 0.35 meters to 0.33 meters with a 10% lateral expansion, a 5.71% reduction. However, the introduction of geosynthetic encasement significantly enhanced the load-bearing capacity of the stone columns and further reduced settlement. The maximum settlement at the embankment's center decreased to 0.24 meters, 0.23 meters, and 0.22 meters for confinement ratios of 0%, 5%, and 10%, respectively. This corresponds to reductions of 31.43%, 34.29%, and 37.14%, respectively, demonstrating the considerable advantage of geosynthetic reinforcement.

Geosynthetic encasement confines the stone column material, preventing lateral spreading and enhancing vertical load-bearing capacity, significantly mitigating settlement. This combined approach ensures more precise and effective results, underscoring the importance of considering both installation effects and geosynthetic reinforcement in the design and construction of stable embankments on soft clay substrates. The parametric analysis further supports this by identifying optimized configurations that maximize stability and minimize settlement, providing essential insights for future geotechnical engineering projects. The findings confirm the effectiveness of stone columns in mitigating settlement in soft clay soils, creating stiffer zones within the soil that lead to a more even distribution of loads and reduced overall settlement.

The wavy settlement pattern underscores the importance of proper stone column design and spacing for uniform load distribution to minimize settlement variations and ensure embankment stability. Additionally, geosynthetic encasement offers further benefits by confining the stone column material and enhancing its load-bearing capacity.
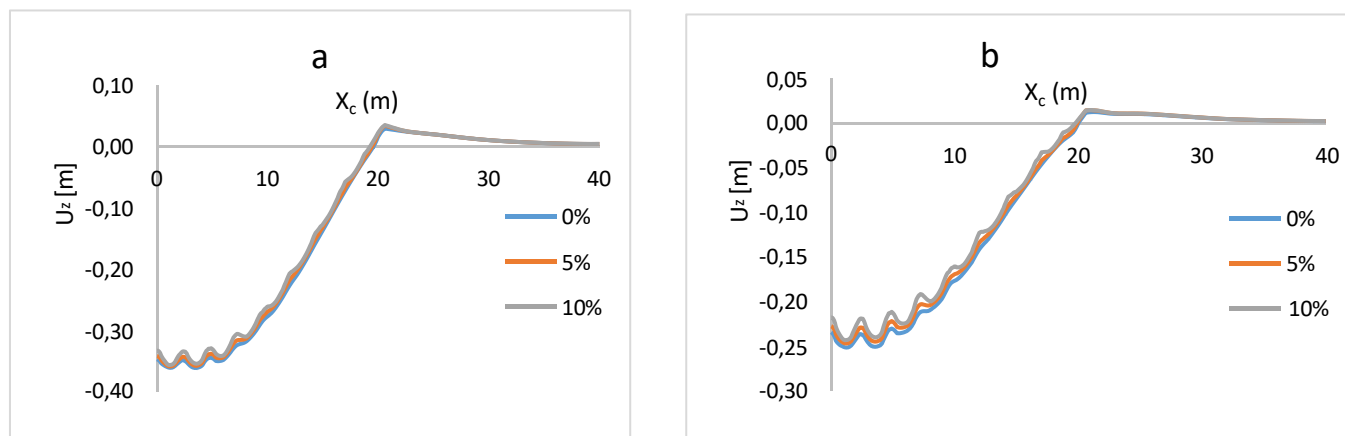
Fig. V. 8 Impact of installation on variation in vertical displacement across section (AA'): **a.** OSC, **b**. GESC.
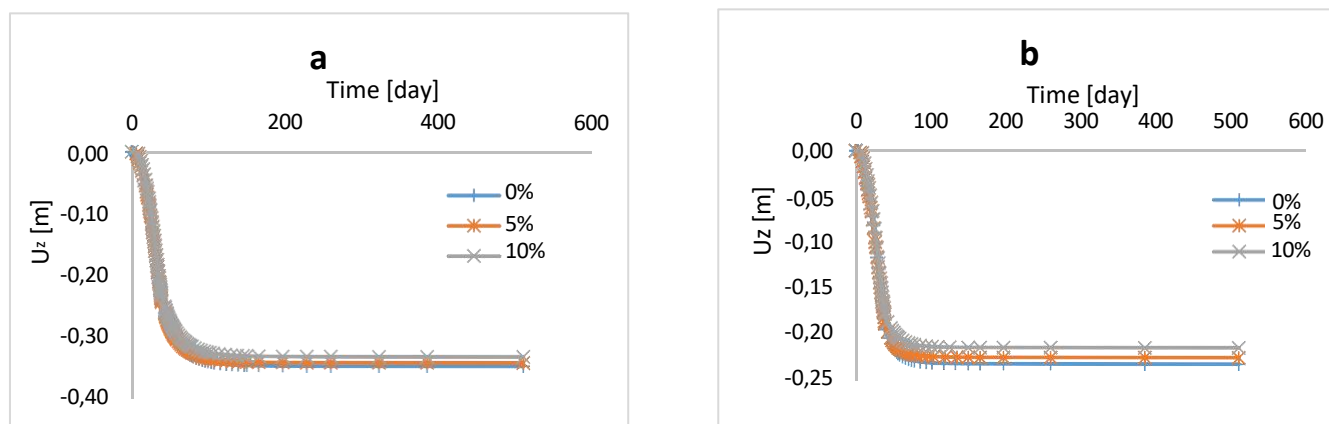
Fig. V. 9 Impact of installation on variation in vertical displacement at point A: **a.** OSC, **b**. GESC

Total displacements u$_z$ (scaled up 5,00 times) (Time 510,4 day)

Maximum value = 0,02863 m

Minimum value = -0,4471 m

0%

Total displacements u$_z$ (scaled up 5,00 times) (Time 510,4 day)

Maximum value = 0,01257 m

Minimum value = -0,3188 m

0%
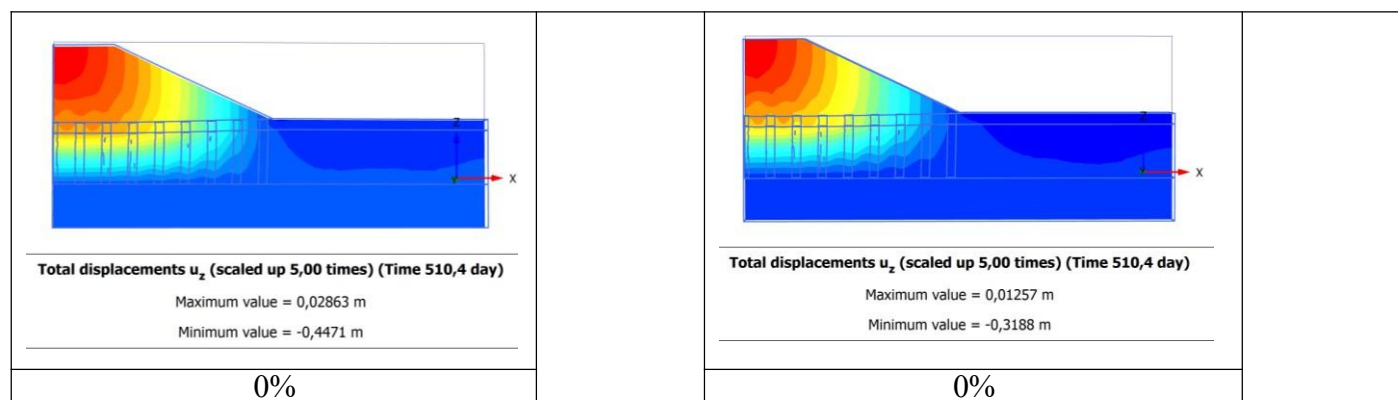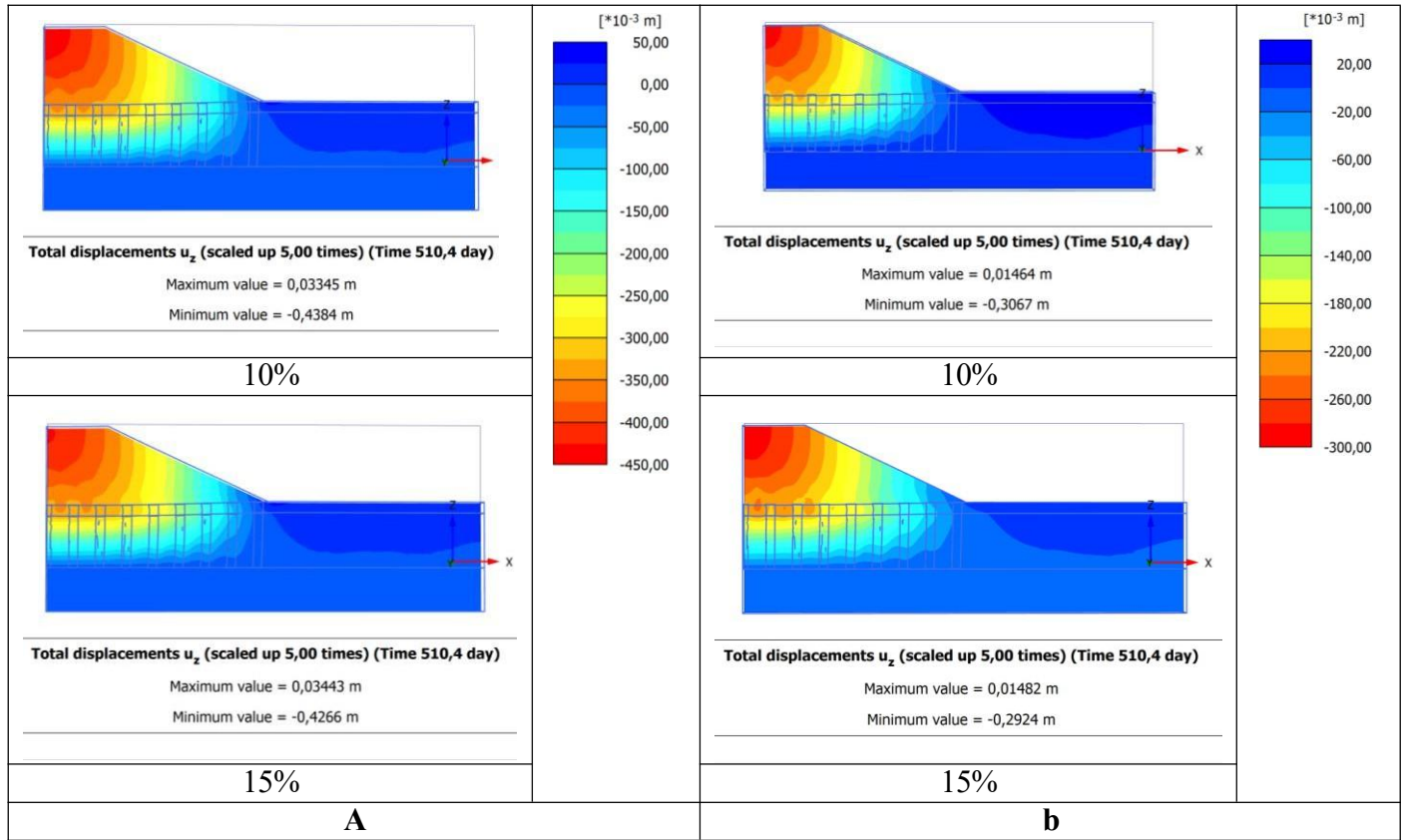
Fig. V. 10 Variation of vertical displacement shading with different values of lateral expansion: **a**. OSC**, b.** GESC.

5.2. Parametric analysis

5.2.1. Geosynthetic strength effect

The stiffness of the geosynthetic encasement determines the hoop stress required to undergo significant strain (Elwakeel and Elsherbini, 2024). This study demonstrates the effectiveness of geotextile encasement in reducing vertical displacement in embankments built on soft clay substrates. Without geotextile encasement (OSC), the original settlement was 35 cm. When columns were encased with geotextiles of varying axial stiffness (*EA*), the following reductions in settlement were observed: EA = 500 kN/m reduced settlement to 31 cm (11.43% reduction), EA = 2000 kN/m reduced settlement to 26 cm (25.71% reduction), and EA = 4000 kN/m reduced settlement to 23 cm (34.29% reduction). These results support the theoretical understanding that geotextile encasement enhances the load-bearing capacity of stone columns by confining the soil and preventing lateral spreading. Previous numerical studies by Alkhorshid et al. (2018), Elsawy (2013), and Yoo et al. (2015) have also explored the impact of the tensile stiffness of geosynthetics on the performance of stone columns (Alkhorshid et al., 2018; Elsawy, n.d.; Yoo, 2015). In this study, the effect of encased stone column stiffness was examined using four different tensile strength values, including 500, 2000, and 4000 kN/m.

The results indicate that as the axial stiffness of the geotextile increases, the reduction in settlement also increases, suggesting that axial stiffer geotextiles provide better confinement and support, thereby enhancing

the stability of the embankment more effectively. These findings have practical implications for designing and constructing embankments on soft clay substrates, allowing engineers to optimize the use of geotextile-encased stone columns to achieve desired stability and settlement reduction levels. The choice of geotextile axial stiffness should be based on the project's specific requirements, balancing material costs with performance needs. While higher axial stiffness geotextiles may be more expensive, their significant reduction in settlement and potential long-term stability benefits can justify the cost. The effect of the axial stiffness of geosynthetic encasement is clearly illustrated in Figures V.11 and V.12.
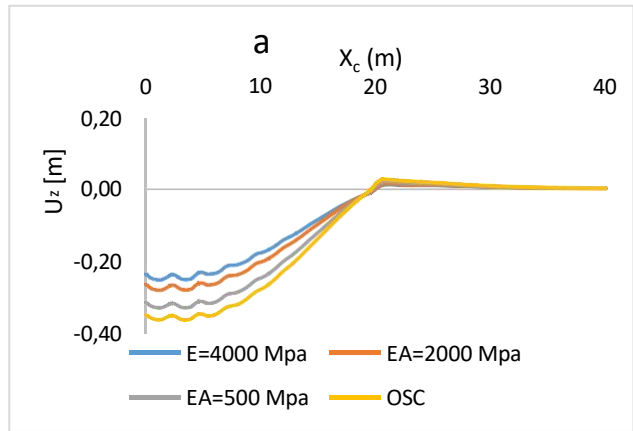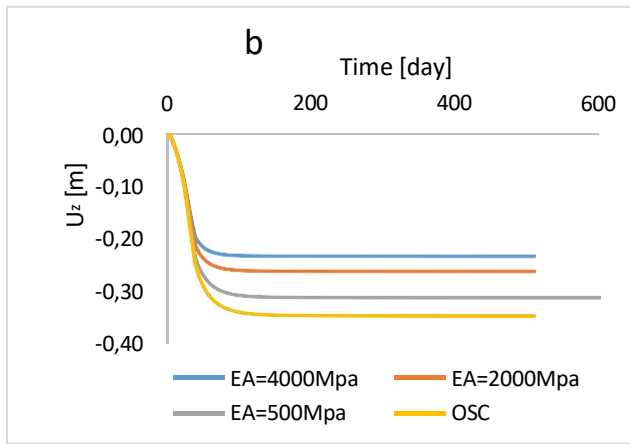
Fig. V. 11 Geosynthetic axial stiffness effect at point A.   **Fig. V. 12** Geosynthetic axial stiffness effect across section (AA').

5.2.2. Method of geosynthetic reinforcement

Stone columns installed in very soft soils often struggle with insufficient lateral confinement, leading to increased bulging and greater surface settlements. This issue is especially significant in soft soil conditions. To address these challenges, this study examines the effectiveness of various geosynthetic reinforcement techniques. The configurations investigated include Vertical Geosynthetic Encased Stone Columns (VESC), Horizontal Geosynthetic Reinforced Stone Columns (HRSC), and combinations of both vertical encasement and horizontal layers (VESC + HRSC). Fig. V.13 shows the different cases studied, ranging from Ordinary Stone Columns (OSC) to various reinforced configurations, such as total vertical encasement (TOT VGESC), 0.5H vertical encasement, and combinations of vertical and horizontal reinforcement. Vertical reinforcement scenarios included stone columns encased with 0.25H, 0.5H, and total vertical encasement (VESC 1/3H, VESC 0.5H, TOT VESC). Horizontal reinforcement involved stone columns reinforced with layers spaced at 0.25m and 0.5m intervals (1/3H HRSC, 0.5H HRSC). Combined reinforcement strategies included TOT VESC + 1/3 H HRSC and TOT VESC + 0.5H HRSC. Figure V.14 illustrates the vertical displacement distribution at point A over time, while Fig.V.15 shows the vertical displacement distribution across section (AA') relative to the distance from the embankment centerline (X_c). The results indicate that stone columns reinforced with both vertical and horizontal geosynthetics (VESC + HRSC) exhibit superior bearing capacity

compared to configurations with only horizontal (HRSC) or vertical (VESC) reinforcement. In Fig.V.15, the vertical displacement follows a sinusoidal pattern, decreasing from the center of the embankment to the toe. The maximum displacement occurs in the cases of OSC and stone columns reinforced with horizontal geosynthetic layers. However, vertical displacement decreases with partial geosynthetic encasement and reduces further in scenarios involving total encasement and combined reinforcement methods.

OSC	TOT V_{ESC}
1/3 H H_{RSC}	1/2 H H_{RSC}
1/3 H V_{RSC}	1/3 H V_{RSC}
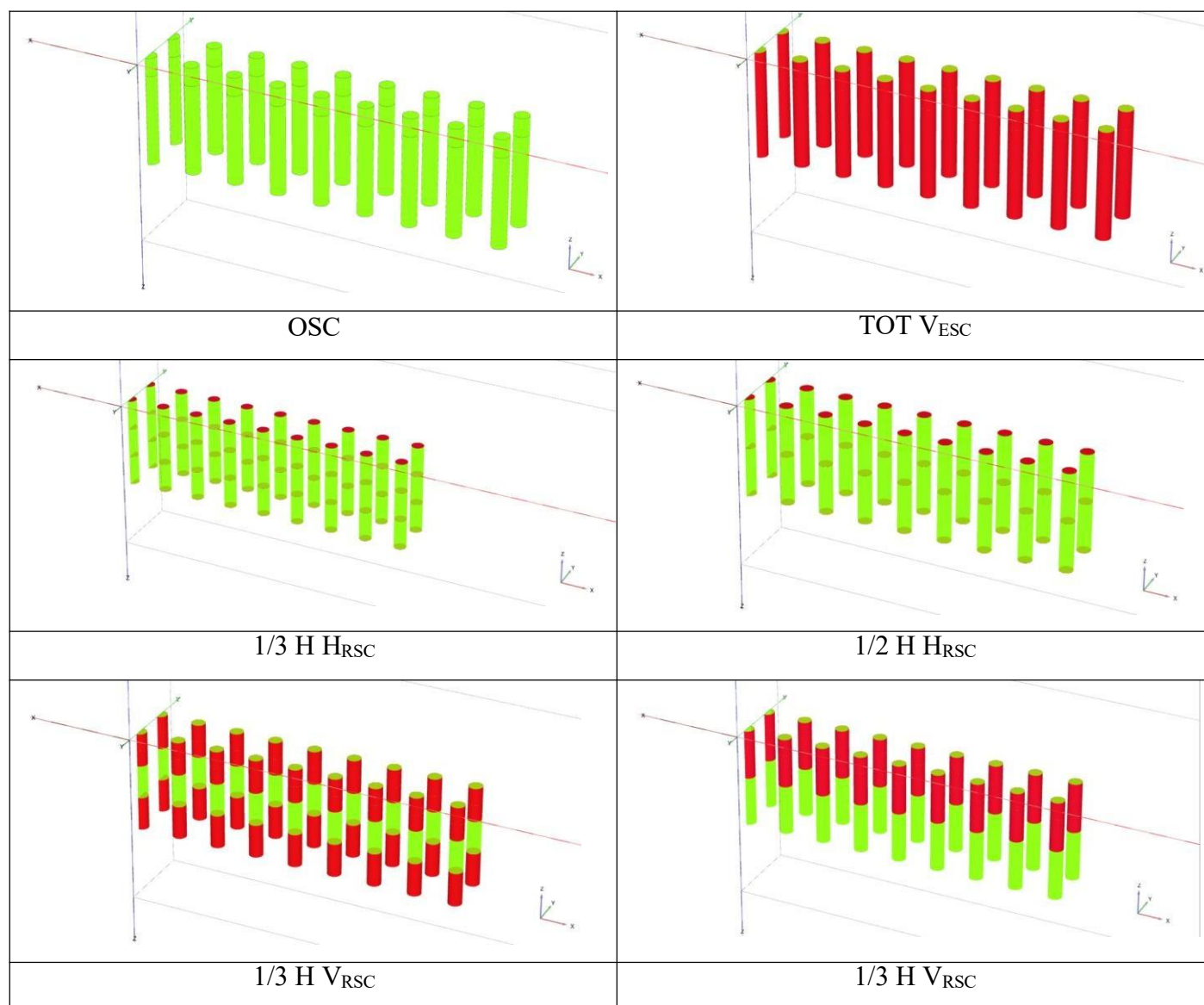
Fig. V. 13 Different Methods of geosynthetic reinforced Stone Columns.
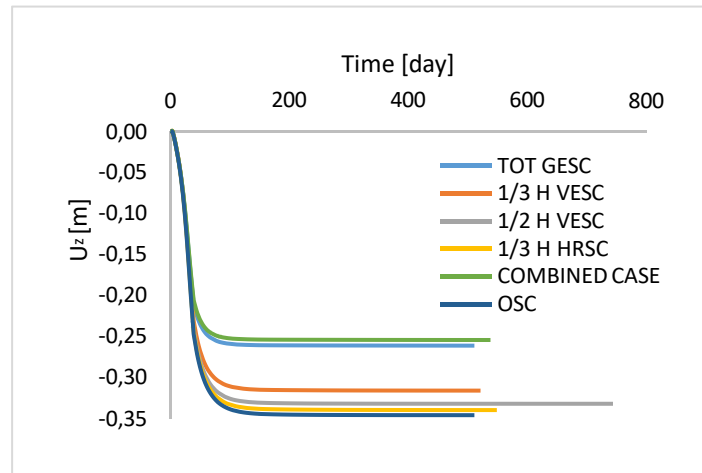
Fig. V. 14 Time-vertical displacement behavior of various studied cases at point A.
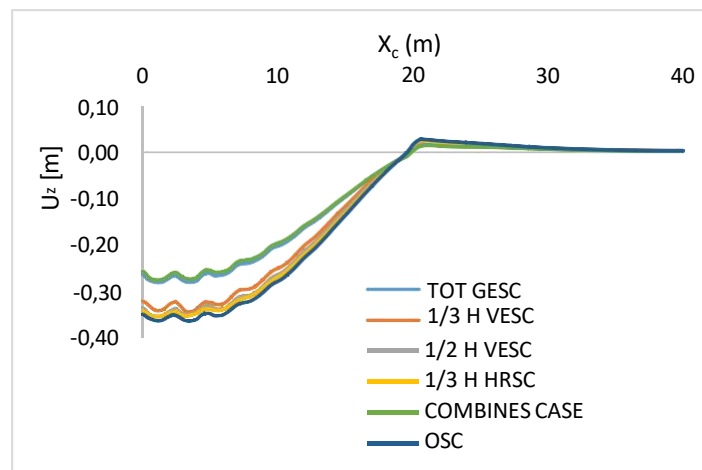
Fig. V. 15 Vertical displacement for different studied cases across section (AA').

5.2.3. Stone column friction angle effect

The analysis conducted in this study underscores the significant influence of the friction angle of stone-column materials on the vertical settlement of geosynthetic-encased stone columns (ESC). Friction angles of 30°, 39°, and 45° were considered, and the results clearly show that higher friction angles lead to reduced vertical displacements. This trend aligns with findings from Alkhorshid et al. (2018), which highlight the importance of the friction angle in enhancing the load-bearing capacity and overall stability of stone columns (Alkhorshid *et al.*, 2018; Elwakeel and Elsherbini, 2024). Figs V.16 and V.17 illustrate the vertical displacement of the ESC over time and distance from the center of the embankment, respectively. The data indicate that increasing the friction angle of the stone column material reduces settlement over time. Specifically, settlements for friction angles of 30°, 39°, and 45° were observed to be 0.25 m, 0.24 m, and 0.23 m, respectively. This suggests that increasing the friction angle by 9° results in a settlement reduction of approximately 0.01 m, highlighting the incremental benefits of optimizing the friction angle of stone-column materials.

 The theoretical basis for these observations lies in the enhanced interlock and resistance provided by materials with higher friction angles. As the friction angle increases, the ability of the stone columns to resist lateral deformation and maintain their structural integrity under load improves, leading to a more stable embankment with reduced vertical displacement. The confinement provided by the geosynthetic encasement further enhances these benefits by preventing lateral spreading of the stone columns, thereby maintaining their vertical load-bearing capacity. These findings have crucial practical implications for the design and construction of embankments on soft clay substrates. Engineers can leverage the knowledge of friction angle effects to optimize the materials used in stone columns, achieving greater stability and reduced settlement. The choice of stone column material should consider not only the inherent properties of the material but also the desired performance outcomes in terms of settlement reduction. Furthermore, the results emphasize the importance of combining geosynthetic encasement with high-friction angle materials to maximize benefits. The combined effect of geosynthetic encasement and optimized friction angles can lead to significant improvements in the performance of stone columns, offering a more cost-effective and efficient solution for stabilizing soft clay substrates. In conclusion, this study demonstrates that the friction angle of stone-column materials is crucial in reducing vertical settlement in geosynthetic-encased stone columns. By selecting materials with higher friction angles and utilizing geosynthetic encasement, engineers can enhance the stability and performance of embankments on soft clay substrates. This research provides valuable insights for future infrastructure projects, offering a pathway to more resilient and durable geotechnical solutions.
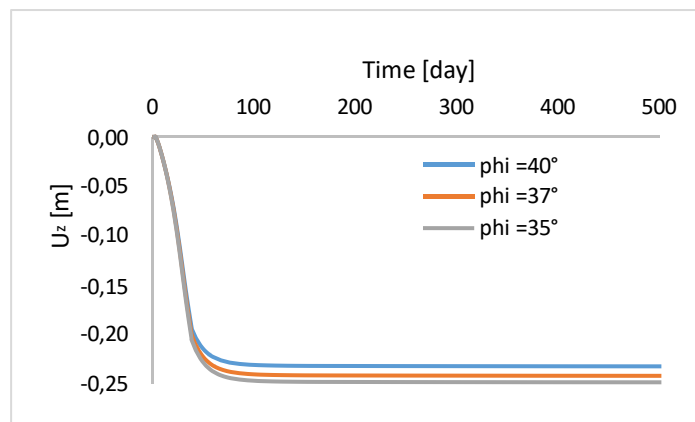
Fig. V. 16 Effect of friction angle on vertical displacement at point A.
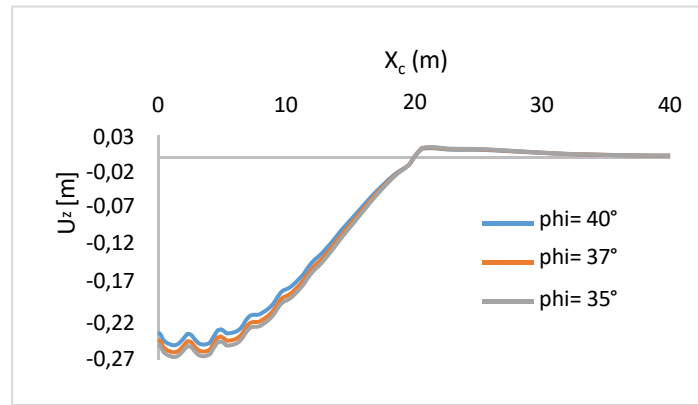
Fig. V. 17 Evolution of vertical displacement across section (AA').

5.2.4. Arrangement effect

The study examined the impact of different arrangements, specifically triangular and square, on the load-bearing capacity of geosynthetic-encased stone columns (GESC). These arrangements are depicted in Fig.V.18. Figs.V.19 and V.20 show how the installation pattern of GESC influences vertical displacement behavior under embankment load intensity (Aslani et al., 2019; Dar and Shah, 2021; Irshad and Mukherjee, 2024). The arrangement of encased stone columns significantly affects vertical displacement in soft clay under embankments. Figs.V.19 and 20 illustrate the vertical displacement at point A and along section (AA'), respectively, for both triangular and square distributions of the encased stone columns. From Fig.V.19, it is clear that vertical displacement at point A is lower for the triangular distribution compared to the square distribution, with values of 0.23 m and 0.26 m, respectively. This indicates that the triangular arrangement more effectively reduces settlement at this critical point. Fig V.20 further depicts the development of vertical displacement along section (AA'). The displacement profile for the square distribution shows a sinusoidal pattern, indicating variations in settlement between the columns. In contrast, the triangular distribution presents a more continuous and uniform decrease in displacement, suggesting a more stable and effective load distribution. These observations highlight that the triangular arrangement of encased stone columns is more effective in minimizing vertical displacement compared to the square arrangement. The closer spacing of columns in the triangular pattern likely enhances performance by providing better support and reducing variability in settlement. This finding is crucial for designing more efficient and stable embankments on soft clay foundations.
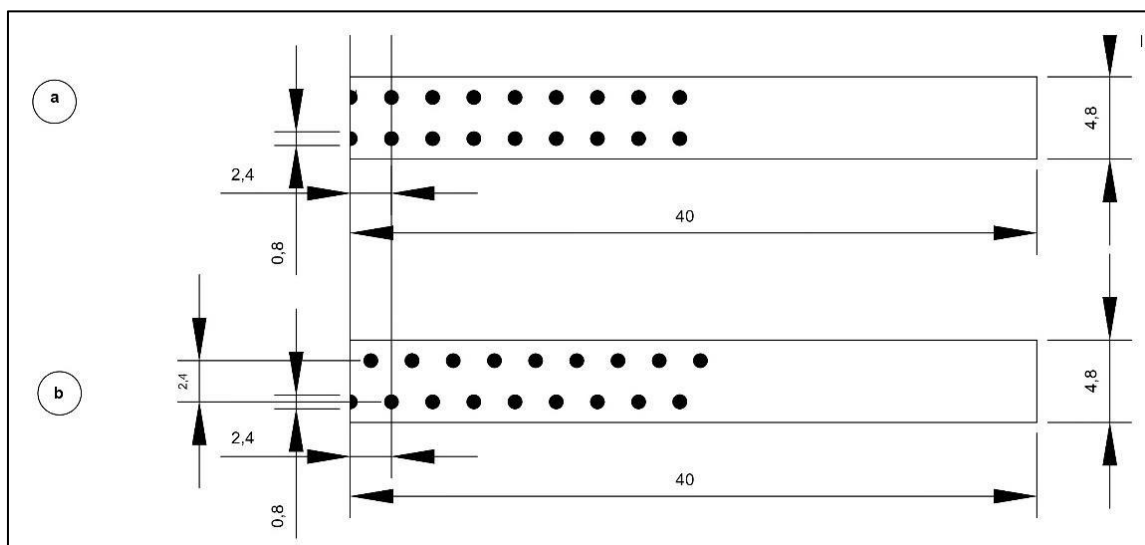
Fig. V. 18 Plan view of the distribution of the stone column: **a.** square pattern**, b.** triangular pattern.
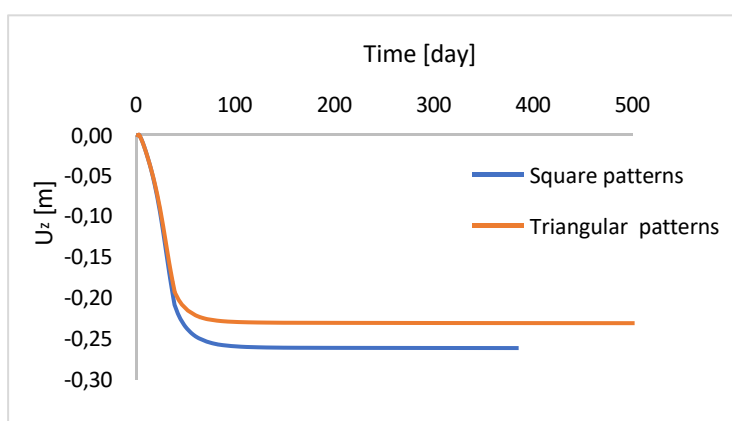
Fig. V. 19 Vertical displacement for different type of patterns at point A.
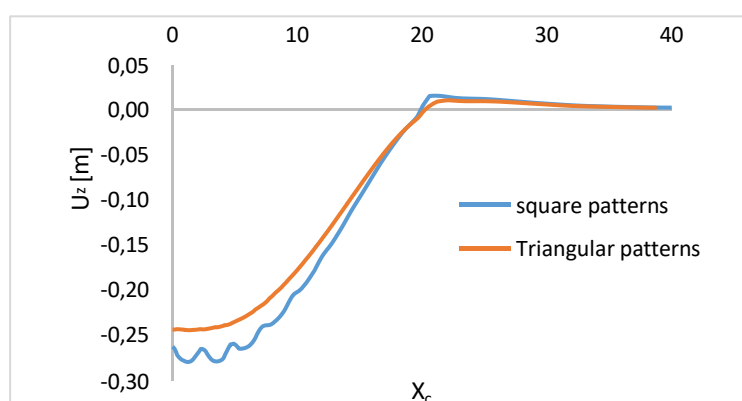
Fig. V. 20 Evolution of vertical displacement for different type of patterns across section (AA').

6. Conclusion

This study provides a thorough analysis of the performance of geosynthetic-encased stone columns (GESC) in soft clay soils beneath embankments using advanced 3D modeling with Plaxis 3D software. The research underscores the significant benefits of incorporating both installation effects and geosynthetic reinforcement in embankment design. The lateral expansion method for installing a group of encased stone columns demonstrates a notable reduction in settlement, highlighting the importance of realistic installation techniques. A detailed parametric study offers valuable insights into the factors influencing settlement reduction, guiding the selection of optimal geosynthetic properties, installation methods, and column arrangements. Increasing the stiffness of the geosynthetic encasement enhances load-bearing capacity and stability by providing better confinement. Various configurations of geosynthetic reinforcement, including horizontal, vertical, and combined methods, were explored, with the combined approach (VESC + HRSC) proving most effective in minimizing vertical displacement. Higher friction angles of stone column materials also result in reduced vertical displacement, emphasizing the importance of material selection. The triangular arrangement of GESC demonstrated superior performance in reducing settlement compared to the square arrangement, offering better support and load distribution. Overall, this research advances the understanding and application of GESC in geotechnical engineering, providing practical solutions for improving embankment stability and performance on soft clay soils. It offers crucial insights for designing resilient infrastructure in challenging geotechnical environments. Future research should continue exploring advanced techniques for integrating installation effects and geosynthetic reinforcement, including further parametric studies on different soil conditions, varying reinforcement configurations, and long-term monitoring of field installations to validate and refine predictive models.

GENERAL CONCLUSION

This thesis has provided a comprehensive analysis of geosynthetic-reinforced stone columns (GESC) in very soft soils, addressing the challenges and advancements in this field. The research is divided into two main sections: bibliographic research and numerical analysis, each contributing to a deeper understanding of GESC technology and its practical applications.

In the first part, the bibliographic research highlights the significance of soil improvement techniques, emphasizing the advantages of geosynthetic reinforcement. The integration of geosynthetics into stone columns offers enhanced radial confinement, reducing lateral expansion and aggregate loss, which greatly improves the columns' performance. The literature review in the second chapter reaffirms that geosynthetics provide a cost-effective and sustainable solution, significantly improving bearing capacity and reducing settlement. This underscores the practical benefits of using GESC in geotechnical engineering, especially in soft soil conditions.

The third chapter synthesizes findings from various studies on GESC, focusing on key parameters such as column diameter, length, and the type of geosynthetic used. It confirms that geogrids are particularly effective due to their superior strength characteristics. This chapter provides valuable insights into optimizing these parameters to enhance GESC performance and reliability.

The numerical analysis in the fourth and fifth chapters advances the understanding of GESC behavior through detailed 3D modeling. The use of advanced numerical techniques, including PLAXIS 3D software, has revealed significant improvements in performance with realistic simulations of installation effects and lateral expansion. The results demonstrate that optimal lateral expansion of up to 15% and triangular column arrangements, combined with vertical and horizontal reinforcements, lead to better performance in reducing settlement and improving load distribution.

This study introduces several novel aspects compared to previous research. It integrates geosynthetic reinforcement with a realistic approach by using the lateral expansion method to simulate installation effects, providing a more accurate representation of field conditions. Unlike other studies that often focus on either geosynthetic encasement or stone columns without addressing installation effects comprehensively, our study offers a combined approach. We employ realistic simulation techniques and extensive numerical analysis, capturing intricate behaviors that simpler methods or 2D models might miss. The synergy between geosynthetic encasement and installation methods significantly enhances performance, while our comprehensive parametric study explores a wide range of factors, offering practical recommendations for real-world applications.

Recommendations

1. Implementation of GESC: Prioritize the use of geosynthetic-encased stone columns for projects involving very soft soils to leverage their enhanced performance and sustainability benefits.

2. Adoption of 3D Numerical Modeling: Utilize advanced 3D numerical modeling techniques to accurately represent field conditions and optimize GESC performance.

3. Optimal Lateral Expansion: Implement lateral expansion methods with an optimal expansion of up to 15% to achieve improved field results.

4. Preferred Column Arrangement: Adopt triangular arrangements of GESC to improve load distribution and minimize settlements.

5. Combined Reinforcement Techniques: Use a combination of vertical and horizontal reinforcements (VESC and HRSC) to enhance performance in soft soil conditions.

6. Further Experimental Research: Conduct additional laboratory and field experiments to validate numerical findings and assess long-term performance and durability.

7. Extended Parameter Studies: Explore a broader range of soil types, column dimensions, and reinforcement configurations to deepen the understanding of GESC behavior.

In conclusion, the integration of geosynthetics into stone column technology represents a significant advancement in ground improvement methods. This research not only enhances theoretical understanding but also offers practical insights and recommendations for constructing stable infrastructure on soft soils. By addressing both theoretical and practical aspects, this thesis contributes to the advancement of geotechnical engineering and the development of resilient infrastructure in challenging soil conditions.

REFERENCES

Al Ammari, K. and Clarke, B. (2016), "Predicting the Effect of Vibro Stone Column Installation on Performance of Reinforced Foundations", World Academy of Science, Engineering and Technology.

Al Ammari, K. and Clarke, B.G. (2018), "Effect of Vibro Stone-Column Installation on the Performance of Reinforced Soil", Journal of Geotechnical and Geoenvironmental Engineering, American Society of Civil Engineers (ASCE), Vol. 144 No. 9, doi: 10.1061/(ASCE)GT.1943-5606.0001914.

Alexiew, D., Brokemper, D., & Lothspeich, S. (2005), "Geotextile Encased Columns (GEC): Load Capacity, Geotextile Selection and Pre-Design Graphs ". 1–14. https://doi.org/10.1061/40777 (156)12

Ali, K., Shahu, J. T., & Sharma, K. G. (2010), "Behaviour of reinforced stone columns in soft soils: an experimental study". In Indian geotechnical conference (pp. 620-628).

Ali, K., Shahu, J.T. and Sharma, K.G. (2015), "Model tests on single and groups of stone columns with different geosynthetic reinforcement arrangement", Https://Doi.Org/10.1680/Gein.14.00002, Thomas Telford Ltd , Vol. 21 No. 2, pp. 103–118, doi: 10.1680/GEIN.14.00002.

Alkhorshid, N.R., Araújo, G.L.S. and Palmeira, E.M. (2018), "Behavior of geosynthetic-encased stone columns in soft clay: Numerical and analytical evaluations", Soils and Rocks, Associacao Brasileira de Mecanica dos Solos, Vol. 41 No. 3, pp. 333–343, doi: 10.28927/SR.413333.

Almeida, M. S. S., Fagundes, D. F., Thorel, L., & Blanc, M. (2020). Geosynthetic-reinforced pile-embankments: numerical, analytical and centrifuge modelling. Https://Doi.Org/10.1680/Jgein.19.00011, 27(3), 301–314. doi: 10.1680/JGEIN.19.00011

Almeida, M. S. S., Hosseinpour, I., & Riccio, M. (2013), "Performance of a geosynthetic-encased column (GEC) in soft ground: numerical and analytical studies ". Geosynthetics international, 20(4), 252-262.

Al-Mosawe, M. J., Abbass, A. J., & Majieed, A. H. (1985), "Prediction of ultimate capacity of a single and groups of stone columns ". In Iraqi conference on Engineering ICE (Vol. 85, pp. 61-68).

Al-Obaidy, N. K. (2000), "Full scale tests on stone piles ", Baghdad University. Master Thesis.

Ambily, A. P., & Gandhi, S. R. (2007), "Behavior of stone columns based on experimental and FEM analysis ", Journal of geotechnical and geoenvironmental engineering, 133(4), 405-415.

Araújo, G.L.S., Palmeira, E.M. and Da Cunha, R.P. (2009), "Geosynthetic Encased Columns in a Tropical Collapsible Porous Clay", Proceedings of the 17th International Conference on Soil Mechanics and Geotechnical Engineering: The Academia and Practice of Geotechnical Engineering, IOS Press, Vol. 1, pp. 889–892, doi: 10.3233/978-1-60750-031-5-889.

Ashour, S. (2016), "The response of stone columns under the cyclic loading (Doctoral dissertation, University of Birmingham). "

Aslani, M., Nazariafshar, J., Ganjian, N., (2019), "Experimental Study on Shear Strength of Cohesive Soils Reinforced with Stone Columns ". Geotechnical and Geological Engineering 37, 2165–2188. https://doi.org/10.1007/S10706-018-0752-Z/METRICS

Ayadat, T. (1990), "Collapse of stone column foundations due to inundation.", University of Sheffield.

Ayadat, T. and Hanna, A.M. (2015), "Encapsulated stone columns as a soil improvement technique for collapsible soil", Https://Doi.Org/10.1680/Grim.2005.9.4.137, Thomas Telford Ltd, Vol. 9 No. 4, pp. 137–147, doi: 10.1680/GRIM.2005.9.4.137.

Ayadat, T., Hanna, A., & Etezad, M. (2008), "Failure process of stone columns in collapsible soils ".

Ayadat, Tahar. (1990), "Collapse of stone column foundations due to inundation ".

Bahi, S. and Houhou, M.N. (2024), "Optimizing ground improvement with encased stone columns: a 3D numerical analysis in very soft clay", World Journal of Engineering, Emerald Publishing, Vol. ahead-of-print No. ahead-of-print, doi: 10.1108/WJE-12-2023-0516/FULL/XML.

Balaam M.P. & Poulous, H.G., (1983), "The Behaviour of Foundations Supported by Clay Stabilised by Stone Columns ". Proc. Speciality Session 5, VIII Euro. Conf. on Soil Mech. & Fdn. Engg., Helsinki, Vol. 2: pp.199-204.

Balaam, N. P., & Booker, J. R. (1981), "Analysis of rigid rafts supported by granular piles. International Journal for Numerical and Analytical Methods in Geomechanics ", 5(4), 379–403. https://doi.org/10.1002/NAG.1610050405

Balaam, N.P. and Booker, J.R. (1985), "Effect of stone column yield on settlement of rigid foundations in stabilized clay", International Journal for Numerical and Analytical Methods in Geomechanics, John Wiley & Sons, Ltd, Vol. 9 No. 4, pp. 331–351, doi: 10.1002/NAG.1610090404.

Barksdale, R.D., Bachus, R.C. and Engineering, G.I. of Technology.S. of C. (1983), "Design and construction of stone columns, vol. I.", Turner-Fairbank Highway Research Center, doi: 10.21949/1503647.

Barron, R.A. (1948), "Consolidation of Fine-Grained Soils by Drain Wells by Drain Wells", Transactions of the American Society of Civil Engineers, American Society of Civil Engineers, Vol. 113 No. 1, pp. 718–742, doi: 10.1061/TACEAT.0006098.

Basack, S., Indraratna, B. and Rujikiatkamjorn, C. (2015), "Modeling the Performance of Stone Column–Reinforced Soft Ground under Static and Cyclic Loads", Journal of Geotechnical and Geoenvironmental

Engineering, American Society of Civil Engineers, Vol. 142 No. 2, p. 04015067, doi: 10.1061/(ASCE)GT.1943-5606.0001378.

Basack, S., Indraratna, B. and Rujikiatkamjorn, C. (2016), "Analysis of the Behaviour of Stone Column Stabilized Soft Ground Supporting Transport Infrastructure", Procedia Engineering, Elsevier Ltd, Vol. 143, pp. 347–354, doi: 10.1016/J.PROENG.2016.06.044.

Bathurst, R.J. and Hatami, K. (2015), "Seismic Response Analysis of a Geosynthetic-Reinforced Soil Retaining Wall", Https://Doi.Org/10.1680/Gein.5.0117, Thomas Telford Ltd, Vol. 5 No. 1–2, pp. 127–166, doi: 10.1680/GEIN.5.0117.

Bathurst, R.J. and Naftchali, F.M. (2021), "Geosynthetic reinforcement stiffness for analytical and numerical modelling of reinforced soil structures", Geotextiles and Geomembranes, Elsevier, Vol. 49 No. 4, pp. 921–940, doi: 10.1016/J.GEOTEXMEM.2021.01.003.

Bazzazian Bonab, S., Lajevardi, S.H., Saba, H.R., Ghalandarzadeh, A. and Mirhosseini, S.M. (2020), "Experimental studies on single reinforced stone columns with various positions of geotextile", Innovative Infrastructure Solutions, Springer, Vol. 5 No. 3, doi: 10.1007/S41062-020-00349-0.

Benmebarek, S., Remadna, A. and Benmebarek, N. (2018), "Numerical Modelling of Stone Column Installation Effects on Performance of Circular Footing", International Journal of Geosynthetics and Ground Engineering, Springer, Vol. 4 No. 3, doi: 10.1007/S40891-018-0140-Z.

Black, J.A., Sivakumar, V., Madhav, M.R. and Hamill, G.A. (2007), "Reinforced Stone Columns in Weak Deposits: Laboratory Model Study", Journal of Geotechnical and Geoenvironmental Engineering, American Society of Civil Engineers, Vol. 133 No. 9, pp. 1154–1161, doi: 10.1061/(ASCE)1090-0241(2007)133:9(1154).

Brinkgreve, R.B., Kumarswamy, S. and Swolfs, W.M. (2016), Plaxis 2016, PLAXISBV, Delft

Carter, J.P., Randolph, M.F. and Wroth, C.P. (1979), "Stress and pore pressure changes in clay during and after the expansion of a cylindrical cavity", International Journal for Numerical and Analytical Methods in Geomechanics, John Wiley & Sons, Ltd, Vol. 3 No. 4, pp. 305–322, doi: 10.1002/NAG.1610030402.

Castro, J. (2014), "Numerical modelling of stone columns beneath a rigid footing", Computers and Geotechnics, Elsevier, Vol. 60, pp. 77–87, doi: 10.1016/J.COMPGEO.2014.03.016.

Castro, J. (2017), "Groups of encased stone columns: Influence of column length and arrangement", Geotextiles and Geomembranes, Elsevier, Vol. 45 No. 2, pp. 68–80, doi: 10.1016/J.GEOTEXMEM.2016.12.001.

Castro, J. and Karstunen, M. (2010), "Numerical simulations of stone column installation", Canadian Geotechnical Journal, Vol. 47 No. 10, pp. 1127–1138, doi: 10.1139/T10-019/ASSET/IMAGES/T10-019IE21H.GIF.

Castro, J. and Sagaseta, C. (2015), "Pore pressure during stone column installation", Https://Doi.Org/10.1680/Grim.9.00015, Thomas Telford Ltd, Vol. 165 No. 2, pp. 97–109, doi: 10.1680/GRIM.9.00015.

Castro, J., Justo, J., Miranda, M., 2024. "An analytical solution for the settlement of encased stone columns beneath rigid footings ". Geotextiles and Geomembranes 52, 451–464. https://doi.org/10.1016/J.GEOTEXMEM.2024.01.001

Castro, J., Sagaseta, C., 2011. "Consolidation and deformation around stone columns: Numerical evaluation of analytical solutions ". Comput Geotech 38, 354–362. https://doi.org/10.1016/J.COMPGEO.2010.12.006

Chen, J. F., Li, L. Y., Xue, J. F., & Feng, S. Z. (2015), "Failure mechanism of geosynthetic-encased stone columns in soft soils under embankment ". Geotextiles and Geomembranes, 43(5), 424–431. https://doi.org/10.1016/J.GEOTEXMEM.2015.04.016

Corneille, S. (2007), "Étude du comportement mécanique des colonnes ballastées chargées par des semelles rigides" ,(Doctoral dissertation, Institut National Polytechnique de Lorraine).

D.T.U 13.2 (1992), "fondations profondes pour le bâtiment", Partie 1 : Cahier des clauses techniques.

Dar, L.A. and Shah, M.Y. (2021), "Three-Dimensional Numerical Study on Behavior of Geosynthetic Encased Stone Column Placed in Soft Soil", Geotechnical and Geological Engineering, Springer Science and.

Das, P., & Pal, S. K. (2013). A study of the behavior of stone column in local soft and loose layered soil. EJGE, 18, 1777-17786.

Dash, S.K. and Bora, M.C. (2013), "Influence of geosynthetic encasement on the performance of stone columns floating in soft clay", Canadian Geotechnical Journal, Vol. 50 No. 7, pp. 754–765, doi: 10.1139/CGJ-2012-0437.

Debbabi, I. E., Saddek, R. M., Rashid, A. S. A., & Muhammed, A. S. (2020), "Numerical modeling of encased stone columns supporting embankments on sabkha soil", Civ. Eng. J, 6(8), 1593-1608.

Debnath, P. and Dey, A.K. (2017), "Bearing capacity of geogrid reinforced sand over encased stone columns in soft clay", Geotextiles and Geomembranes, Elsevier, Vol. 45 No. 6, pp. 653–664, doi: 10.1016/J.GEOTEXMEM.2017.08.006.

Demir, A., Sarici, T., Laman, M., Bagriacik, B., & Ok, B. (2013), "An experimental study on behaviour of geosynthetic reinforced stone columns", In 2nd International Balkans Conference on Challenges of Civil Engineering.

Deshpande, T.D., Kumar, S., Begum, G., Basha, S.A.K., Rao, B.H., (2021), "Analysis of Railway Embankment Supported with Geosynthetic-Encased Stone Columns in Soft Clays: A Case Study "International Journal of Geosynthetics and Ground Engineering 7. https://doi.org/10.1007/S40891-021-00288-5

Dhouib, A. (1956-. . . .)., Magnan, J.-P. (1949-. . . .)., & Mestat, Philippe. (2004), "Comportement des semelles sur colonnes ballastees. ASEP-GI 2004 : SYMPOSIUM INTERNATIONAL SUR L'AMELIORATION DES SOLS EN PLACE, 9-10 SEPTEMBRE 2004.

Dhouib, A., & Blondeau, F. (2005), "Colonnes ballastées", Edition Revues des Ponts et Chaussées, 142-144.

Dhouib, A., Gambin, M. P., Jacquemin, S., & Soyez, B. (1998), " Une nouvelle approche de la stabilité des remblais sur sols mous traités par colonnes ballastées", Revue francaise de Geotechnique, (82), 37-48.

di Prisco, C. and Galli, A. (2011), "Mechanical behaviour of geo-encased sand columns: small scale experimental tests and numerical modelling", Geomechanics and Geoengineering, Taylor & Francis, Vol. 6 No. 4, pp. 251–263, doi: 10.1080/17486025.2011.578756.

Dobson, T., & Slocombe, B. (1982), "Deep densification of granular fills", In Internal Publication, GKN Keller Foundation Company, presented at ASCE 2nd Geotechnical Conference, Las Vegas, Nev.

DU LCPC, M. O. (1971). Essai pressiométriqlle normal.

EBGEO, G. (2011), "Recommendations for design and analysis of earth structures using geosynthetic reinforcements", German Geotechnical Society, Berlin.

Ellouze, S., Bouassida, M., Bensalem, Z. and Znaidi, M.N. (2017), "Numerical analysis of the installation effects on the behaviour of soft clay improved by stone columns", Geomechanics and Geoengineering, Taylor and Francis Ltd., Vol. 12 No. 2, pp. 73–85, doi: 10.1080/17486025.2016.1164903.

Elsawy, M.B.D., n.d. Behaviour of soft ground improved by conventional and geogrid-encased stone columns, based on FEM study. https://doi.org/10.1680/gein.13.00017

Elshazly, H., Elkasabgy, M. and Elleboudy, A. (2008), "Effect of inter-column spacing on soil stresses due to vibro-installed stone columns: Interesting findings", Geotechnical and Geological Engineering, Vol. 26 No. 2, pp. 225–236, doi: 10.1007/S10706-007-9159-Y.

Elwakeel, A.O., Elsherbini, R.M., (2024), "Effect of Column Material Internal Angle of Friction and the Geotextile Stiffness on the Behavior of Group of Geosynthetic-Encased Stone Column", Indian Geotechnical Journal 2024 1–15. https://doi.org/10.1007/S40098-024-01005-5

Farah, R.E. and Nalbantoglu, Z. (2020), "Behavior of Geotextile-Encased Single Stone Column in Soft Soils", Arabian Journal for Science and Engineering, Springer, Vol. 45 No. 5, pp. 3877–3890, doi: 10.1007/S13369-019-04299-3/METRICS.

Fattah, M.Y., Zabar, B.S. and Hassan, H.A. (2016), "Experimental Analysis of Embankment on Ordinary and Encased Stone Columns", International Journal of Geomechanics, American Society of Civil Engineers, Vol. 16 No. 4, p. 04015102, doi: 10.1061/(ASCE)GM.1943-5622.0000579.

Foray, P., Flavigny, E., Nguyen, N.T., Lambert, S. and Briançon, L. (2009), "Modélisation numérique 3D de colonnes ballastées et application", Proceedings of the 17th International Conference on Soil Mechanics and Geotechnical Engineering: The Academia and Practice of Geotechnical Engineering, IOS Press, Vol. 3, pp. 2382–2385, doi: 10.3233/978-1-60750-031-5-2382.

Gäb, M., Schweiger, H., Thurner, R. and Adam, D. (2007), "Field trial to investigate the performance of a floating stone column foundation", Millpress.

Gao, J., Zhang, Y., Wang, C. and Yuan, C. (2021), "Behavior characteristics of geosynthetic-encased stone column under cyclic loading", Transportation Geotechnics, Elsevier, Vol. 28, p. 100554, doi: 10.1016/J.TRGEO.2021.100554.

Ghaemi, A., Zhian, T., Pirzadeh, B., Hashemi Monfared, S. and Mosavi, A. (2021), "Reliability-based design and implementation of crow search algorithm for longitudinal dispersion coefficient estimation in rivers", Environmental Science and Pollution Research, Springer Science and Business Media Deutschland GmbH, Vol. 28 No. 27, pp. 35971–35990, doi: 10.1007/S11356-021-12651-0/FIGURES/13.

Ghazavi, M. and Nazari Afshar, J. (2013), "Bearing capacity of geosynthetic encased stone columns", Geotextiles and Geomembranes, Vol. 38, pp. 26–36, doi: 10.1016/J.GEOTEXMEM.2013.04.003.

Ghazavi, M., Ehsani Yamchi, A., Nazari Afshar, J., (2018), "Bearing capacity of horizontally layered geosynthetic reinforced stone columns", Geotextiles and Geomembranes 46, 312–318. https://doi.org/10.1016/J.GEOTEXMEM.2018.01.002

Gholaminejad, A., Mahboubi, A. and Noorzad, A. (2020), "Encased stone columns: coupled continuum – discrete modelling and observations", Https://Doi.Org/10.1680/Jgein.20.00017, Thomas Telford Ltd , Vol. 27 No. 6, pp. 581–592, doi: 10.1680/JGEIN.20.00017.

Ghorbani, A., Hosseinpour, I., Shormage, M., (2021), "Deformation and Stability Analysis of Embankment over Stone Column-Strengthened Soft Ground", KSCE Journal of Civil Engineering 25, 404–416. https://doi.org/10.1007/s12205-020-0349-y

Gibson, R. E. (1961). In situ measurement of soil properties with the pressuremeter. Civil Engrg. and Pub. Wks. Rev, 56(568), 615-618.

Gniel, J. and Bouazza, A. (2009), "Improvement of soft soils using geogrid encased stone columns", Geotextiles and Geomembranes, Elsevier, Vol. 27 No. 3, pp. 167–175, doi: 10.1016/J.GEOTEXMEM.2008.11.001.

Gniel, J., & Bouazza, A. (2010), "Construction of geogrid encased stone columns: A new proposal based on laboratory testing", Geotextiles and Geomembranes, 28(1), 108–118. doi: 10.1016/J.GEOTEXMEM.2009.12.012

Golait, Y.S., Padade, A.H., (2017), "Analytical and Experimental Studies on Cemented Stone Columns for Soft Clay Ground Improvement", International Journal of Geomechanics 17. https://doi.org/10.1061/(ASCE)GM.1943-5622.0000779

GREENWOOD DA. (1970), "Mechanical improvement of soils below ground surface", Trid.Trb.Org, pp. 11–22.

Greenwood, D. A. (1991), "Load tests on stone columns", ASTM International.

Greenwood, J. A., & Tripp, J. H. (1970), "The contact of two nominally flat rough surfaces", Proceedings of the institution of mechanical engineers, 185(1), 625-633.

Grizi, A., Al-Ani, W. and Wanatowski, D. (2022), "Numerical Analysis of the Settlement Behavior of Soft Soil Improved with Stone Columns", Applied Sciences 2022, Vol. 12, Page 5293, Multidisciplinary Digital Publishing Institute, Vol. 12 No. 11, p. 5293, doi: 10.3390/APP12115293.

Guetif, Z., Bouassida, M., & Debats, J. M. (2003). "Parametric study of the improvement due to vibrocompacted columns installation in soft soils". In Proceedings of the 13th African Regional Conference of Soil Mechanics and Geotechnical Engineering (pp. 463-466).

Guetif, Z., Bouassida, M., Debats, J.M., (2007), "Improved soft clay characteristics due to stone column installation", Comput Geotech 34, 104–111. https://doi.org/10.1016/j.compgeo.2006.09.008

Halder, P. and Manna, B. (2022), "Performance evaluation of piled rafts in sand based on load-sharing mechanism using finite element model", International Journal of Geotechnical Engineering, Taylor & Francis, Vol. 16 No. 5, pp. 574–591, doi: 10.1080/19386362.2020.1729297.

Han, J. and Ye, S.L. (2002), "A Theoretical Solution for Consolidation Rates of Stone Column-Reinforced Foundations Accounting for Smear and Well Resistance Effects", International Journal of Geomechanics, American Society of Civil Engineers, Vol. 2 No. 2, pp. 135–151, doi: 10.1061/(ASCE)1532-3641(2002)2:2(135).

Han, J., & Ye, S. (1991), "Field tests of soft clay stabilized by stone columns in coastal areas of China", In

Handy, R.L. (2001), "Does Lateral Stress Really Influence Settlement?", Journal of Geotechnical and Geoenvironmental Engineering, American Society of Civil Engineers (ASCE), Vol. 127 No. 7, pp. 623–626, doi: 10.1061/(ASCE)1090-0241(2001)127:7(623).

Hataf, N., & Nabipour, N. (2013). Experimental investigation on bearing capacity of geosynthetic encapsulated stone columns. In Proc. 18th Int. Conf. on Soil Mech. and Geotech. Eng., Paris.

Hatami, K., Bathurst, R.J., (2011), "Development and verification of a numerical model for the analysis of geosynthetic-reinforced soil segmental walls under working stress conditions", https://doi.org/10.1139/t05-040 42, 1066–1085. https://doi.org/10.1139/T05-040

Hosseinpour, I., Soriano, C. and Almeida, M.S.S. (2019), "A comparative study for the performance of encased granular columns", Journal of Rock Mechanics and Geotechnical Engineering, Chinese Academy of Sciences, Vol. 11 No. 2, pp. 379–388, doi: 10.1016/J.JRMGE.2018.12.002.

Huang, B., Bathurst, R.J. and Hatami, K. (2009), "Numerical Study of Reinforced Soil Segmental Walls Using Three Different Constitutive Soil Models", Journal of Geotechnical and Geoenvironmental Engineering, American Society of Civil Engineers, Vol. 135 No. 10, pp. 1486–1498, doi: 10.1061/(ASCE)GT.1943-5606.0000092.

Hughes, J.M.O., Withers, N.J. and Greenwood, D.A. (2015), "A field trial of the reinforcing effect of a stone column in soil", Https://Doi.Org/10.1680/Geot.1975.25.1.31, Thomas Telford Ltd , Vol. 25 No. 1, pp. 31–44, doi: 10.1680/GEOT.1975.25.1.31.

Iqbal, M.A., Wang, Y., Miah, M.M. and Osman, M.S. (2021), "Study on Date–Jimbo–Kashiwara–Miwa Equation with Conformable Derivative Dependent on Time Parameter to Find the Exact Dynamic Wave Solutions", Fractal and Fractional 2022, Vol. 6, Page 4, Multidisciplinary Digital Publishing Institute, Vol. 6 No. 1, p. 4, doi: 10.3390/FRACTALFRACT6010004.

Irshad, A., Mukherjee, S., (2024), "Numerical study on performance of Raft Foundation resting on stone column reinforced soft clay subjected to eccentric load", Recent Advances in Material, Manufacturing, and Machine Learning 331–339. https://doi.org/10.1201/9781003450252-39/NUMERICAL-STUDY-PERFORMANCE-RAFT-FOUNDATION-RESTING-STONE-COLUMN-REINFORCED-SOFT-CLAY-SUBJECTED-ECCENTRIC-LOAD-ASHEEQUL-IRSHAD-SIDDHARTHA-MUKHERJEE

Jabir, H.A., Abid, S.R., Murali, G., Ali, S.H., Klyuev, S., Fediuk, R., Vatin, N., et al. (2020), "Experimental Tests and Reliability Analysis of the Cracking Impact Resistance of UHPFRC", Fibers 2020, Vol. 8, Page 74, Multidisciplinary Digital Publishing Institute, Vol. 8 No. 12, p. 74, doi: 10.3390/FIB8120074.

Jamshidi Chenari, R. and Bathurst, R.J. (2023), "Influence of geosynthetic stiffness on bearing capacity of strip footings seated on thin reinforced granular layers over undrained soft clay", Geotextiles and Geomembranes, Elsevier, Vol. 51 No. 1, pp. 43–55, doi: 10.1016/J.GEOTEXMEM.2022.09.006.

Jayarajan, J. and Karpurapu, R. (2021), "Bearing Capacity and Settlement Response of Ordinary and Geosynthetic Encased Granular Columns in Soft Clay Soils: Analysis and Design Charts", Indian Geotechnical Journal, Springer, Vol. 51 No. 2, pp. 237–253, doi: 10.1007/S40098-020-00457-9/METRICS.

Jefferson, I., Gaterell, M., Thomas, A.M. and Serridge, C.J. (2015), "Emissions assessment related to vibro stone columns", Https://Doi.Org/10.1680/Grim.2010.163.1.71, Thomas Telford Ltd , Vol. 163 No. 1, pp. 71–77, doi: 10.1680/GRIM.2010.163.1.71.

Kadhim, S.T., Parsons, R.L. and Han, J. (2018), "Three-dimensional numerical analysis of individual geotextile-encased sand columns with surrounding loose sand", Geotextiles and Geomembranes, Elsevier, Vol. 46 No. 6, pp. 836–847, doi: 10.1016/J.GEOTEXMEM.2018.08.002.

Kahyaoğlu, M.R. and Doğan, T. (2022), "Numerical Study on the Deformation Behavior of Geosynthetic-Encased Stone Columns Supporting Embankments", Teknik Dergi, Teknik Dergi, doi: 10.18400/tekderg.949826.

Kardgar, H. (2018), "Investigation of the Bearing Capacity of Foundations on Encased Stone Columns Using Finite Element Method", International Journal of Integrated Engineering, Vol. 10 No. 1, pp. 103–108, doi: 10.30880/ijie.2018.10.01.016.

Kelesoglu, M.K. and Durmus, C. (2022), "Numerical Plane-Strain Modelling of Stone Columns: Installation Process, Single and Group Column Behaviour", KSCE Journal of Civil Engineering, Korean Society of Civil Engineers, Vol. 26 No. 8, pp. 3402–3415, doi: 10.1007/S12205-022-1671-3/METRICS.

Kempfert H. (2006), "Excavations and Foundations in Soft Soil". Berlin: Springer-Verlag Berlin Heidelberg.

KEMPFERT, H. Geotextile-Encased Columns (GEC) for Foundation of a Dike on Very Soft Soils.

Killeen, M.M. and Mccabe, B.A. (2014), "Settlement performance of pad footings on soft clay supported by stone columns: A numerical study", Soils and Foundations, Elsevier, Vol. 54 No. 4, pp. 760–776, doi: 10.1016/J.SANDF.2014.06.011.

Kirsch F. (2006), "Vibro stone column installation and its effect on ground improvement", Numerical Modelling of Construction Processes in Geotechnical Engineering for Urban Environment, Bochum, Germany, pp. 115–124.

Kirsch, Klaus and Fabian. (2016), "Ground Improvement By Vibratory Deep Compaction".

Kumar Shukla, S., & Yin, J.-H. (2006), "Fundamentals of Geosynthetic Engineering", Fundamentals of Geosynthetic Engineering. https://doi.org/10.1201/9781482288445

Kumar, R., & Jain, P. K. (2013), "Expansive soft soil improvement by geogrid encased granular pile", International Journal on Emerging Technologies, 4(1), 55-61.

Lambe, T. W., and Whitman, R. V. (1969), "Soil Mechanics". John Wiley and Sons, New York, pp. 514-520.

Lee, D., Yoo, C., Park, S., & Jung, S. (2008), "Field Load Tests of Geogrid Encased Stone Columns In Soft Ground", OnePetro. https://dx.doi.org/

Lee, D.-Y. and Yoo, C.-S. (2011), "Laboratory Investigation on Construction Method of Geogrid Encased Stone Column", Journal of the Korean Geotechnical Society, Korean Geotechnical Society, Vol. 27 No. 2, pp. 73–80, doi: 10.7843/KGS.2011.27.2.073.

Lee, F.H., Juneja, A. and Tan, T.S. (2015), "Stress and pore pressure changes due to sand compaction pile installation in soft clay", Https://Doi.Org/10.1680/Geot.2004.54.1.01, Thomas Telford Ltd , Vol. 54 No. 1, pp. 01–16, doi: 10.1680/GEOT.2004.54.1.01.

Madhav, M. R., & Vitkar, P. P. (1978), "Strip footing on weak clay stabilized with a granular trench or pile", Canadian geotechnical journal, 15(4), 605-609.

Maleki, M. and Imani, M. (2022), "Active lateral pressure to rigid retaining walls in the presence of an adjacent rock mass", Arabian Journal of Geosciences 2022 15:2, Springer, Vol. 15 No. 2, pp. 1–11, doi: 10.1007/S12517-022-09454-Z.

Maleki, M. and Mir Mohammad Hosseini, S.M. (2019), "Seismic Performance of Deep Excavations Restrained by Anchorage System Using Quasi Static Approach", Journal of Seismology and Earthquake Engineering, International Institute of Earthquake Engineering and Seismology, Vol. 21 No. 2, pp. 11–21, doi: 10.48303/JSEE.2019.240810.

Maleki, M. and Mir Mohammad Hosseini, S.M. (2022), "Assessment of the Pseudo-static seismic behavior in the soil nail walls using numerical analysis", Innovative Infrastructure Solutions, Springer Science and Business Media Deutschland GmbH, Vol. 7 No. 4, pp. 1–18, doi: 10.1007/S41062-022-00861-5/METRICS.

Maleki, M. and Nabizadeh, A. (2021), "Seismic performance of deep excavation restrained by guardian truss structures system using quasi-static approach", SN Applied Sciences, Springer Nature, Vol. 3 No. 4, pp. 1–17, doi: 10.1007/S42452-021-04415-9/FIGURES/32.

McCabe, B. A., & Killeen, M. M. (2017), "Small stone-column groups: mechanisms of deformation at serviceability limit state", International Journal of Geomechanics, 17(5), 04016114.

McKelvey, D., Sivakumar, V., Bell, A. and Graham, J. (2015), "Modelling vibrated stone columns in soft clay", Https://Doi.Org/10.1680/Geng.2004.157.3.137, Thomas Telford Ltd , Vol. 157 No. 3, pp. 137–149, doi: 10.1680/GENG.2004.157.3.137.

Miranda, M. and Da Costa, A. (2016), "Laboratory analysis of encased stone columns", Geotextiles and Geomembranes, Elsevier, Vol. 44 No. 3, pp. 269–277, doi: 10.1016/J.GEOTEXMEM.2015.12.001.

Miranda, M., Da Costa, A., Castro, J. and Sagaseta, C. (2017), "Influence of geotextile encasement on the behaviour of stone columns: Laboratory study", Geotextiles and Geomembranes, Elsevier, Vol. 45 No. 1, pp. 14–22, doi: 10.1016/J.GEOTEXMEM.2016.08.004.

Miranda, M., Fernández-Ruiz, J., Castro, J., (2021), "Critical length of encased stone columns", Geotextiles and Geomembranes 49, 1312–1323. https://doi.org/10.1016/J.GEOTEXMEM.2021.05.003

Mitchell, J. M., & Jardine, F. M. (2002). A guide to ground treatment (Vol. 573, p. 2002). London: CIRIA.

Moghadam, M.J., Ashtari, K., (2020), "Numerical Analysis of Railways on Soft Soil Under Various Train Speeds", Transportation Infrastructure Geotechnology 7, 103–125. https://doi.org/10.1007/S40515-019-00092-9

Moradi, R., Marto, A., Rashid, A.S.A., Moradi, M.M., Ganiyu, A.A. and Horpibulsuk, S. (2018), "Bearing capacity of soft soil model treated with end-bearing bottom ash columns", Environmental Earth Sciences, Springer Verlag, Vol. 77 No. 3, pp. 1–9, doi: 10.1007/S12665-018-7287-8/METRICS.

Moseley, M.P., Kirsch, K. (Eds.), (2004), "Ground Improvement". https://doi.org/10.1201/9780203489611

Murakonda, P., Maheshwari, P., (2020), "Soil–Structure Interaction of Plates on Extensible Geosynthetic-Stone Column Reinforced Earth Beds", Geotechnical and Geological Engineering 38, 3067–3086. https://doi.org/10.1007/s10706-020-01207-7

Murugesan, S. and Rajagopal, K. (2006), "Geosynthetic-encased stone columns: Numerical evaluation", Geotextiles and Geomembranes, Vol. 24, pp. 349–358, doi: 10.1016/j.geotexmem.2006.05.001.

Murugesan, S., & Rajagopal, K. (2009), "Experimental and Numerical investigations on the behaviour of geosynthetic encased stone columns", In Proceedings of Indian Geotechnical Conference, Guntur, India (pp. 480-484).

Muzammil, S.P., Varghese, R.M. and Joseph, J. (2018), "Numerical Simulation of the Response of Geosynthetic Encased Stone Columns Under Oil Storage Tank", International Journal of Geosynthetics and Ground Engineering, Springer, Vol. 4 No. 1, pp. 1–12, doi: 10.1007/S40891-017-0122-6/METRICS.

Naeini, S.A. and Gholampoor, N. (2019), "Effect of Geotextile Encasement on the Shear Strength Behavior of Stone Column-Treated Wet Clays", Indian Geotechnical Journal, Springer, Vol. 49 No. 3, pp. 292–303, doi: 10.1007/S40098-018-0329-Z/METRICS.

Nafees, A., Javed, M.F., Musarat, M.A., Ali, M., Aslam, F. and Vatin, N.I. (2021), "FE Modelling and Analysis of Beam Column Joint Using Reactive Powder Concrete", Crystals 2021, Vol. 11, Page 1372, Multidisciplinary Digital Publishing Institute, Vol. 11 No. 11, p. 1372, doi: 10.3390/CRYST11111372.

Nagula, S.S., Nguyen, D.M., Grabe, J., (2018), "Numerical modelling and validation of geosynthetic encased columns in soft soils with installation effect", Geotextiles and Geomembranes 46, 790–800. https://doi.org/10.1016/J.GEOTEXMEM.2018.07.011

Najjar, S., Sadek, S., & Bou Lattouf, H. (2013), "The drained strength of soft clays with partially penetrating sand columns at different area replacement ratios", in 18th international conference on soil mechanics and geotechnical engineering (pp. 939-942).

Najjar, S.S., Sadek, S. and Maakaroun, T. (2010), "Effect of Sand Columns on the Undrained Load Response of Soft Clays", Journal of Geotechnical and Geoenvironmental Engineering, American Society of Civil Engineers, Vol. 136 No. 9, pp. 1263–1277, doi: 10.1061/(ASCE)GT.1943-5606.0000328.

Nasiri, M. and Hajiazizi, M. (2019), "An experimental and numerical investigation of reinforced slope using geotextile encased stone column", Https://Doi.Org/10.1080/19386362.2019.1651029, Taylor & Francis, Vol. 15 No. 5, pp. 543–552, doi: 10.1080/19386362.2019.1651029.

Nav, M.A., Rahnavard, R., Noorzad, A. and Napolitano, R. (2020), "Numerical evaluation of the behavior of ordinary and reinforced stone columns", Structures, Elsevier, Vol. 25, pp. 481–490, doi: 10.1016/J.ISTRUC.2020.03.021.

Nazari Afshar, J. and Ghazavi, M. (2014), "A simple analytical method for calculation of bearing capacity of stone-column", International Journal of Civil Engineering, International Journal of Civil Engineering, Vol. 12 No. 1, pp. 15–25.

Nguyen, N.-T., Foray, P. and Flavigny, E. (2007), "Prise en compte de l'effet de la mise en place dans la modélisation numérique en 3D des colonnes ballastées dans l'argile molle", AFM, Maison de la Mécanique, 39/41 rue Louis Blanc - 92400 Courbevoie.

Ouyang, F., Wu, Z., Wang, Y., Wang, Z., Cao, J., Wang, K., Zhang, J., (2024), "Field tests on partially geotextile encased stone column-supported embankment over silty clay", Geotextiles and Geomembranes 52, 95–109. https://doi.org/10.1016/J.GEOTEXMEM.2023.09.005

Poorooshasb, H.B. and Meyerhof, G.G. (1997), "Analysis of behavior of stone columns and lime columns", Computers and Geotechnics, Elsevier, Vol. 20 No. 1, pp. 47–70, doi: 10.1016/S0266-352X(96)00013-4.

Prasad, S. S. G., & Satyanarayana, P. V. V. (2016), "Improvement of soft soil performance using stone columns improved with circular geogrid discs", Indian Journal of Science and Technology.

Priebe, H.J. (1995), "The design of vibro replacement : Ground Engineering".

Pulko, B. and Majes, B. (2005), "Simple and accurate prediction of settlements of stone column reinforced soil", IOS Press, pp. 1401–1404, doi: 10.3233/978-1-61499-656-9-1401.

Pulko, B., Majes, B. and Logar, J. (2011), "Geosynthetic-encased stone columns: Analytical calculation model", Geotextiles and Geomembranes, Elsevier, Vol. 29 No. 1, pp. 29–39, doi: 10.1016/J.GEOTEXMEM.2010.06.005.

Rahmani, F., Hosseini, S.M., Khezri, A. and Maleki, M. (2022), "Effect of grid-form deep soil mixing on the liquefaction-induced foundation settlement, using numerical approach", Arabian Journal of Geosciences 2022 15:12, Springer, Vol. 15 No. 12, pp. 1–15, doi: 10.1007/S12517-022-10340-X.

Raithel, M. and Kempfert, H.-G. (2000), "Calculation Models For Dam Foundations With Geotextile Coated Sand Columns", OnePetro, 19 November.

Raithel, M., Kirchner, A., Schade, C., & Leusink, E. (2005), "Foundation of constructions on very soft soils with geotextile encased columns-state of the art", Innovations in Grouting and Soil Improvement, 1-11.

Raithel, M., Küster, V., & Lindmark, A. (2004). Geotextile-Encased Columns-a foundation system for earth structures, illustrated by a dyke project for a works extension in Hamburg. In Nordic Geotechnical Meeting NGM (pp. 1-10). Citeseer.

Rajesh, S. (2017), "Time-dependent behaviour of fully and partially penetrated geosynthetic encased stone columns", Http://Dx.Doi.Org/10.1680/Jgein.16.00015, Thomas Telford Ltd , Vol. 24 No. 1, pp. 60–71, doi: 10.1680/JGEIN.16.00015.

Rashid, A. S. A., Kueh, A. B. H., & Mohamad, H. (2018), "Behaviour of soft soil improved by floating soil–cement columns", Https://Doi.Org/10.1680/Jphmg.15.00041, 18(2), 95–116. https://doi.org/10.1680/JPHMG.15.00041

Recommendations for Design and Analysis of Earth Structures using Geosynthetic Reinforcements – EBGEO. (2012), Second Edition.

Remadna, A., Benmebarek, S. and Benmebarek, N. (2020), "Numerical Analyses of the Optimum Length for Stone Column Reinforced Foundation", International Journal of Geosynthetics and Ground Engineering, Springer, Vol. 6 No. 3, doi: 10.1007/s40891-020-00218-x.

Rezaei, M.M., Lajevardi, S.H., Saba, H., Ghalandarzadeh, A., Zeighami, E., (2019), "Laboratory Study on Single Stone Columns Reinforced with Steel Bars and Discs", International Journal of Geosynthetics and Ground Engineering 5, 1–14. https://doi.org/10.1007/S40891-019-0154-1/METRICS

Rowe, R.K. and Ho, S.K. (1997), "Continuous Panel Reinforced Soil Walls on Rigid Foundations", Journal of Geotechnical and Geoenvironmental Engineering, American Society of Civil Engineers, Vol. 123 No. 10, pp. 912–920, doi: 10.1061/(ASCE)1090-0241(1997)123:10(912).

Rowe, R.K. and Ho, S.K. (2011), "Horizontal deformation in reinforced soil walls", Https://Doi.Org/10.1139/T97-062, NRC Research Press Ottawa, Canada , Vol. 35 No. 2, pp. 312–327, doi: 10.1139/T97-062.

Sadaoui, O., and R. Bahar. (2017), "Field Measurements and Back Calculations of Settlements of Structures Founded on Improved Soft Soils by Stone Columns." European Journal of Environmental and Civil Engineering 23 (1): 85–111. doi:10.1080/19648189.2016.1271358.

Sexton, B.G. and McCabe, B.A. (2015), "Modeling stone column installation in an elasto-viscoplastic soil", International Journal of Geotechnical Engineering, Vol. 9 No. 5, pp. 500-512, doi: 10.1179/1939787914Y.0000000090

Shahu, J.T., Madhav, M.R. and Hayashi, S. (2000), "Analysis of soft ground-granular pile-granular mat system", Computers and Geotechnics, Elsevier, Vol. 27 No. 1, pp. 45–62, doi: 10.1016/S0266-352X(00)00004-5.

Shamsi, M., Ghanbari, A., Nazariafshar, J., (2019), "Behavior of sand columns reinforced by vertical geotextile encasement and horizontal geotextile layers", Geomechanics and Engineering 19, 329–342. https://doi.org/10.12989/gae.2019.19.4.329

Sharma, R. S., Kumar, B. P., & Nagendra, G. (2004), "Compressive load response of granular piles reinforced with geogrids", Canadian geotechnical journal, 41(1), 187-192.

Shehata, H.F., Sorour, T.M. and Fayed, A.L. (2021), "Effect of stone column installation on soft clay behavior", International Journal of Geotechnical Engineering, Taylor and Francis Ltd., Vol. 15 No. 5, pp. 530–542, doi: 10.1080/19386362.2018.1478245.

Shen, P., Xu, C. and Han, J. (2020), "Centrifuge tests to investigate global performance of geosynthetic-reinforced pile-supported embankments with side slopes", Geotextiles and Geomembranes, Elsevier, Vol. 48 No. 1, pp. 120–127, doi: 10.1016/J.GEOTEXMEM.2019.103527.

Shenkman, R., & Ponomaryov, A. (2016), "experimental and numerical studies of geotextile encased stone columns in geological conditions of perm region of Russia", Procedia engineering, 143, 530-538.

Shivashankar, R., Babu, M. R. D., Nayak, S., & Rajathkumar, V. (2011), "Experimental Studies on Behaviour of Stone Columns in Layered Soils", Geotechnical and Geological Engineering, 29(5), 749–757. https://doi.org/10.1007/S10706-011-9414-0/METRICS

Shukla, S. K., & Yin, J. H. (2006), "Fundamentals of geosynthetic engineering", CRC Press.

Singh, I., Sahu, A.K., (2019), "A review on stone columns used for ground improvement of soft soil", International Journal of Innovative Technology and Exploring Engineering 8, 466–468. https://doi.org/10.11159/icgre19.132

Sivakumar, V., Boyd, J. L., Black, J. A., & McNeil, J. A. (2010), "Effects of granular columns in compacted fills", Proceedings of the Institution of Civil Engineers-Geotechnical Engineering, 163(4), 189-196.

Sukmak, G., Sukmak, P., Horpibulsuk, S., Hoy, M. and Arulrajah, A. (2021), "Load Bearing Capacity of Cohesive-Frictional Soils Reinforced with Full-Wraparound Geotextiles: Experimental and Numerical Investigation", Applied Sciences 2021, Vol. 11, Page 2973, Multidisciplinary Digital Publishing Institute, Vol. 11 No. 7, p. 2973, doi: 10.3390/APP11072973.

Tallapragada, K. R., Golait, Y. S., & Zade, A. S. (2011), "Improvement of bearing capacity of soft soil using stone column with and without encasement of geosynthetics", International Journal of Science and Advanced Technology, 1(7), 50-59.

Tan, S. A., & Ng, K. S. (2013). "Stone columns foundation analysis with concentric ring approach". In Proceedings of the Third International Symposium on Computational Geomechanics (ComGeo III), Krakow (pp. 495-504).

Tan, S.A., Ng, K.S. and Sun, J. (2014), "Column Group Analyses for Stone Column Reinforced Foundation", American Society of Civil Engineers, pp. 597–608, doi: 10.1061/9780784413265.048.

Tan, S.A., Tjahyono, S., Oo, K.K., (2008), "Simplified Plane-Strain Modeling of Stone-Column Reinforced Ground", Journal of Geotechnical and Geoenvironmental Engineering 134, 185–194. https://doi.org/10.1061/(ASCE)1090-0241(2008)134:2(185)

Tandel, Y. K., Solanki, C. H., & Desai, A. K. (2013), "Laboratory experimental analysis on encapsulated stone column", Archives of Civil Engineering, 359-379.

Thakur, A., Rawat, S. and Gupta, A.K. (2021), "Experimental study of ground improvement by using encased stone columns", Innovative Infrastructure Solutions, Springer Science and Business Media Deutschland GmbH, Vol. 6 No. 1, pp. 1–13, doi: 10.1007/S41062-020-00383-Y/METRICS.

Thorburn, S. (1975). Building structures supported by stabilized ground. Geotechnique, 25(1), 83-94.

Van Eekelen, S.J.M. and Han, J. (2020), "Geosynthetic-reinforced pile-supported embankments: State of the art", Geosynthetics International, ICE Publishing, Vol. 27 No. 2, pp. 112–141, doi: 10.1680/JGEIN.20.00005/ASSET/IMAGES/SMALL/JGEIN.20.00005-F15.GIF.

VESIC AS. (1972), "Expansion of Cavities in Infinite Soil Mass", Journal of the Soil Mechanics and Foundations Division, 98(3), 265–290. https://doi.org/10.1061/JSFEAQ.0001740

Viswanadham, B.V.S. and König, D. (2004), "Studies on scaling and instrumentation of a geogrid", Geotextiles and Geomembranes, Elsevier, Vol. 22 No. 5, pp. 307–328, doi: 10.1016/S0266-1144(03)00045-1.

Wang, K., Liu, M., Cao, J., Niu, J., Zhuang, Y., (2023), "Bearing Characteristics of Composite Foundation Reinforced by Geosynthetic-Encased Stone Column: Field Tests and Numerical Analyses", Sustainability 2023, Vol. 15, Page 5965 15, 5965. https://doi.org/10.3390/SU15075965

WATTS, K.S., CHOWN, R.C., SERRIDGE, C.J. and CRILLY, M.S. (2001), "Vibro stone columns in soft clay soil: a trial to study the influence of column installation on foundation performance", International Conference on Soil Mechanics and Geotechnical Engineering, A A. Balkema, Lisse, pp. 1867–1870.

Watts, K.S., Johnson, D., Wood, L.A. and Saadi, A. (2000), "An instrumented trial of vibro ground treatment supporting strip foundations in a variable fill", Geotechnique, ICE Publishing, Vol. 50 No. 6, pp. 699–708, doi: 10.1680/GEOT.2000.50.6.699.

Weber, T.M., Plötze, M., Laue, J., Peschke, G. and Springman, S.M. (2015), "Smear zone identification and soil properties around stone columns constructed in-flight in centrifuge model tests", Https://Doi.Org/10.1680/Geot.8.P.098, Thomas Telford Ltd , Vol. 60 No. 3, pp. 197–206, doi: 10.1680/GEOT.8.P.098.

Wehr, J. (2006), "The undrained cohesion of the soil as criterion for the column installation with a depth vibrator", In Proceedings of the international symposium on vibratory pile driving and deep soil Vibratory compaction. TRANSVIB, Paris (pp. 157-162).

Wu, C. Sen, Hong, Y. S., & Lin, H. C. (2009), "Axial stress–strain relation of encapsulated granular column", Computers and Geotechnics, 36(1–2), 226–240. doi: 10.1016/J.COMPGEO.2008.01.003

Xu, F., Moayedi, H., Foong, L.K., Moghadam, M.J. and Zangeneh, M. (2021), "Laboratory and numerical analysis of geogrid encased stone columns", Measurement: Journal of the International Measurement Confederation, Elsevier B.V., Vol. 169, doi: 10.1016/J.MEASUREMENT.2020.108369.

Xu, Z., Zhang, L. and Zhou, S. (2021), "Influence of encasement length and geosynthetic stiffness on the performance of stone column: 3D DEM-FDM coupled numerical investigation", Computers and Geotechnics, Elsevier, Vol. 132, p. 103993, doi: 10.1016/J.COMPGEO.2020.103993.

Yasser, F., Altahrany, A. and Elmeligy, M. (2022), "Numerical investigation of the settlement behavior of hybrid system of floating stone columns and granular mattress in soft clay soil", International Journal of Geo-Engineering, Springer, Vol. 13 No. 1, pp. 1–26, doi: 10.1186/S40703-022-00177-4/FIGURES/33.

Ye, G., Cai, Y., & Zhang, Z. (2017), "Numerical study on load transfer effect of Stiffened Deep Mixed column-supported embankment over soft soil", KSCE Journal of Civil Engineering, 21(3), 703–714. https://doi.org/10.1007/S12205-016-0637-8/METRICS

Yoo, C. and Abbas, Q. (2020), "Laboratory investigation of the behavior of a geosynthetic encased stone column in sand under cyclic loading", Geotextiles and Geomembranes, Elsevier Ltd, Vol. 48 No. 4, pp. 431–442, doi: 10.1016/J.GEOTEXMEM.2020.02.002.

Yoo, C., & Abbas, Q. (2019), "Performance of geosynthetic-encased stone column-improved soft clay under vertical cyclic loading", Soils and Foundations, 59(6), 1875–1890. doi: 10.1016/J.SANDF.2019.08.006

Yoo, C., (2015), "Settlement behavior of embankment on geosynthetic-encased stone column installed soft ground – A numerical investigation", Geotextiles and Geomembranes 43, 484–492. https://doi.org/10.1016/J.GEOTEXMEM.2015.07.014

Yu, Y. and Bathurst, R.J. (2016), "Influence of Selection of Soil and Interface Properties on Numerical Results of Two Soil–Geosynthetic Interaction Problems", International Journal of Geomechanics, American Society of Civil Engineers, Vol. 17 No. 6, p. 04016136, doi: 10.1061/(ASCE)GM.1943-5622.0000847.

Yu, Y. and Bathurst, R.J. (2017), "Probabilistic assessment of reinforced soil wall performance using response surface method", Https://Doi.Org/10.1680/Jgein.17.00019, Thomas Telford Ltd , Vol. 24 No. 5, pp. 524–542, doi: 10.1680/JGEIN.17.00019.

Zhang, L. and Zhao, M. (2015), "Deformation Analysis of Geotextile-Encased Stone Columns", International Journal of Geomechanics, American Society of Civil Engineers, Vol. 15 No. 3, p. 04014053, doi: 10.1061/(ASCE)GM.1943-5622.0000389

Zhang, L., Xu, Z., Zhou, S., (2020), "Vertical cyclic loading response of geosynthetic-encased stone column in soft clay", Geotextiles and Geomembranes 48, 897–911. https://doi.org/10.1016/J.GEOTEXMEM.2020.07.006

Zhao, T.H., Khan, M.I. and Chu, Y.M. (2023), "Artificial neural networking (ANN) analysis for heat and entropy generation in flow of non-Newtonian fluid between two rotating disks", Mathematical Methods in the Applied Sciences, John Wiley & Sons, Ltd, Vol. 46 No. 3, pp. 3012–3030, doi: 10.1002/MMA.7310.

Zhou, Y., Kong, G., Yang, Q. and Li, H. (2019), "Deformation analysis of geosynthetic-encased stone column using cavity expansion models with emphasis on boundary condition", Geotextiles and Geomembranes, Elsevier, Vol. 47 No. 6, pp. 831–842, doi: 10.1016/J.GEOTEXMEM.2019.103498.

Zhuang, Y., Cheng, X. and Wang, K. (2020), "Analytical solution for geogrid-reinforced piled embankments under traffic loads", Https://Doi.Org/10.1680/Jgein.19.00023, Thomas Telford Ltd , Vol. 27 No. 3, pp. 249–260, doi: 10.1680/JGEIN.19.00023.